Mass transfer to a turbulent fluid with and without chemical reaction

T. K. SHERWOOD and J. M. RYAN

Chemical Engineering Department, Massachusetts Institute of Technology, Cambridge, Mass.

Abstract—A new theory based on a turbulent boundary layer model is developed to describe mass transfer with a simultaneous, fast, irreversible reaction. Data on dissolution of a rotating cylinder of benzzoic acid into aqueous caustic are compared with this theory and with the theories based on the film and penetration models.

Comparison of the data on dissolution into water with a form of the Deissler analogy points up the fact that the various modern analogies between heat, mass and momentum transfer predict that the Stanton number should be proportional to $\sqrt{f}$ at high Prandtl or Schmidt numbers, whereas the data show direct proportionality. This suggests a basic error in the usual procedure by which analogies are developed.

Résumé—Les auteurs développent une théorie nouvelle basée sur la couche limite turbulente pour décrire le transfert de masse avec une réaction instantanée rapide et irréversible. Les résultats sur la dissolution d'un cylindre d'acide benzoïque animé d'un mouvement de rotation dans une solution de soude caustique sont comparés avec cette théorie et avec les théories de films et de pénétration.

La comparaison des résultats sur la dissolution dans l'eau au moyen des formules d'analogie de Deissler indique le fait que les analogies diverses entre le transfert de chaleur, de masse et de quantité de mouvement prévoient un nombre de Stanton proportionnel à $\sqrt{f}$ pour de grands nombres de Prandtl et de Schmidt, tandis que les résultats montrent une proportionnalité directe. Ceci suggère une erreur de base dans le procédé usuel de développement des analogies.

Zusammenfassung—Auf der Grundlage eines Modells der turbulenten Grenzschicht wird eine neue Theorie der Stoffübertragung mit gleichzeitiger schneller, nicht umkehrbarer Reaktion abgeleitet. Die Werte der Auflösung eines rotierenden Zylinders aus Benzoesäure in wässrigen Laugen werden mit dieser Theorie und mit der Theorie der Film- und der Durchdringungs-vorstellung verglichen.

Ein Vergleich der Auflösungswerte in Wasser mit der Analogie nach Deissler zeigt, dass die verschiedenen modernen Analogien zwischen Wärme-, Stoff und Impulsübertragung eine Proportionalität zwischen der Stanton–Zahl und $\sqrt{f}$ bei hohen Prandtl- oder Schmidt-Zahlen voraussagen, während die Messwerte eine direkte Proportionalität zeigen. Das deutet auf einen grundsätzlichen Irrtum bei der üblichen Ableitung der Analogien hin.

UNDERSTANDING of the process of mass transfer between phases is basic to the development of such important chemical engineering operations as gas absorption, solvent extraction, distillation, drying and leaching. Although industrial operations frequently involve simultaneous diffusion and chemical reaction, most of the theoretical and experimental investigations of mass transfer between two phases have been concerned with the physics of the transfer of a single diffusing substance.

In comparing theory with data on heat or mass

81

transfer to a turbulent stream, it has usually been found convenient to treat the case of a round tube through which the fluid passes in steady, fully-developed turbulent flow. This is a situation about which much is known, but is complicated by the fact that the bulk stream temperatures or concentrations vary with distance from the tube inlet, so that analysis of data to obtain transfer coefficients is often difficult. Use of a rotating cylinder avoids this difficulty, since the temperature or concentration depend only on radial distance.

EXPERIMENTAL

Benzoic acid was melted, cast and machined to fill a 0·80 mm-deep recess, 63·5 mm-long, cut in a 30·5 mm-o.d. stainless or lacquered-steel cylinder. The benzoic acid was machined smooth and flush with the steel. The cylinder so prepared was rotated on a vertical axis at the centre of a 10·2 cm-i.d. glass container holding 1555 cm^3 of liquid. The recess holding the acid was at the vertical centre of the 20·3 cm-high container. Ball bearings were provided at both top and bottom, and the cylinder rotated by a variable-speed drive operable over a speed range from 2 to 6000 rev/min. Plexiglass end plates with neoprene seals at top and bottom were held in place by external steel tie rods, and the whole was immersed in a constant-temperature water bath.

Special pains were taken to exclude air, both to avoid the introduction of CO_2, and to eliminate the air bubbles which tended to collect at the rotating surface. Access to the container was through a 6 mm hole in the top plate, sealed by a rubber membrane during a test. No free air–liquid surface existed in this hole. A 0·40 mm-wide annulus, 25 mm long between the hole in the top plate and the rotating cylinder, formed a liquid seal.

A first series of tests was made with distilled CO_2-free water, taken from a vessel kept in the constant-temperature bath. The tests varied in length from 0·5 to 4 hr, during which times the water became 10 – 40 per cent saturated in benzoic acid, and the diameter of the test cylinder, measured before and after the test, decreased by about 2 per cent. Eight to ten samples of 5 – 6 cm^3 each were taken at intervals during the test, using a hypodermic needle to withdraw them through a rubber membrane. Samples were immediately replaced by the same volumes of water. Twenty-five tests at 25°C, two at 33°C and one at 17°C were made over a range of Reynolds numbers from 136 to 103,400.

A second set of tests with aqueous NaOH solutions was carried out in similar fashion, but the tests were shorter in duration (14 min minimum). Samples were neutralized with identical additions of standard HCl and back-titrated with the alkaline solution used in the test. Twenty-five tests were made at 25°C, using initial NaOH normalities from 0·0090 to 0·64 ; in two cases the initial solution contained both sodium hydroxide and sodium benzoate.

REDUCTION OF DATA

In the case of the dissolution tests using water, graphs of $\ln (1 - C_{A0}/C_{Aw})$ versus time gave excellent straight lines ; $k_A^{'}$ was calculated from the measured slopes. Small corrections were made in the measured values of C_{A0} to allow for the replacement of the small samples by water.

Similar corrections for sampling were made in the tests with caustic. In addition, allowance was made for the fact that k_A varied during the test as NaOH concentration decreased. If k_A varies linearly with the bulk NaOH concentration C_{B0}, the slope being $k_{ai} \gamma/C_{Aw}$, then $1/\gamma \ln \{1 - \gamma [(C_{B0})_{initial} - C_{B0}]/C_{Aw}\}$ should be linear in time. This was found to be the case, and k_A at zero time (k_{ai}) was calculated from the slopes of such graphs. Since the changes in NaOH concentration during a test were small, the result is quite insensitive to the assumed value of γ, and k_{ai} is accurately established.

Values of $k_A^{'}$ and k_A obtained by these procedures were calculated using an area based on the measured length and arithmetic mean of initial and final diameters of the cast test section. Surface speed u_w was calculated from the mean diameter and the measured speed of rotation. The known physical properties of the solutions were employed in the calculation of N_{Re}.

SEIDELL's [1] data on solubility of benzoic acid

in water and sodium benzoate were used; the water data were checked closely by measurements of the solubility of pieces of the cast test sections. Chang's [2] values of the molecular diffusion coefficient of benzoic acid in water were used. These are checked closely at 25°C by King and Brodie [3], but are 10 per cent higher than reported by Bennett and Lewis [4]. The Schmidt number σ for benzoic acid–water at 25°C was taken as 870.

Part I

Mass Transfer without Chemical Reaction

(1) Results—physical dissolution

The data for twenty-eight tests in which benzoic acid was dissolved in water are plotted on Fig. 1 as $k°/u_w$ versus N_{Re}. Twenty-five were at 25°C; three at other temperatures are corrected to 25°C by assuming $k°$ to vary with $\sigma^{-0.644}$, σ being the Schmidt number. The points fall reasonably close to a well-defined line (to avoid confusion on the graph, this line is not shown).

The most extensive comparable data are those of Eisenberg et al. [5], who carried out similar tests, employing several sizes of rotating cylinders and containers. The cylinder radius, R_w, was varied from 0.97 to 2.99 cm and the container radius R_e, from 3.03 to 6.84 cm. Though the ratio of gap width to inner cylinder diameter

varied from 0.104 to 4.88, an excellent correlation was obtained using N_{Re} based on R_w; the effect of R_e and gap width appeared to be unimportant, at least for the geometries tested. σ was varied from 835 to 11,500 by using different diffusing species, and N_{St} found to be proportional to $\sigma^{-0.644}$. The solid line shown on Fig. 1 is a close representation of their one hundred or more tests with benzoic acid and water ($\sigma = 870$). It is evident that the agreement between the present data and those of Eisenberg et al. is remarkably good.

Also shown on Fig. 1 are five tests reported by King and Brodie [3], who used a 2.2 cm diameter cylinder of benzoic acid rotated in 500 cm³ of water. The recent results of Bennett and Lewis [4], also shown, have been adjusted to 25°C by assuming $k°$ to be proportional to $\sigma^{-0.644}$. Their cylinder diameter was 1.0 cm, rotated in a 3 cm container. The four sets of data would appear to fix the relationship for benzoic acid–water within 10 per cent to a high degree of probability.

(2) Theory—physical dissolution

As described in a recent review by one of the authors [6], the various analogies relating mass, heat and momentum transfer agree well with the considerable amount of data on mass and heat transfer for fully developed turbulent flow in
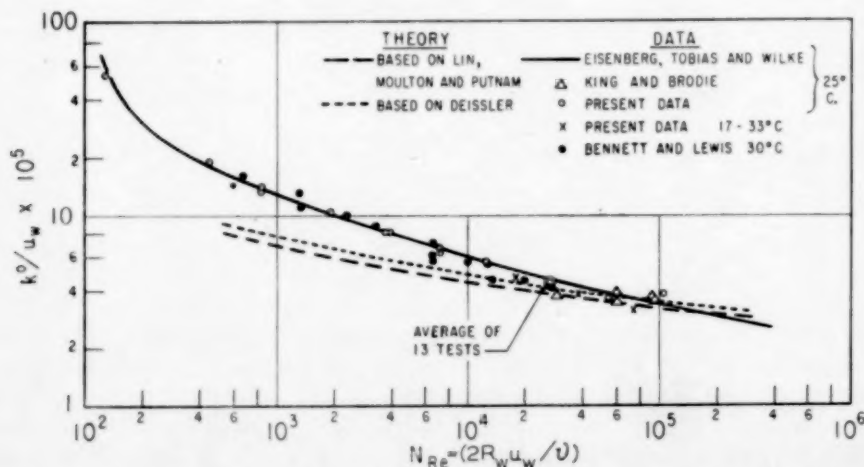

Fig. 1. Data on rate of solution of cylinders of solid benzoic acid rotated in water.

round tubes. These are developed from the following rate equation:

$$N = -(D + \epsilon) \frac{dC}{dy} \qquad (1)$$

where N is the molal flux, C the concentration, y the distance from the phase boundary, and D and ϵ are the molecular and eddy diffusion coefficients. D may be assumed constant in dilute solutions, but ϵ varies from zero at the wall to very large values (relative to D) in the main turbulent stream.

In order to obtain integrated forms of equation (1), it is necessary to relate ϵ and y. In many of the theories ϵ is assumed to be equal or proportional to the eddy viscosity, and so obtained from known velocity gradients. VON KÁRMÁN [7] employed the generalized $u^+ - y^+$ correlation in smooth tubes for this purpose and obtained good agreement with data on heat and mass [8] transfer in tubes for values of σ from 0·5 to 25. His integration of equation (1) assumed ϵ to be zero for $0 < y^+ < 5$. KAYS and BJORKLUND [9] show a similar analysis to agree well with their data on heat transfer from a rotating cylinder to air. The theory fails completely, however, at large values of σ.

In liquid systems D is so small that the slight turbulence very near the wall can be quite important, and in this range the eddy viscosity cannot be obtained from existing data on velocity profiles. Various authors, therefore, have proposed empirical relations relating ϵ to y, and so obtained relations for the wall flux N_w. The most successful analyses of this kind appear to be those of DEISSLER [10] and of LIN et al. [11].

For the region of $0 < y^+ < 26$, DEISSLER writes:

$$\epsilon/\nu = n^2 u^+ y^+ \left[1 - \exp\left(-n^2 u^+ y^+\right)\right] \qquad (2)$$

where the empirical constant n is determined from data at high Schmidt numbers to be 0·124, and u^+ is related to y^+ by the generalized velocity correlation for smooth tubes. For $u^+ < 4$, u^+ may be taken equal to y^+, and for $u^+ < 1$ the equation reduces to $\epsilon/\nu = n^4 (y^+)^4$. Equation (2) was developed and tested for flow in round tubes, but will be assumed to apply very near the surface

of a rotating cylinder, where most of the resistance to mass transfer at high Schmidt numbers is concentrated. In the region near the wall LIN et al. assume ϵ/ν to be proportional to $(y^+)^3$; the result is not greatly different if their form is used in place of DEISSLER's.

On integration, with N_w assumed constant, equation (1) becomes:

$$\frac{C_w - C}{N_w} Q = \int_0^{y^+} \frac{dy^+}{1/\sigma + \epsilon/\nu} = \phi(y^+, \sigma) \qquad (3)$$

Here C is the concentration at distance y^+ from the wall, Q is introduced to represent $\sqrt{(\tau_w g_c/\rho)}$, and σ is the dimensionless Schmidt group, ν/D. The function $\phi(y^+, \sigma)$ is the indicated integral.

In order to obtain mass transfer coefficients and Stanton numbers, equation (2) will be employed from the wall to $y^+ = 26$, and the Reynolds analogy used from $y^+ = 26$ to the bulk stream concentration at y_0^+. The latter may be written:

$$\frac{Q}{N} dC = du^+ \qquad (4)$$

whence:

$$\phi(y_0^+) - \phi(26) = u_0^+ - u_{26}^+ = \sqrt{(2/f)} - 12 \cdot 85 \qquad (5)$$

This increment varies from about 3 to 8 as N_{Re} increases from 10,000 to 100,000. Since it is a small part of the total integral, it will be taken as constant at 5·75, equivalent to using equation (3) with the limit $y^+ = 200$ in place of y_0^+.

From equation (3) it follows that the total integral may be written:

$$\frac{u_0}{k^\circ} \sqrt{\frac{f}{2}} = \frac{1}{N_{St}} \sqrt{\frac{f}{2}} = \phi(200, \sigma) \qquad (6)$$

where $\tau_w g_c$ is replaced by $(1/2) f \rho u_0^2$. The top line of Fig. 2 represents this integral and provides a basis for calculating k°; it checks the DEISSLER asymptotic equation for high values of σ.

It seems not unreasonable to assume that the conditions very near the wall should be the same for a rotating cylinder as for flow in a round tube at the same f. Away from the wall, however, the turbulence pattern is quite different in the two systems.
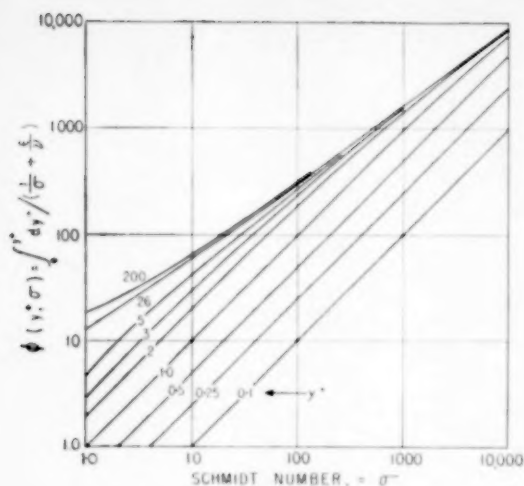
Fig. 2. Graph of $\phi(y^+, \sigma)$.

Let R_w be the radius of the rotating cylinder, and R_e be the radius of the outer fixed cylinder confining the fluid in an annulus of gap width $R_e - R_w$. Let the Reynolds number N_{Re} be defined as $2R_w u_w/\nu$, where u_w is the peripheral speed of the rotating cylinder. At very low speeds the flow is laminar, as in a narrow-gap rotating-cup viscometer. There is an intermediate speed range in which a series of three-dimensional vortices may be noted [12, 13, 14], above which the motion is turbulent. The present study is confined to the fully turbulent regime.

Since the turning torque is the same at any radius,

$$\tau_w R_w^2 = \tau r^2 \qquad (7)$$

Townsend [15] gives the following expression for the turbulent flow condition:

$$-\tau g_c = \mu r \frac{d(u/r)}{dr} - \overline{\rho v_r u_t} \qquad (8)$$

where $\overline{v_r u_t}$ is the time-mean product of the fluctuating components of velocity in the radial and tangential directions. The velocity profile over the principal portion of the gap has been shown by Taylor [16] and Wendt [17] to be given closely by:

$$ur = 0.5 u_w R_w \qquad (9)$$

If the eddy viscosity ϵ_v is defined by:

$$-\tau g_{c/\rho} = (\nu + \epsilon_v) r \frac{d(u/r)}{dr} \qquad (10)$$

and the friction coefficient is based on cylinder radius and cylinder peripheral velocity, then equations (9) and (10) may be combined to give:

$$\epsilon_v/\nu = \frac{f}{4} N_{Re} - 1 \qquad (11)$$

This suggests that ϵ_v and ϵ are constant except near the inner and outer walls of the rotating-cylinder system.

Equating ϵ_v and ϵ, equations (2) and (11) may be employed to relate ϵ to y^+ for the entire region from wall to bulk fluid [18]. This is not worth while for the analysis of data at high values of σ, however, since the intersection of equations (2) and (11) occurs at $y^+ = 4.7$ for $N_{Re} = 750$, $y^+ = 8.3$ for $N_{Re} = 11,500$ and $y^+ = 11.3$ for $N_{Re} = 53,200$. The resistance beyond $y^+ = 4.7$ is very small for $\sigma = 870$ (benzoic acid in water), so the use of equation (11) would hardly change the results of the analysis based on Deissler to $y^+ = 26$ and the Reynolds analogy to y_0^+.

(3) *Comparison of theory with data on physical dissolution*

In order to compare equation (6) with the data on physical dissolution, it is necessary to have values of f for rotating cylinders. These are obtainable from the work of Theodorsen and Regier [19], who employed both smooth and rough cylinders of several sizes rotating in oils, kerosene, water and air. Their data are well represented by the single line A-A on Fig. 3.
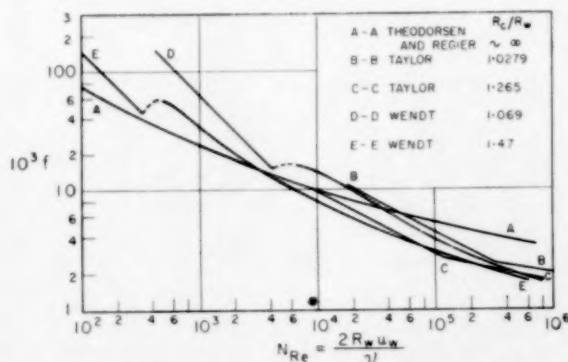

Fig. 3. Friction coefficients for rotating cylinders.

85

That f var s with gap width is suggested by the data of Taylor [16] and Wendt [17], but the nature of the variation has not been established.

Experimental and calculated values of N_{St} are compared on Fig. 1, which shows lines representing equation (6) for both the Deissler and the Lin et al. functions. The comparison is seen to be poor, especially at low values of N_{Re}, where the discrepancy is about 50 per cent.

Both theoretical lines are based on analyses of transfer processes in tubes, and it may be that a different relation between ϵ and y^+ should be employed for rotating cylinders. It is also possible that Theodorsen and Regier's values of f are inapplicable, since their cylinders were rotated in a large space and all of the mass transfer data were obtained with confined cylinders. Fig. 3 suggests that finite gap widths give steeper f curves, more in line with the mass transfer data of Fig. 1.

A more interesting speculation, however, relates to the possibility that the form of equation (6) is wrong. Following von Kármán, ϵ has been taken to be a function of y^+. Suppose, instead, that the proper distance parameter were assumed to be the dimensionless group y^{++}, defined by:

$$y^{++} = \frac{y\,\tau_w\,g_c}{u_0\,\nu\,\rho} = \frac{y}{u_0\,\nu}\,Q^2 = \frac{yu_0}{\nu}\frac{f}{2} \qquad (12)$$

i.e., $\epsilon/\nu = f_2(y^{++})$, instead of $\epsilon/\nu = f_1(y^+)$.

Deissler and Lin et al. compare their "analogies" with heat and mass transfer data over quite narrow ranges of N_{Re} (10,000 to 100,000). Assuming Deissler's function $f_1(y^+)$ to have been well chosen for $N_{Re} = 50,000$, then the use of $f_2(y^{++})$ would require the values of $k°/u_w$ as calculated by Deissler to be multiplied by the ratio of $\sqrt{(f/2)}$ at N_{Re} to $\sqrt{(f/2)}$ at $N_{Re} = 50,000$. The latter value is given by Theodorsen and Regier as $\sqrt{0.00325}$. Adjustment by this procedure of the dashed line of Fig. 1 representing Lin et al. would result in a curve of predicted values checking the best line through the data points within 10 per cent. Similar adjustment of the Deissler line would give similarly good agreement between predicted and experimental values.

There are several reasons to believe that ϵ/ν should be a function of y^{++} instead of y^+. Most important is the success of the many correlations of experimental mass and heat transfer data in the form of graphs of j_H or j_D versus N_{Re}. Where the drag is due to skin friction, these follow $f/2$, not $\sqrt{(f/2)}$, as called for by equation (6).

If ϵ is taken to be a function of y^+, as was done by von Kármán and later workers, the mass and heat transfer analogies take the form:

$$N_{St} = \frac{2}{f} + \sqrt{\left(\frac{2}{f}\right)}f(\sigma) \qquad (13)$$

If u^+ is assumed to be a universal function of y^{++} instead of y^+, the result is similar except that $\sqrt{(2/f)}$ becomes $2/f$ in the second term on the right. The Reynolds analogy still holds for $\sigma = 1$, and at high values of σ the nature of the variation of N_{St} with σ is unchanged, since the first term on the right is then negligible.

The universal velocity distribution relating u^+ and y^+ seems well established by the experiments of Nikuradse, Reichardt and others. Most of the older data were obtained at high Reynolds numbers, with little variation in f. Recent data of Corcoran and Sage [20] give higher values of u^+ at any specified y^+; use of y^{++} instead of y^+ would introduce a correction factor in the right direction.

Schlicting's [21] review of the history of the $u^+ \sim y^+$ correlation indicates that the choice of y^+ as a parameter was based largely on dimensional arguments. It would be of interest to explore the possible advantage of y^{++} in the velocity correlation.

Whether or not the modified distance parameter y^{++} has application to velocity correlations, it may be concluded that ϵ/ν for mass and heat transfer must be expressed as a function of wall distance in terms of y^{++} rather than y^+ if N_{St} is to be proportional to f at high values of σ.

Fig. 4 demonstrates the general nature of the $j_D \sim j_H \sim f/2$ correlation for rotating cylinders, and supports the statement that N_{St} is proportional to f rather than $\sqrt{f}$. The data of Fig. 1 are represented by the line for the Eisenberg et al. correlation at $\sigma = 870$. Several results of Cotter and Schmidt [22] for vaporization of naphthalene
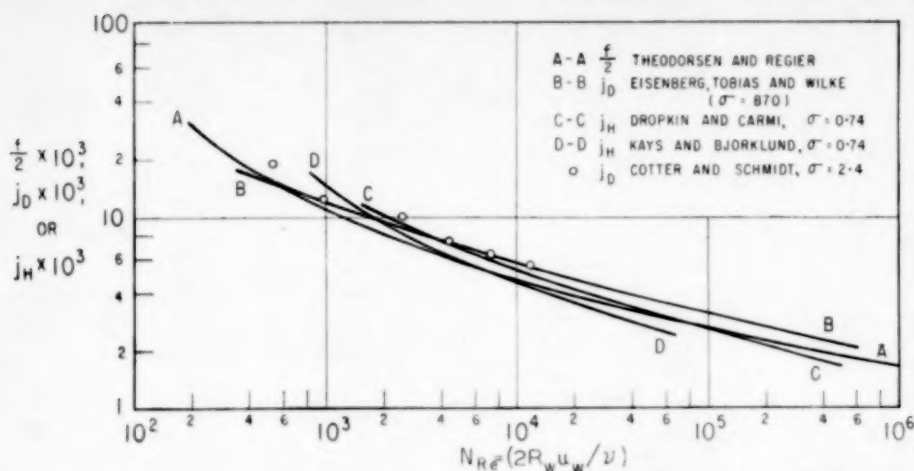
Fig. 4. Comparison of data on heat transfer, mass transfer and friction for rotating cylinders.

from a 2·44-cm diameter cylinder rotating in air are seen to agree well, though σ was less than 1 per cent of the values for the liquid systems. The two sets of data [9, 23] on heat transfer to air fall somewhat low at high Reynolds numbers, but do not agree well with each other. The recent data of SEBAN and JOHNSON [24] on heat transfer from a 6·35-cm cylinder rotating in oil and in water (for $N_{Re} > 2000$, with negligible free convection) fall some $10 - 15$ per cent above the mass-transfer data. The friction data of THEODORSEN and REGIER are in reasonable agreement with the experimental curves for j_D and j_H.

Fig. 4 represents a remarkable correlation, in that it brings together data on heat transfer, mass transfer and friction for cylinders rotating in gases and liquids over a range of Reynolds and Schmidt numbers of more than one-thousand fold.

PART II

Mass Transfer with Chemical Reaction

(1) Theory—rapid, irreversible reaction

The theoretical treatments of mass transfer with chemical reaction have generally led to expressions defining a multiplying factor to apply to the coefficient for transfer without chemical reaction. These have been based on two models: (a) the stagnant film, and (b) an interface being continually replaced by fresh surface.

The first, developed originally by HATTA [25] on the basis of the stagnant–film model, leads to the relation:

$$\frac{k_A}{k_A^\circ} = 1 + \frac{D_B C_{B0}}{D_A C_{Aw}} \tag{14}$$

This is for the case of a solute A entering the fluid and reacting irreversibly and instantaneously with solute B diffusing toward the phase boundary from the bulk fluid (see Fig. 5). The transfer
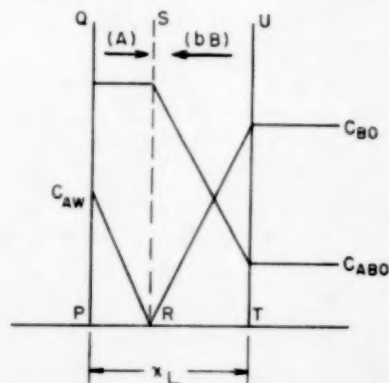

Fig. 5. Film model employed by HATTA.

coefficient k_A is defined as the ratio of the molal flux N_A to the concentration difference $(C_{Aw} - 0)$ and k_A° is the corresponding transfer coefficient D_A/x_L for the diffusion of A from interface to bulk without chemical reaction (no B present).

87

Retaining the stagnant film model, Sherwood and Wei [26] have shown how the Hatta theory may be modified to allow for the dissociation of electrolytes in water, where the molecular diffusion coefficients D_A and D_B have little meaning. For solution of benzoic acid in water, with dissociation of benzoic acid neglected, their result may be written (see Appendix):

$$\frac{k_A}{k_A^\cdot} = 1 + \frac{2RT}{D_a}\frac{\lambda'_-}{F_a^2} \times$$

$$\left\{ \sqrt{\left[1 + \frac{C_{B0}}{C_{AB0}}\left(\frac{\lambda'_-}{\lambda_-} - 1\right)\right]} + 1 \right\}^{-1} \frac{C_{B0}}{C_{Aw}} \quad (15)$$

where F_a is the Faraday and λ'_-, λ_- are the limiting (zero concentration) ionic conductances of OH^- and Bz^- ions, respectively. C_{Aw} is the concentration of benzoic acid at the phase boundary; C_{B0} and C_{AB0} are the bulk solution concentrations of sodium hydroxide and total sodium, respectively. It follows from equation (15) that because of the rapidity of OH^- diffusion, k_A increases some 50 per cent faster with C_{B0}/C_{Aw} than suggested by the Hatta form.

The second model involves transient penetration of diffusing species into a renewable interface. The use of this model for the development of a theory of transfer with simultaneous, rapid second-order reaction has been described by Danckwerts [27] and others [28, 29, 30, 31], without allowance for varying diffusion rates of the different ions formed by dissociation. The calculated increase of k_A with C_{B0}/C_{Aw} is not greatly different than predicted by Hatta [32].

It is now proposed to employed a third model — the turbulent boundary layer*. Following the pattern of the Hatta theory, assume that A reacts rapidly and irreversibly with b moles of B at some plane a distance y_R^+ from the surface. Then:

$$\frac{(C_{Aw} - 0)}{N_A} Q = \phi(y_R^+, \sigma_A) = \frac{Q}{k_A} \quad (16)$$

*Note added in proof: Three recent articles treat diffusion and chemical reaction in *laminar* boundars layers. These are: Friedlander S. K. and Litt M., *Chem. Engng. Sci.* 1958 7 229; Potter O. D., *Trans. Inst. Chem. Engrs.* 1958 36 415; Chambre P. L. and Young J. D., *Phys. Fluids* 1958 1 48.

$$\frac{(0 - C_{B0})}{N_B} Q = Q\frac{C_{B0}}{bN_A}$$

$$= \phi(y_0^+, \sigma_B) - \phi(y_R^+, \sigma_B) \quad (17)$$

With no B present A diffuses without reacting, and:

$$\frac{(C_w - C_0)}{N_A} Q = \frac{Q}{k_A^\cdot} = \phi(y_0^+, \sigma_A) \quad (18)$$

This assumes that the limit C_0 corresponds to the limit y_0^+, an assumption shown by Rannie [33] to be acceptable for $\sigma < 1$.

$$\frac{k_A}{k_A^\cdot} = \frac{\phi(y_0^+, \sigma_A)}{\phi(y_R^+, \sigma_A)}$$

$$= \frac{C_{B0}}{bC_{Aw}}\frac{\phi(y_0^+, \sigma_A)}{[\phi(y_0^+, \sigma_B) - \phi(y_R^+, \sigma_B)]} \quad (19)$$

In order to evaluate this relation, it is necessary to relate ϵ to y^+ and obtain values of the integral represented by ϕ. Before doing this, however, it is of interest to inspect three limiting cases, for which ϵ need not be known.

(a) $\sigma_A = \sigma_B$. Equation (19) reduces to:

$$\frac{k_A}{k_A^\cdot} = \frac{C_{B0}}{bC_{Aw}}\frac{1}{\{1 - [\phi(y_R^+)/\phi(y_0^+)]\}}$$

$$= \frac{C_{B0}}{bC_{Aw}}\frac{1}{[1 - (k_A^\cdot/k_A)]} \quad (20)$$

whence:

$$\frac{k_A}{k_A^\cdot} = 1 + \frac{C_{B0}}{bC_{Aw}} \quad (21)$$

which is identical with the Hatta equation, since $D_A = D_B$.

(b) $y_R^+ < 1$. ϵ/ν approaches zero at the wall, and in the limit $\phi(y_R^+, \sigma) \to y_R^+ \sigma$, as seen from equation (6). Then:

$$\frac{k_A}{k_A^\cdot} = \frac{\phi(y_0^+, \sigma_A)}{y_R^+ \sigma_A} \quad (22)$$

$$\frac{k_B^\cdot}{k_A^\cdot} = \frac{\phi(y_0^+, \sigma_A)}{\phi(y_0^+, \sigma_B)} \quad (23)$$

$$\frac{C_{B0}}{C_{Aw}} = \frac{\phi(y_0^+, \sigma_B) - y_R^+ \sigma_B}{y_R^+ \sigma_A} \quad (24)$$

whence:

$$\frac{k_A}{k_A^\circ} = \frac{k_B^\circ}{k_A^\circ}\left[\frac{\sigma_B}{\sigma_A} + \frac{C_{B0}}{bC_{Aw}}\right] \qquad (25)$$

If the coefficient k° is represented as being proportional to a power function of D ($k_A^\circ \propto D^a$), then:

$$\frac{k_A}{k_A^\circ} = \left(\frac{\sigma_B}{\sigma_A}\right)^{1-a}\left[1 + \frac{D_B}{D_A}\frac{Cb_{B0}}{bC_{Aw}}\right] \qquad (26)$$

The condition $y_R^+ < 1$ applies approximately if k_A/k_A° is greater than 20 at $\sigma_A = 1$; greater than 7 at $\sigma_A = 10$; greater than 3·5 at $\sigma_A = 100$, or greater than 1·7 at $\sigma_A = 1,000$.

(c) k_A/k_A° near 1·0. This is the case of y_R^+ being very large, so that the value of σ is not important, and the result is the same as for $\sigma_A = \sigma_B$:

$$\frac{k_A}{k_A^\circ} = 1 + \frac{C_{B0}}{bC_{Aw}} \qquad (27)$$

These three limiting situations define the variation of k_A within quite narrow limits, though no assumption as to the variation of the eddy diffusivity has been made.

The complete theory, using the DEISSLER expression for ϵ, follows by substitution into equation (19) of the integral defined by equation (3). Computed values of this integral as a function of y^+ and σ are given in Fig. 2; y_0^+ is taken to be 200 for the reasons given earlier. The ordinates of Fig. 2 represent the mass transfer resistance from the wall to any y^+; the use of these values is seen to lead to a theory similar to HATTA's but with resistance per unit length varying with distance from the wall.

(2) Results—with chemical reaction

Fig. 6 shows the data obtained for the dissolution of benzoic acid into aqueous NaOH solutions of several normalities. The range of variables (N_{Re}, C_{B0}) was limited by the attainable precision and reproducibility. At low NaOH concentrations the effect of the caustic was small and the ratio k_A/k_A° sensitive; at the highest normalities and Reynolds numbers the tests were necessarily of short duration and sufficient benzoic acid was dissolved to distort the rotating cylinder. The points plotted, however, represent initial rates.
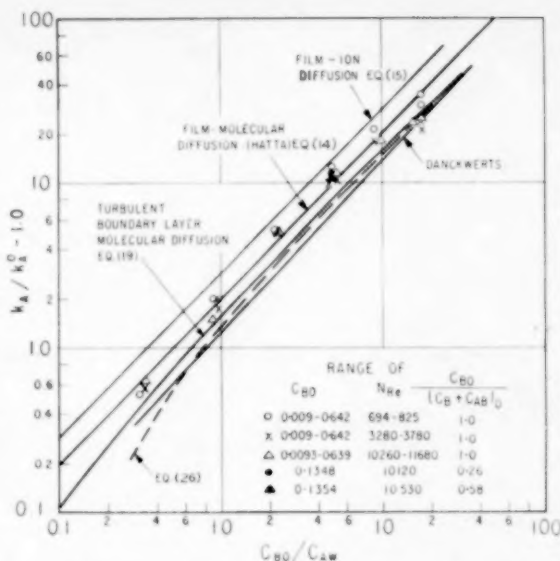

FIG. 6. Data on solution of benzoic acid into aqueous NaOH compared with several theories.

The data follow the general trend of the several theories, and show the curvature predicted by the turbulent transport model. It is evident, however, that the points fall some 0 – 50 per cent above the line representing equation (19), the discrepancy being the greatest near the middle of the range. The HATTA equation fits the data somewhat better than the new theory; since the film model is not realistic, this must be considered fortuitous.

The lack of agreement between the data and the boundary layer theory is not attributable to the possible error in the analogy approach discussed in an earlier section, since here we are concerned only with the ratio of coefficients with and without chemical reaction. More probably, the difficulty lies in the failure of the theory to allow for the increased speed of diffusion of OH$^-$ ions in a multiple-ion system. The data points fall roughly half-way between the boundary layer theory based on molecular diffusion, and the film theory based on ion diffusion. They fall about as much above the theory for molecular diffusion in a boundary layer as the film ion-diffusion theory falls above the film molecular-diffusion theory.

Allowance for the increase in C_{Aw} with accumulation of sodium benzoate near the wall would affect both ordinate and abscissa of the points but would not greatly change their positions relative to the theoretical lines.

It appears difficult to extend the theory further until more is known about turbulent mixing. In the zone where the reactants meet, there is a fine-grained turbulence of small eddies. Some of these are acid and some basic, though the region may be statistically neutral. The lines of mean concentration, as represented by Fig. 5, probably cross rather than meet at zero concentration. Gross mixing is accomplished by the motion of the eddies; ultimate mixing necessary for chemical reaction by molecular and ion diffusion. The development of a complete theory must await the solution of the problem basic to most studies involving turbulence — the mechanism of the dissipation of eddies.

APPENDIX

SHERWOOD and WEI [26] employed average concentration gradients and concentrations in using the VINOGRAD and McBAIN equations for ion diffusion. It is now noted that this is unnecessary; integrated forms are not difficult to obtain in certain cases.

For example, the second case treated by SHERWOOD and WEI (non-dissociating acid diffusing and reacting with base) involves the diffusion of Bz^-, OH^- and Na^+ ions in the right-hand portion of the film pictured in Fig. 5. The Na^+ flux is set equal to zero:

$$N_+ = 0 = - \frac{RT \lambda_+}{F_a^2} \times$$
$$\left[G_+ - C_+ \frac{\lambda_+ G_+ - \lambda_- G_- - \lambda_-' G_-'}{\lambda_+ C_+ + \lambda_- C_- + \lambda_-' C_-'} \right] \quad (28)$$

where the subscripts refer to anion and cation, and the prime to OH^-. G represents the gradient dC/dy. The condition of electrical neutrality requires the C_+ be equal to the sum of C_- and C_-'. This is introduced and the equation integrated to obtain:

$$C_+ \sqrt{\left\{ \lambda_- + (\lambda_-' - \lambda_-) \frac{C_-'}{C_+} \right\}} = \text{constant} \quad (29)$$

The constant is evaluated in terms of the concentrations at the two boundaries. The equation for N', similar to equation (28), is written and C_- eliminated to give:

$$N_-' = - D_-' \left[\frac{2\lambda_-}{\lambda_-' - \lambda_-} \right] \frac{dC_+}{dy} \quad (30)$$

where: $$D_-' = \frac{RT \lambda_-'}{F_a^2} \quad (31)$$

Integration and substitution of limits leads to equation (15). This is identical with the result obtained by SHERWOOD and WEI.

NOTATION

a = exponent in equation (26)
b = moles of B reacting with one mole of A
C = concentration   g mole/cm^3
C_{A0}, C_{B0} = concentration of reacting solutes A or B in bulk fluid stream   g mole/cm^3
C_{Aw} = concentration of diffusing solute A at phase boundary   g mole/cm^3
C_0 = concentration in bulk stream   g mole/cm^3
C_+, C_- = concentration of cation, anion   g equiv/cm^3
D_A, D_B = molecular diffusion coefficients of species A, B cm^2/sec
F_a = Faraday,   96,500 C/g equiv.
f = friction factor   dimensionless
G = concentration gradient dC/dy
g_c = mass-force conversion factor = unity in c.g.s. system
$j_D = N_{St} N_{Sc}^{2/3}$ (for mass transfer)
$j_H = N_{St} N_{Pr}^{2/3}$ (for heat transfer)
k_A = mass transfer coefficient, = N_w / C_{Aw} cm/sec
$k_A°$, $k_B°$ = mass transfer coefficient of species A or B for transfer without chemical reaction
k_{ai} = initial (zero time) mass transfer coefficient in batch test   cm/sec
N = mass transfer flux   g mole/(sec)(cm^2)
n = empirical constant in equation (2)
N_{Pr} = Prandtl number
N_{Re} = Reynolds number $2R_w u_w / \nu$
N_{Sc} = Schmidt number ν / D
N_{St} = Stanton number $k°/u_w$
N_w = mass transfer flux at wall   g mole/(sec)(cm^2)
N_+, N_- = ion flux   g equiv/(sec)(cm^2)
$Q = \sqrt{\tau_w g_c / \rho} = u_0 \sqrt{(f/2)}$, or $u_w \sqrt{(f/2)}$
r = radial distance from axis   cm
R = gas constant   8·314 J/(°K)(g mole)
R_c = radius of container   cm
R_w = radius of cylinder   cm
T = temperature   °K
u = time – mean velocity   cm/sec
u^+ = dimensionless velocity u/Q
u_0^+ = value of u^+ corresponding to bulk stream velocity
u_0 = average velocity of main stream, (relative to wall)   cm/sec

u_t = fluctuating velocity, tangential   cm²/sec
u_w = peripheral speed of cylinder surface   cm/sec
v_r = fluctuating velocity, radial   cm/sec
x_L = film thickness   cm
y = distance from wall or phase boundary   cm
y^+ = dimensionless distance from wall yQ/ν
y^{++} = dimensionless distance defined by equation (12)
y_0^+ = value of y^+ corresponding to bulk stream concentration
y_R^+ = value of y^+ at reaction zone
γ = rate of change of k_A with C_{B0} during batch test

ϵ = eddy conductivity   cm²/sec
λ_-, λ_-' = limiting (zero concentration) ionic conductances of anions (A) (cm²/)(V) (g equiv.)
λ_+ = limiting ionic conductance of cation (A) (cm²)/(V) (g equiv.)
μ = viscosity   g/(sec) (cm)
ρ = density   g/cm³
σ = Schmidt number, N_{Sc}; or Prandtl number, N_{Pr}
τ = shear stress at radius r dyn/cm²
τ_w = shear stress at wall   dyn/cm²
ν = kinematic viscosity, $= \mu/\rho$ cm²/sec
$\phi(y^+, \sigma)$ = integral defined by equaton (3)

REFERENCES

[1] SEIDELL A. *Solubilities of Inorganic and Metal Organic Compounds* (3rd Ed. Van Nostrand, New York 1940.
[2] CHANG S. Y. S. M. Thesis in Chemical Engineering. Massachusetts Institute of Technology 1949.
[3] KING C. V. and BRODIE S. S. *J. Amer. Chem. Soc.* 1937 **59** 1375.
[4] BENNETT J. A. R. and LEWIS J. B. Report A.E.R.E. CE/R 1998. United Kingdom Atomic Energy Authority, 1957
[5] EISENBERG M., TOBIAS C. W. and WILKE C. R. *Chem. Engng. Progr.* 1955 **51** Symposium Series No. 16, p. 1.
[6] SHERWOOD T. K. Paper presented at the Philadelphia meeting. *Amer. Inst. Chem. Engrs.* June 24 1958.
[7] VON KARMAN T. *Trans. Amer. Soc. Mech. Engrs.* 1939 **61** 705.
[8] SHERWOOD T. K. *Trans. Amer. Inst. Chem. Engrs.* 1940 **36** 817.
[9] KAYS W. M. and BJORKLUND I. S. *Trans. Amer. Soc. Mech. Engrs.* 1958 **80** 70.
[10] DEISSLER R. G. NACA Report 1210, 1955.
[11] LIN C. S., MOULTON R. W. and PUTNAM G. L. *Industr. Engng. Chem.* 1953 **45** 636.
[12] GOLDSTEIN S. (Editor) *Modern Developments in Fluid Mechanics.* Vol. 2 p. 385. Oxford University Press 1938.
[13] PAI SHIH-I. NACA Technical Note 892 1943.
[14] TAYLOR G. I. *Phil. Trans. Roy. Soc.* 1923 **A 223** 289.
[15] TOWNSEND A. A. *The Structure of Turbulent Shear Flow.* Cambridge University Press 1956.
[16] TAYLOR G. I. *Proc. Roy. Soc.* 1935 **A 151** 494 ; *Ibid.* 1936 **A 157** 546.
[17] WENDT F. *Ingen.-Arch.* 1933 **4** 577.
[18] RYAN J. M. Sc.D. Thesis in Chemical Engineering. Massachusetts Institute of Technology 1958.
[19] THEODORSEN T. and REGIER A. NACA Technical Report 793 1944.
[20] CORCORAN W. H. and SAGE B. H. *Amer. Inst. Chem. Engrs. J.* **2**. 1956 **2** 251.
[21] SCHLICTING H. *Boundary Layer Theory* (Translated by J. Kerstin). McGraw-Hill, New York 1955.
[21] COTTER J. E. and SCHMIDT G. L. S.B. Thesis in Chemical Engineering. Massachusetts Institute of Technology 1956.
[23] DROPKIN D. and CARMI A. *Trans. Amer. Soc. Mech. Engrs.* 1957 **79** 741.
[24] SEBAN R. A. and JOHNSON H. A. NACA Contract No. NAW 6502. Institute of Engineering Research, University of California 1958.
[25] HATTA S. *Technical Reports. Tohôku Imp. Univ.* 1928 – 29 **8** 1 ; PIGFORD R. L. in *Absorption and Extraction* by SHERWOOD T. K. and PIGFORD R. L. pp. 320. McGraw-Hill, New York 1952.
[26] SHERWOOD T. K. and WEI J. C. *Amer. Inst. Chem. Engrs. J.* 1955 **1** 522.
[27] DANCKWERTS P. V. *Trans. Faraday Soc.* 1950 **46** 300, 701 ; *Industr. Engng. Chem.* 1951 **43** 1460.
[28] HOFTYZER P. J. and VAN KREVELEN D. W. *Trans. Inst. Chem. Engrs.* 1954 **32** Supplement No. 1 560.
[29] PERRY R. H. and PIGFORD R. L. *Industr. Engng. Chem.* 1953 **45** 1247.
[30] PIGFORD R. L. in *Absorption and Extraction* by SHERWOOD T. K. and PIGFORD R. L. p. 332. McGraw-Hill 1952.
[31] VIVIAN J. E. and PEACEMAN D. W. *Amer. Inst. Chem. Engrs. J.* 1956 **2** 437.
[32] DANCKWERTS P. V. and KENNEDY A. M. *Trans. Inst. Chem. Engrs.* 1954 **32** Supplement No. 1 p. 549.
[33] RANNIE W. D. *J. Aero. Sci.* 1956 **23** 485.

Sinkversuche mit isometrischen Teilchen in Flüssigkeiten

K. C. R. Chowdhury und W. Fritz

Institut für Chemische Technik der Technischen Hochschule, Karlsruhe, Germany

Zusammenfassung—Es wird die Abhängigkeit der Sinkgeschwindigkeit isometrischer (regulärer) Teilchen von deren Form untersucht. Für den Stokesschen (0 < Re < 0, 2) und den Newtonschen Strömungsbereich (Re > 1000) werden mit Hilfe des von Wadell eingeführten Kugelwertes der isometrischen Teilchen formelmässige Zusammenhänge zwischen der Sinkgeschwindigkeit und der Teilchenform aufgestellt.

Abstract—The relationship between the settling velocity of isometric (regular) particles and their shape is investigated. A mathematical equation, embracing the regions of Stoke (0 < Re < 0,2) and Newtonian (Re > 1000) types of flow, between the above qualities is put forward in terms of sphericity as defined by Wadell.

Résumé—Les auteurs ont étudié la relation entre la vitesse de sédimentation des particules isométriques (régulières) et leur forme. Dans les domaines d'écoulement de Stokes (0 < Re < 0,2) et de Newton (Re > 1000) on a établi sous forme de formules les relations entre la vitesse de sédimentation et la forme des particules à l'aide de la constante introduite pour des sphères par Wadell.

1 Einleitung

Bei den mechanischen Trennverfahren kann man zwei Prinzipien unterscheiden [1]:

1. das Absetzprinzip
2. das Siebprinzip.

Die praktische Anwendung der Absetzverfahren, bei denen sich feste Teilchen in einer Flüssigkeit bewegen, ist vielfach der Erforschung der theoretischen Grundlagen vorausgeeilt. Die vorliegende Arbeit soll daher zur Klärung der theoretischen Zusammenhänge beitragen.

Bewegt sich ein Teilchen in einer Flüssigkeit, so erfährt es einen Widerstand, d.h. auf das Teilchen wird eine Kraft ausgeübt, die entgegengesetzt der Bewegungsrichtung an ihm angreift. Die Bestimmung der Widerstände von Körpern, die sich in Flüssigkeiten bewegen, und die Ableitung von Formeln für die Sinkgeschwindigkeiten dieser Körper in Flüssigkeiten beschäftigte die Forschung seit langer Zeit. Zunächst wurden Beziehungen zur Berechnung der Widerstände, die bewegte Kugeln in einer Flüssigkeit erfahren, gefunden. In der Technik hat man es jedoch meist mit unregelmässig geformten Körpern zu tun, so dass die abgeleiteten Formeln nur angenäherte Gültigkeit haben.

Während sich eine frühere Arbeit von Ludwig [2] mit der Sinkgeschwindigkeit von Scheiben und Zylindern beschäftigte, untersucht die vorliegende Arbeit für isometrische (reguläre) Teilchen, wie Würfel, Oktaeder und Tetraeder, den Zusammenhang zwischen dem Widerstand, den ein solches Teilchen in einer Flüssigkeit erfährt, bzw. dessen Sinkgeschwindigkeit und der Teilchenform.

1.1 Mathematische Grundlagen

Der Widerstand W, den ein in einer Flüssigkeit bewegtes Teilchen erfährt, wird allgemein folgendermassen formuliert [3, 4]:

$$W = \psi \, F \, \rho_F \frac{v^2}{2} \tag{1}$$

Nach der Abhängigkeit des Widerstandskoeffizienten ψ von der Reynoldsschen Zahl Re unterscheidet man drei Bereiche:

(a) Stokesscher Bereich (0 < Re < 0, 2). In diesem Bereich gilt $\psi = 24/\text{Re}$. Die Stokessche

Formel für den Widerstand von Kugeln ($F = d^2\pi/4$ $Re = v_K d/\nu = v_K d\rho_F/\eta$) erhält man durch Einsetzen dieser Werte in Gleichung (1):

$$W = 3\pi\eta \, dv_K \qquad (2)$$

(b) Allenscher Bereich ($30 < Re < 300$). Hier ist $\psi = 10/\sqrt{Re}$, so dass die Allensche Formel für den Widerstand von Kugeln lautet

$$W = \frac{5\,\pi}{4\sqrt{Re}} \, d^2 \rho_F v_K^2 \qquad (3)$$

(c) Newtonscher Bereich ($Re > 1000$). In diesem Bereich ist ψ unabhängig von Re, d.h. $\psi = \text{const.} = C_W$. Damit ergibt sich die Newtonsche Formel für den Widerstand von Kugeln

$$W = C_W \frac{d^2\,\pi}{4} \rho_F \frac{v_K^2}{2} \qquad (4)$$

Die Gebiete zwischen diesen Bereichen werden von keiner Formel exakt erfasst, so dass man auf graphische Darstellungen angewiesen ist. Aus der dynamischen Grundgleichung Kraft = Masse $\times$ Beschleunigung folgt für das Sinken eines Teilchens in einer Flüssigkeit (A = Auftrieb, S = Schwerkraft, W = Widerstand)

$$m\frac{dv}{dt} = S\text{-}A\text{-}W \qquad (5)$$

Hat das Teilchen seine maximale Sinkgeschwindigkeit erreicht, so ist $dv/dt = 0$, d.h.

$$W = S\text{-}A \qquad (6)$$

Durch Einsetzen der Werte für eine Kugel folgt daraus für deren Sinkgeschwindigkeit allgemein

$$v_K^2 = \frac{4g}{3\,\psi} \frac{\rho_T - \rho_F}{\rho_F} d \qquad (7)$$

Somit ergibt sich für die Sinkgeschwindigkeit v_K einer Kugel

(a) im Stokesschen Bereich mit $\psi = 24/Re$

$$v_K = \frac{d^2}{18\eta} (\rho_T - \rho_F) g \qquad (8)$$

(b) im Allenschen Bereich mit $\psi = 10/\sqrt{Re}$

$$v_K = \sqrt[3]{\left[\frac{4g^2}{225\eta} \frac{(\rho_T - \rho_F)^2}{\rho_F}\right] d} \qquad (9)$$

(c) im Newtonschen Bereich mit $\psi = \text{const.}$ $= C_W$

$$v_K = \sqrt{\left(\frac{4g}{3\,C_W} \frac{\rho_T - \rho_F}{\rho_F} d\right)} \qquad (10)$$

bzw. mit

$$K_N = \sqrt{\left(\frac{4}{3\,C_W}\right)} \qquad (11)$$

$$v_K = K_N \sqrt{\left(g \frac{\rho_T - \rho_F}{\rho_F} d\right)} \qquad (12)$$

1.2 Einfluss des Wandeffektes auf den Widerstand und die Sinkgeschwindigkeit

Die Stokessche Formel (Gleichung 2) für den Widerstand, den eine bewegte Kugel in einer Flüssigkeit erfährt, setzt voraus, dass im Gültigkeitsbereich dieser Formel ($0 < Re < 0,2$) das Flüssigkeitsvolumen unendlich ausgedehnt ist. Bei endlichen Gefässdimensionen muss zur Eliminierung des Einflusses der Gefässwände auf den Widerstand die Stokessche Widerstandsformel ergänzt werden. Von den zahlreichen vorgeschlagenen Korrekturfaktoren zur Berücksichtigung des Wandeffektes wurde hier der von LADENBURG [5] verwendet. Danach beträgt der Widerstand einer Kugel vom Durchmesser d, die längs der Achse eines Zylinders mit dem Durchmesser D fällt:

$$W = 3\pi\eta dv_K (1 + 2,4 \, d/D) \qquad (13)$$

1.3 Definition der Teilchengrösse und Charakterisierung der Teilchenform

Die Definition der Teilchengrösse ist bei Teilchen, die von der Kugelform abweichen, nicht einheitlich. So herrscht in der Literatur einige Verwirrung bezüglich dieser Definition und es besteht eine Vielfalt von Begriffen.

In dieser Arbeit wird zur Festlegung der Teilchengrösse nur der von WADELL [6] vorgeschlagene " wahre Nenndurchmesser " d_K verwendet. Der " wahre Nenndurchmesser " d_K ist definiert als der Durchmesser einer Kugel, die bei gleicher Dichte dasselbe Volumen hat wie das betrachtete, nicht kugelförmige Teilchen.

Zur Charakterisierung der Teilchenform wird hier der ebenfalls von WADELL [7] eingeführte " Kugelwert " K_W benutzt; dieser ist definiert als das Verhältnis der Oberfläche O_K einer Kugel zu der Oberfläche O_{NK} eines nicht kugelförmigen

Teilchens, wobei Kugel und nicht kugelförmiges Teilchen dasselbe Volumen, also denselben wahren Nenndurchmesser d_K haben (Abb. 1a):

$$K_W = \frac{O_K}{O_{NK}} \qquad (14)$$

(a)

Würfel
Volumen V_{NK}
Oberfläche O_{NK}

Kugel
Volumen $V_K = V_{NK}$
Oberfläche O_K
Durchmesser $d = d_K$

$$K_W = \frac{O_K}{O_{NK}}$$

(b)

Würfel
Volumen V_{NK}
einbeschriebene Kugel
Durchmesser d

Kugel
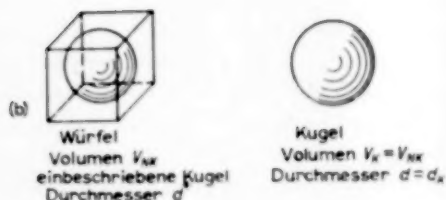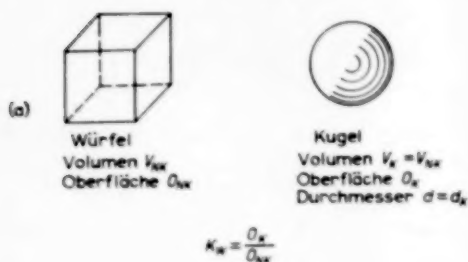Volumen $V_K = V_{NK}$
Durchmesser $d = d_K$

ABB. 1. Definition des Kugelwertes K_W am Beispiel des Würfels
(a) allgemeine Definition
(b) Definition für isometrische Teilchen.

Für isometrische Teilchen lässt sich noch eine andere Formulierung des Kugelwertes K_W angeben. Für solche Teilchen gilt allgemein [8]:

$$\frac{O}{V} = \frac{6}{d^*} \qquad (15)$$

($d^* =$ Durchmesser der dem isometrischen Teilchen einbeschriebenen Kugel).

Daraus folgt:

$$\frac{O_K}{V_K} = \frac{6}{d_K} \quad \text{(für Kugel)},$$

$$\frac{O_{NK}}{V_{NK}} = \frac{6}{d^*} \quad \text{(für isometrische Teilchen)} \qquad (16)$$

Nach der Definition des Kugelwertes muss $V_K = V_{NK}$ sein, d.h.

$$O_K \, d_K = O_{NK} \, d^* \qquad (17)$$

Aus Gleichung (17) ergibt sich mit Gleichung (14) für den Kugelwert isometrischer Teilchen

$$K_W = \frac{d^*}{d_K} \qquad (18)$$

Der Kugelwert isometrischer Teilchen lässt sich also ausdrücken durch das Verhältnis des Durchmessers d^* der dem Teilchen einbeschriebenen Kugel zum Durchmesser d_K der dem Teilchen volumengleichen Kugel (Abb. 1b).

2 EXPERIMENTELLER TEIL

2.1 *Versuchsanordnung*

Die Versuchsanordnung (Abb. 2) besteht aus einem Glaszylinder a mit einem inneren Durchmesser $D = 76$ mm und einer Länge von 1150 mm; dieser Glaszylinder dient als Raum für die Sinkversuche. Er kann auch gegen einen
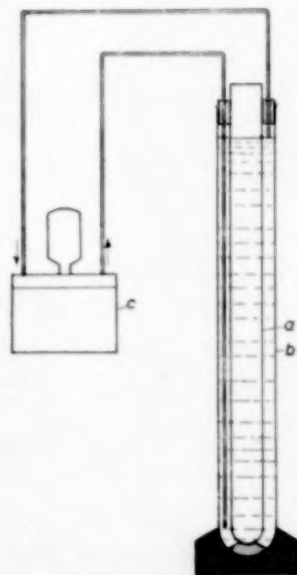
ABB. 2. Schema der Versuchsanordnung.

Glaszylinder mit einem inneren Durchmesser $D = 42,5$ mm und einer Länge von 1150 mm ausgewechselt werden. Glaszylinder (a) befindet sich auf einer Korkunterlage in einem zweiten Glaszylinder (b) mit einem inneren Durchmesser $D = 100$ mm und einer Länge von 1150 mm. Ein Korkring verschliesst den Zylinder (b) und

dient gleichzeitig als Halterung für (a). Der Ring-raum, der durch die beiden Zylinder gebildet wird, wird von Wasser durchflossen, dessen Temperatur durch den Thermostaten (c) auf $\pm 0,1\,°C$ konstant gehalten wird. Die Sinkstrecke im Glaszylinder (a) ist durch zwei Marken festgelegt, die $(500 \pm 0,5)$ mm voneinander entfernt sind. Die obere Marke befindet sich 450 mm unterhalb des Flüssigkeitsspiegels, während die untere Marke 150 mm vom Boden entfernt ist, um einen Einfluss des Bodens auf die Sinkgeschwindigkeit auszuschalten.

2.2 Versuchsteilchen und Versuchsflüssigkeiten

Bei den Sinkversuchen wurden Tetraeder, Würfel und Oktaeder aus Kunststoff ($\rho_T = 1,213$ bis $1,314\,g/cm^3$) sowie Kugeln aus Glas ($\rho_T = 2,930\,g/cm^3$) und Stahl ($\rho_T = 7,760\,g/cm^3$) in Abmessungen von $0,95$ bis 45 mm verwendet. Es wurden die Sinkgeschwindigkeiten einzelner Teilchen gemessen. Teilchen, an denen Luft-

bläschen hafteten und solche, die entlang der Wandung des Glaszylinders sanken, wurden bei der Auswertung nicht berücksichtigt. Als Versuchsflüssigkeiten dienten destilliertes Wasser, wässrige Calciumchlorid-, Zucker- und Glyzerin-lösung, ferner Mineralöl. Die Viskositäten dieser Flüssigkeiten konnten noch durch Änderung der Temperatur variiert werden; der Viskositäts-bereich erstreckte sich so von $\eta = 6,4 \times 10^{-3}$ bis $7,48\,g/cm$ sec. Die Dichten der Flüssigkeiten lagen zwischen $\rho_F = 0,9037$ und $1,314\,g/cm^3$.

3 Versuchsergebnisse

Aus den gemessenen Sinkgeschwindigkeiten — im Stokesschen Bereich ($0 < Re < 0,2$) wurden diese zur Berücksichtigung des Wandeffektes nach der Ladenburgschen Formel korrigiert (siehe Abschnitt 1.2) — lässt sich mittels Gleichung (7) durch Einsetzen des wahren Nenndurchmessers d_K an Stelle von d der Widerstandskoeffizient ψ_K berechnen, wobei der Index K ausdrücken soll,
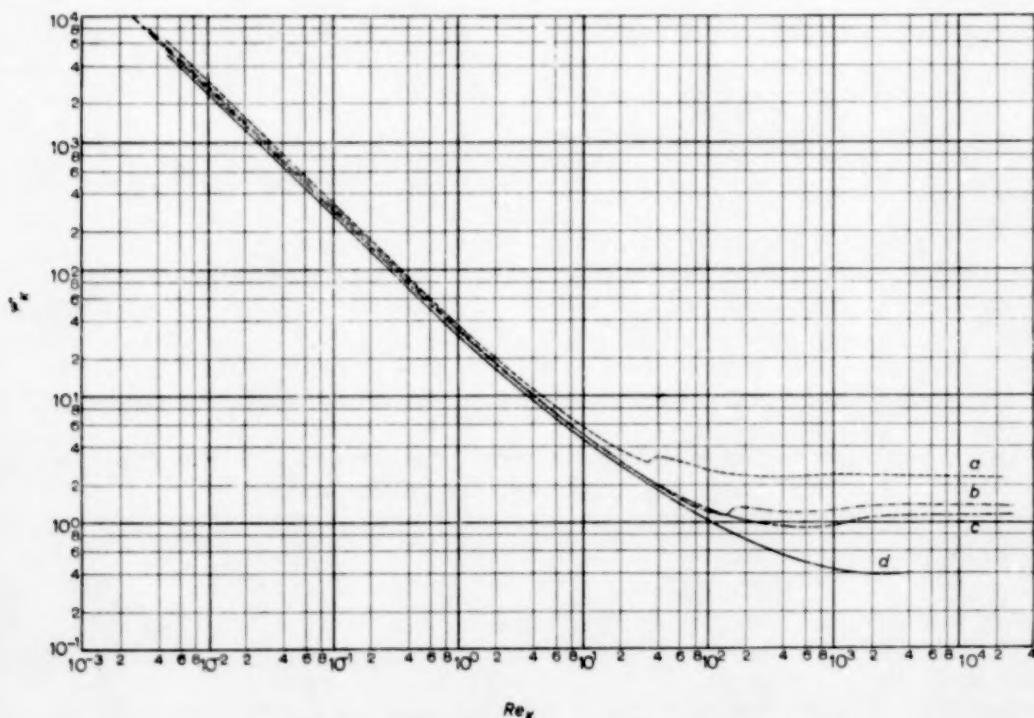

Abb. 3. Widerstandskoeffizient ψ_k als Funktion der Reynoldsschen Zahl Re_k (a = Tetraeder, b = Würfel, c = Oktaeder, d = Kugel).

dass der Berechnung der wahre Nenndurchmesser d_K zugrunde gelegt wurde. Auch die entsprechenden Reynoldsschen Zahlen Re_K wurden mit Hilfe des wahren Nenndurchmessers d_K berechnet.

Für den Bereich Reynoldsscher Zahlen von etwa 0,003 bis 20,000 sind die Widerstandskoeffizienten ψ_K als Funktion von Re_K im doppeltlogarithmischen Netz in Abb. 3 dargestellt. Die Kurven $\psi_K = f(Re_K)$ für Tetraeder (a, Kugelwert $K_W = 0,670$), Würfel (b, Kugelwert $K_W = 0,806$), Oktaeder (c, Kugelwert $K_W = 0,846$) und Kugeln (d, Kugelwert $K_W = 1$) liegen mit abnehmendem Kugelwert übereinander, d.h. je höher der Kugelwert ist, desto niedriger liegen die Kurven, desto niedriger ist auch der Widerstandskoeffizient ψ_K. Lediglich im Bereich von etwa $Re_K = 20$ bis $Re_K = 140$ liegt die Kurve für Oktaeder (c) über der für Würfel (b), obwohl Oktaeder einen höheren Kugelwert haben.

3.1 Berechnung der Sinkgeschwindigkeiten nicht kugelförmiger Teilchen im Stokesschen Bereich $(0 < Re < 0,2)$

Die Stokessche Formel zur Berechnung der Sinkgeschwindigkeit, Gleichung (8), gilt nur für kugelförmige Teilchen. Um auch die Sinkgeschwindigkeit nicht kugelförmiger Teilchen nach dieser Gleichung berechnen zu können, führen wir einen Formkorrekturfaktor ein durch die Beziehung

$$v_{NK} = K v_K \qquad (19)$$

Darin ist v_{NK} die Sinkgeschwindigkeit eines nicht kugelförmigen Teilchens, dessen wahrer Nenndurchmesser d_K gleich dem Durchmesser d einer volumengleichen Kugel ist, die unter denselben Bedingungen mit der Geschwindigkeit v_K sinkt. Aus Gleichung (19) erhält man durch Einsetzen von Gleichung (8) und mit $d = d_K$ nach einfacher Umformung für den Formkorrekturfaktor

$$K = \frac{18 \, \eta \, v_{NK}}{d_K^2 \, g \, (\rho_T - \rho_F)} \qquad (20)$$

Mittels Gleichung (20) lassen sich die Formkorrekturfaktoren aus den experimentell ermittelten Sinkgeschwindigkeiten berechnen. Zur Eliminierung des Wandeffektes, der vom Verhältnis d_K/D abhängt (siehe Abschnitt 1.2), wurden die nach Gleichung (20) berechneten Formkorrekturfaktoren jeweils für eine bestimmte Teilchenform graphisch über d_K aufgetragen. Die Formkorrekturfaktoren sind von d_K linear abhängig, d.h. $K = a d_K + b$. Die Konstanten a und b der Geradengleichung wurden nach der Methode der Summe der kleinsten Fehlerquadrate von GAUSS [9] bestimmt. Für $d_K = 0$ erhält man den reinen Formkorrekturfaktor (= Ordinatenabschnitt b). Die Extrapolation auf den wahren Nenndurchmesser $d_K = 0$ ist gleichbedeutend mit der Voraussetzung des Stokesschen Gesetzes eines unendlich ausgedehnten Flüssigkeitsvolumens.

Zum Vergleich wurden die Sinkversuche sowohl in einem Glaszylinder mit 42, 5 mm Innendurchmesser als auch in einem solchen mit einem Innendurchmesser von 76, 0 mm durchgeführt. Die aus den Messergebnissen beider Versuchsreihen ermittelten Formkorrekturfaktoren zeigten gute Übereinstimmung (Tabelle 1).

Zwischen dem Kugelwert K_W und dem Korrekturfaktor K besteht eine einfache mathematische Beziehung. Wird der Logarithmus des Kugelwertes als Funktion des Formkorrekturfaktors

Tabelle 1. *Formkorrekturfaktoren* K *für Tetraeder, Würfel, Oktaeder und Kugeln* (D = *Innendurchmesser des Versuchszylinders*, K$_W$ = *Kugelwert*)

Versuchsreihe	Tetraeder $K_W = 0,670$	Würfel $K_W = 0,806$	Oktaeder $K_W = 0,846$	Kugel $K_W = 1$
1 ($D = 42,5$ mm)	0,85	0,91	0,94	1
2 ($D = 76,0$ mm)	0,85	0,93	0,94	1
Mittelwerte	0,85	0,92	0,94	1

aufgetragen, so ergibt sich eine Gerade, d.h. $\log K_W = aK + b$ (Abb. 4). Die Konstanten errechnen sich aus den Daten der Tabelle 1:
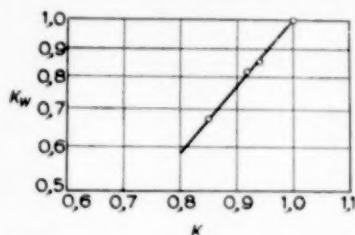

ABB. 4. Zusammenhang zwischen Kugelwert K_W und Formkorrekturfaktor K.

$a = 1,159$, $b = -1,159$. Damit wird $\log K_W = 1,159 K - 1,159$, woraus durch Umformung folgt:

$$K = 1 + 0,862 \times \log K_W \qquad (21)$$

Nach dieser Gleichung, die für Tetraeder, Würfel, Oktaeder und Kugeln mit einer Genauigkeit von $\pm 1\%$ erfüllt ist, lassen sich aus den Kugelwerten die Formkorrekturfaktoren und damit die Sinkgeschwindigkeiten v_{NK} dieser Teilchen im Stokesschen Bierech berechnen nach der Gleichung

$$v_{NK} = \frac{K d_K^2}{18\,\eta} (\rho_T - \rho_F)\,g, \qquad (22)$$

die sich aus Gleichung (19) durch Einsetzen von Gleichung (8) mit $d = d_K$ ergibt.

3.2 Berechnung der Sinkgeschwindigkeiten nicht kugelförmiger Teilchen im Newtonschen Bereich ($Re > 1000$)

Die Konstante K_N der Newtonschen Formel für die Sinkgeschwindigkeit, Gleichung (12), kann unmittelbar aus den experimentell ermittelten Sinkgeschwindigkeiten berechnet werden, wenn in Gleichung (12) für $d = d_K$ und für v_K die Sinkgeschwindigkeit v_{NK} der nicht kugelförmigen Teilchen gesetzt wird. Es zeigte sich, dass für eine bestimmte Teilchenform K_N unabhängig vom wahren Nenndurchmesser d_K ist.

Die aus den Sinkgeschwindigkeiten berechneten Werte von K_N sind in Tabelle 2 aufgeführt und in Abb. 5 als Funktion des Kugelwertes K_W dargestellt.
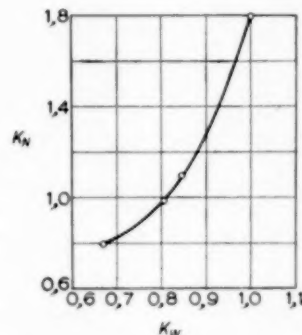
ABB. 5. Konstante K_N der Gleichung (12) als Funktion des Kugelwertes K_W.

Die Kurve der Abb. 5 hat in erster Näherung parabolischen Verlauf; sie kann als Parabel dritten Grades angesehen werden mit der allgemeinen Gleichung $y = a + bx + cx^2 + dx^3$. Die Berechnung der Konstanten dieser Gleichung aus den Werten der Tabelle 2 ergibt für K_N:

$$K_N = 2,22 - 3,04\,K_W - 1,11\,K_W^2 + 3,71\,K_W^3 \quad (23)$$

Mit Hilfe dieser Beziehung, die für Tetraeder, Würfel, Oktaeder und Kugeln mit einer Genauigkeit von $\pm 1\%$ erfüllt ist, lassen sich aus den Kugelwerten K_W die Konstanten K_N für diese Teilchen berechnen. Deren Sinkgeschwindigkeit ergibt sich aus folgender Gleichung

$$v_{NK} = K_N \sqrt{\left(g \frac{\rho_T - \rho_F}{\rho_F} d_K \right)} \qquad (24)$$

Tabelle 2. Konstante K_N der Gleichung (12) für Tetraeder, Würfel, Oktaeder und Kugel

Teilchenform	Tetraeder	Würfel	Oktaeder	Kugel
Kugelwert K_W	0,670	0,806	0,846	1
K_N	$0,79 \pm 0,01$	$0,98 \pm 0,01$	$1,09 \pm 0,01$	$1,79 \pm 0,01$

die aus Gleichung (12) durch Setzen von $v_K = v_{NK}$ und $d = d_K$ folgt. Im Bereich zwischen dem Stokesschen und dem Newtonschen Bereich lassen sich keine Beziehungen über den Zusammenhang von Sinkgeschwindigkeit und Teilchenform, die durch den Kugelwert charakterisiert ist, aufstellen.

Erklärung der Formelzeichen

(Die Formelzeichen bedeuten Grössen. Die bevorzugten Einheiten sind in Klammern angegeben)

C_W = Konstante der Newtonschen Widerstandformel

D = Durchmesser des Messrohres   cm

d = Durchmesser einer Kugel   cm

d^* = Durchmesser der einem isometrischen Teilchen einbeschriebenen Kugel   cm

d_K = wahrer Nenndurchmesser = Durchmesser einer Kugel, die bei gleicher Dichte dasselbe Volumen hat wie ein nicht kugelförmiges Teilchen   cm

F = angeströmte Querschnittfläche eines Teilchens cm^2

g = Erdbeschleunigung cm/sec^2

K = Formkorrekturfaktor

$K_N = \sqrt{(4/3\, C_W)}$

K_W = Kugelwert = $\dfrac{\text{Oberfläche einer Kugel}}{\text{Oberfläche eines Teilchens mit gleichem Volumen}}$

m = Masse eines Teilchens   g

O = Oberfläche eines Teilchens cm^2

Re = Reynoldssche Zahl

Re_K = Reynoldssche Zahl unter Zugrundelegung des wahren Nenndurchmessers d_K

t = Zeit   sec

V = Volumen eines Teilchens cm^3

v = Relativgeschwindigkeit zwischen Teilchen und Flüssigkeit   cm/sec

W = Widerstand $g\,cm/sec^2$

η = Dynamische Zähigkeit der Versuchsflüssigkeit   g/cm sec

ν = Kinematische Zähigkeit der Versuchsflüssigkeit cm^2/sec

ψ = Widerstandkoeffizient

ψ_K = Widerstandkoeffizient unter Zugrundelegung des wahren Nenndurchmessers d_K

ρ_F = Dichte der Versuchsflüssigkeit g/cm^3

ρ_T = Dichte eines Teilchens g/cm^3

Bei O, V und v gelten die Indizes

K = für kugelförmige Teilchen

NK = für nicht kugelförmige Teilchen, welche dasselbe Volumen und denselben wahren Nenndurchmesser d_K haben.

LITERATUR

[1] HENGLEIN F. A. *Grundriss der chemischen Technik* (9. Aufl.) Verlag Chemie, Weinheim 1955.

[2] LUDWIG J. *Chemikerztg.* 1955 **79** 774.

[3] *Handbuch der Experimentalphysik* (hrsgeg. von W. WIEN und F. HARMS) Bd IV, 2. Teil, S. 237. Akademische Verlagsgesellschaft, Leipzig 1932.

[4] *Der Chemie-Ingenieur* (hrsgeg. von A. EUCKEN und M. JAKOB) Bd I, 2. Teil, S. 116. Akademische Verlagsgesellschaft, Leipzig 1933.

[5] LADENBURG R. *Ann. Phys.* 1907 **23** 447.

[6] WADELL H. *J. Franklin Inst.* 1934 **217** 459.

[7] WADELL H. *J. Geol.* 1933 **41** 310.

[8] HENGLEIN F. A. *Grundriss der chemischen Technik* (9. Aufl.) S. 28. Verlag Chemie, Weinheim 1955.

[9] KÜSTER F. W. *Logarithmische Rechentafeln*, (56. bis 60. Aufl.) S. 208. Walter de Gruyter, Berlin 1947.

Vapour–liquid equilibria at reduced pressures : n-butanol–ethyl benzene ; aniline–p-cymene

S. R. M. Ellis* and M. Razavipour

Abstract—The increasing importance of vacuum distillation in the petroleum, chemical and allied industries has drawn attention to the need for accurate vapour–liquid equilibria results at reduced pressure.

Vapour–liquid equilibria results are presented for the azeotropic systems n-butanol ethyl–benzene, and p-cymene aniline at pressures from 50 to 760 mm Hg. A test is made for the thermodynamic consistency of the data, and the limitations of the correlating equations for isobaric conditions are discussed.

Résumé—L'importance croissante de la distillation sous vide dans l'industrie du pétrole, l'industrie chimique et autres industries connexés a àttiré l'attention sur le besoin de résultats précis des équilibres liquide–vapeur à pression réduite.

Les auteurs présentent les résultats des équilibres liquide–vapeur poru les systémes azéotropiques n-butanol – éthylbenzéne et p-isopropyloluéne – aniline pour des pressions de 50 à 760 mm Hg. Ils vérifient la consistance thermodynamique des données et discutent des limites des équations correspondantes pour des conditions isobares.

Zusammenfassung—Die steigende Bedeutung der Vakuumdestillation in den Erdöl-, chemischen und verwandten Industrien erfordert genaue Kenntnis der Dampfflüssiggleichgewichte bei kleinen Drucken.

Dampfflüssiggleichgewichte werden für die azeotropischen Systeme n-Butanol – Äthylbenzol und p-Cymolanilin bei Drücken von 50 bis 760 Torr mitgeteilt. Die thermodynamische Konsistenz der Daten wurde nachgeprüft und die Begrenzung der Beziehungsgleichungen für isobare Bedingungen diskutiert.

APPARATUS

THE still used was the recirculating type, previously described [1], and the pressures ranged from 100 to 760 mm Hg.

When the still was operated at 50 mm it was necessary to modify the heater unit for even boiling. The clearance between the inner and outer walls of the bayonet heater unit was reduced from 4 mm to 1 mm. The tube joining the top of the boiler to the Cottrel coil was reduced from 8 mm to 6 mm. These modifications had two main advantages ; firstly, the velocity of the liquid over the heating surface was increased, thus improving the rate of heat transfer ; secondly, when any " bumping " occurred, the volume of liquid forced from the boiler into the still was smaller, and had a comparatively small effect on the smooth running of the apparatus.

PRESSURE CONTROL

When the still was operated under vacuum the pressure was controlled by the control system shown on Fig. 1. The actual automatic controller uses a sintered disk glass and was similar to that suggested by M. L. Frederick [2]. The chambers D and B were two cylindrical glasses $3\frac{1}{2}$in. high and 1in. diameter, connected by a U-shape tube, H, $\frac{1}{4}$in. diameter. The chamber D could be closed off from the pump by the stopcock E while the stopcock C disconnected the still from the pump. The required pressure was obtained in chamber D by leaving open the stopcocks C and E until the manometer, M, indicated the required pressure and then stopcocks C and E were closed. The pressure in chamber D was the operating pressure of the still and an increase in pressure in the still resulted in a movement of mercury in the manostat

---

* Chemical Engineering Department, University of Birmingham, Edgbaston, Birmingham, 15
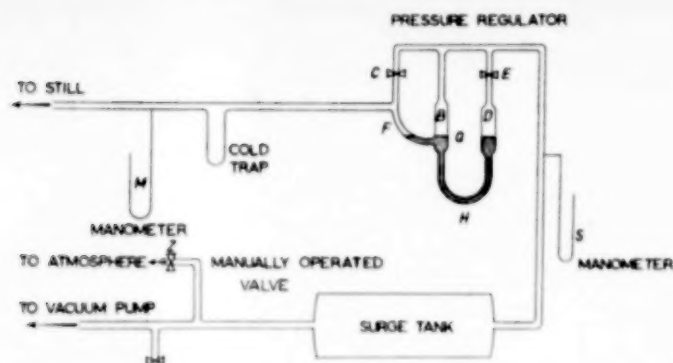
FIG. 1. Pressure control system.

tube so as to open the sealed disk, Q, between B and F. When the pressure in the chamber D was equal to that in the still, the mercury rose thus sealing the disk again.

At the end of the run, cocks C and E were opened in order to bleed air into the still, so that samples could be taken. An auxiliary manometer, S, which indicated the pressure of chamber B was installed to prevent disturbing the apparatus. Before opening the cocks, air was let through by opening the valve Z until the pressure in B became nearly equal to that in D, the cocks C and E were then both opened together. A further advantage in using the manometer S, was that the pressure in chamber D could be altered during the runs if required.

MATERIAL USED AND METHODS OF ANALYSIS

Analar grade ethylbenzene and n-butanol were purified in a 30 plate Oldershaw column at atmospheric pressure while aniline and p-cymene were purified by fractionation in the same apparatus at reduced pressure. The physical properties of the purified materials are tabulated in Table 1.

The vapour pressures of ethylbenzene and p-cymene were calculated using the Antoine equation reported by the National Bureau of Standards [6]. Data by STULL [7] were used for n-butanol; the log of the vapour pressure was plotted against the log of the vapour pressure of pure water at the same temperature. Equations were then derived from the resulting straight line plots. Vapour pressure results for aniline were taken from TIMMERMANS [3].

For the analysis of the binary mixtures the refractive index-composition plots at 20°C were determined for ethyl benzene–n-butanol and aniline–p-cymene mixtures. The results are presented in Table 2. An Abbé refractometer was used for refractive index measurements.

Table 1.

Materials	Refractive index at 20°C		Density 20/4		Boiling point °C.	
	Purified	Literature	Purified	Literature	Purified	Literature
Ethylbenzene	1·4958	1·4958 [3]	0·8671	0·8671 [3]	136·1	136·1 [3]
n-Butanol	1·3993	1·3993 [3]	0·8097	0·8097 [3]	117·7	117·7 [3]
Aniline	1·5862	1·5862 [3]	1·0219	1·0218 [3]	184·1	184·35 [3] [4]
p-cymene	1·4903	1·4908 [5]	0·8571	0·8573 [6]	177·7	177·2 [6]

Table 2

p-cymene–aniline		Ethyl benzene–p-cymene	
Mol. % p-cymene	R.I. at 20°C	Mol. % n-butanol	R.I. at 20°C
0·00	1·5862	0·00	1·4958
8·18	1·5725	9·55	1·4892
18·88	1·5585	10·48	1·4876
28·10	1·5470	19·75	1·4800
39·40	1·5350	27·85	1·4731
48·45	1·5270	40·15	1·4623
58·50	1·5178	49·75	1·4533
68·50	1·5097	59·90	1·4433
79·00	1·5023	69·85	1·4333
88·80	1·4959	79·90	1·4223
100·00	1·4903	89·90	1·4113
		100·00	1·3993

EXPERIMENTAL RESULTS

Vapour liquid equilibrium results for the system ethyl benzene–*n*-butanol for 760, 500, 300, 100 and 50 mm Hg are presented graphically on FIG. 2 while results for the system aniline–*p*-cymene are shown on FIG. 3. Typical experimental results are shown in Tables 3 – 6.

The equilibrium results for ethyl benzene–*n*-

butanol on FIG. 2 shows that a minimum boiling azeotrope exists at all pressures investigated, with the azeotrope composition becoming less rich in *n*-butanol as the pressure is reduced. It will also be noted that the concentration of butanol in the vapour decreases as the pressure is reduced.

Fig. 3 shows that there is a minimum boiling azeotrope in the system aniline–*p*-cymene. The concentration of *p*-cymene in the vapour increases as the pressure is increased.
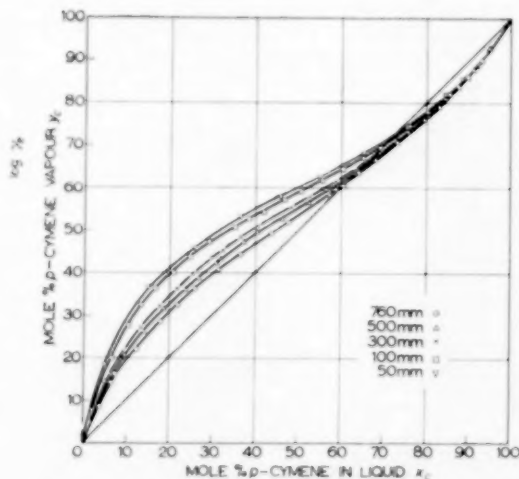
FIG. 3.   Vapour–liquid compositions for aniline–*p*-cymene.

FIG. 2.   Vapour–liquid compositions for *n*-butanol–ethylbenzene.

CORRELATION OF EQUILIBRIUM RESULTS

Activity coefficients were calculated by the equation

$$\gamma = \frac{\pi\, y}{P_0\, x}$$

where π = total pressure

P_0 = vapour pressure of pure component at boiling point.

y = mole fraction of component in the vapour phase.

x = mole fraction of component in the liquid phase.

Table 3.   Ethylbenzene (e)–n-butanol (b)

Run no.	Total pressure (mm)	Boiling point (°C)	Composition		Activity coefficients	
			Liquid x_b	Vapour y_b	log γ_b	log γ_e
1	760	117·20	96·95	95·55	0·0003	0·3973
2	760	116·75	92·70	90·00	0·0010	0·3757
3	760	116·20	88·10	84·95	0·0071	0·3482
4	760	115·85	83·10	80·55	0·0154	0·3112
5	760	115·85	78·35	76·90	0·0207	0·2783
6	760	115·85	72·85	72·85	0·0289	0·2502
7	760	115·80	66·80	70·05	0·0506	0·2068
8	760	116·05	61·90	66·80	0·0589	0·1882
9	760	116·35	57·35	64·70	0·0729	0·1619
10	760	116·65	52·70	62·10	0·0870	0·1437
11	760	116·95	47·65	60·00	0·1110	0·1182
12	760	117·50	42·90	57·95	0·1326	0·0966
13	760	118·15	37·10	55·00	0·1630	0·0737
14	760	119·05	31·70	51·90	0·1918	0·0577
15	760	120·30	25·70	48·05	0·2308	0·0381
16	760	121·80	19·75	43·35	0·2891	0·0232
17	760	123·90	14·90	38·30	0·3147	0·0086
18	760	126·80	9·80	29·05	0·3329	0·0072
19	760	129·75	5·60	20·25	0·3757	0·0028
20	760	131·45	4·15	15·80	0·3736	0·0003

Table 4.   Ethyl benzene (e)–n-butanol (b)

Run no.	Total pressure (mm)	Boiling point (°C)	Composition		Activity coefficients	
			Liquid x_b	Vapour y_b	log γ_b	log γ_e
1	100	67·95	96·00	90·05	0·0188	0·5042
2	100	67·35	93·25	84·40	0·0182	0·4825
3	100	66·35	89·85	79·00	0·0282	0·4527
4	100	65·85	85·40	73·90	0·0309	0·3946
5	100	65·00	80·40	68·00	0·0400	0·3736
6	100	64·55	75·30	63·85	0·0515	0·3351
7	100	64·20	70·10	60·35	0·0658	0·2989
8	100	64·00	63·65	56·50	0·0837	0·2581
9	100	63·65	59·10	54·50	0·1070	0·2324
10	100	63·80	54·10	52·15	0·1234	0·2012
11	99·7	63·60	48·50	49·95	0·1553	0·1730
12	100·3	63·80	42·70	47·75	0·1880	0·1448
13	100	63·70	36·80	45·95	0·2380	0·1166
14	100	64·35	32·60	43·60	0·2541	0·0954
15	100	64·45	28·05	41·90	0·2997	0·0803
16	100	64·25	22·80	39·25	0·3958	0·0718
17	100	65·40	17·70	30·35	0·4171	0·0429
18	99·85	65·85	12·90	32·15	0·4899	0·0332
19	100	67·80	6·40	23·60	0·6166	0·0245
20	100·6	69·90	4·00	16·65	0·6265	0·0147

Table 5.   p-cymene (c) – Aniline (a)

Run no.	Total pressure (mm)	Boiling point (°C)	Composition		Activity coefficients	
			Liquid x_c	Vvapour y_c	$\log \gamma_c$	$\log \gamma_a$
1	760	174·80	93·00	89·90	0·0112	0·2691
2	760	174·05	87·50	83·90	0·0163	0·2288
3	760	173·60	83·00	79·25	0·0193	0·2109
4	760	173·20	79·50	76·00	0·0242	0·1972
5	760	173·00	73·25	70·80	0·0316	0·1702
6	760	172·90	68·00	66·80	0·0400	0·1486
7	760	172·85	64·00	63·90	0·0476	0·1342
8	760	172·80	60·50	60·50	0·0486	0·1300
9	760	172·85	58·75	59·50	0·0538	0·1250
10	760	172·85	57·30	58·25	0·0554	0·1232
11	760	173·00	47·60	52·00	0·0844	0·0930
12	760	173·10	43·60	49·50	0·0945	0·0819
13	760	173·75	36·50	44·50	0·1230	0·0641
14	760	174·30	31·40	40·90	0·1465	0·0552
15	760	174·90	25·70	36·50	0·1774	0·0406
16	760	175·55	21·75	32·50	0·1919	0·0370
17	760	176·10	17·75	28·75	0·2217	0·0320
18	760	177·30	12·30	22·40	0·2694	0·0270
19	760	178·75	7·40	16·40	0·3297	0·0006
20	760	179·30	6·40	14·40	0·3300	0·0149
21	760	180·60	3·80	8·80	0·3340	0·0181

Table 6.   p-cymene (c) – Aniline (a)

| Run no.	Total pressure (mm)	Boiling point (°C)	Compositions		Activity coefficients	
			Liquid x_c	Vapour y_c	$\log \gamma_c$	$\log \gamma_a$
1	99·5	107·30	93·00	90·00	0·0135	0·3602
2	100·0	107·00	89·50	86·10	0·0172	0·3444
3	100·0	106·80	85·40	82·10	0·0198	0·3147
4	100·4	106·70	80·50	77·75	0·0256	0·2871
5	100·4	106·80	76·00	74·60	0·0306	0·2525
6	99·8	106·40	69·10	69·60	0·0452	0·2248
7	99·5	106·30	65·30	67·40	0·0566	0·2054
8	99·25	106·40	60·60	64·50	0·0668	0·1842
9	99·6	106·55	55·75	61·90	0·0847	0·1639
10	99·9	107·00	50·70	59·20	0·1009	0·1401
11	100·3	107·55	46·80	57·25	0·1143	0·1190
12	100	107·90	42·00	54·40	0·1234	0·1025
13	100	108·20	38·50	52·75	0·1519	0·0875
14	100·3	109·00	29·20	48·25	0·2212	0·0529
15	100·1	109·15	24·90	44·00	0·2516	0·0620
16	99·7	109·75	20·80	40·00	0·2732	0·0528
17	100	110·70	16·75	36·70	0·3167	0·0384
18	99·75	111·40	13·40	32·65	0·3507	0·0354
19	99·5	112·85	10·40	27·75	0·3676	0·0242
20	100·3	114·35	6·60	20·00	0·4047	0·0282
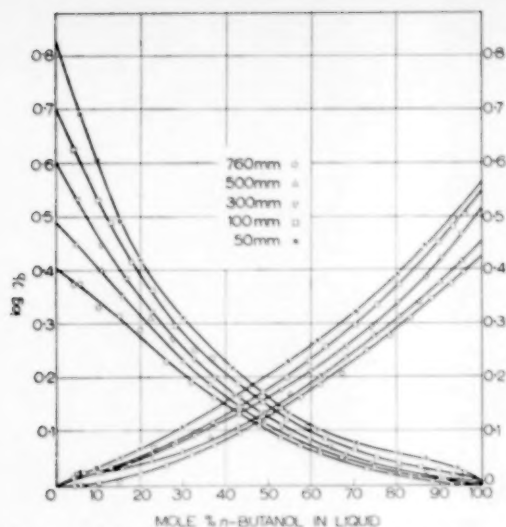
FIG. 4. Activity coefficient curves for n-butanol–ethyl-benzene.
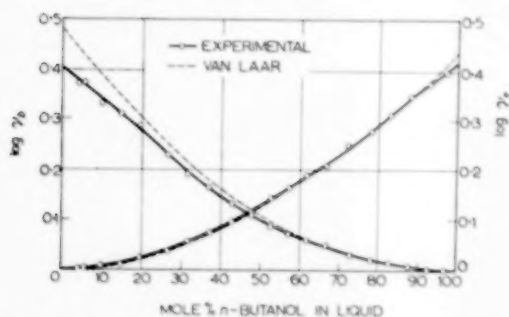
FIG. 5. Activity coefficient curves for n-butanol–ethyl-benzene at 760 mm Hg.
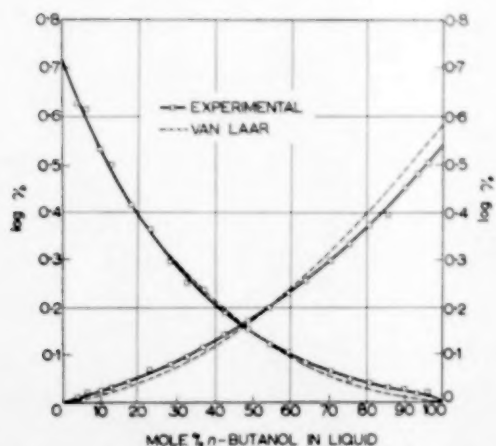
FIG. 6. Activity coefficient curves for n-butanol–ethyl-benzene at 100 mm Hg.
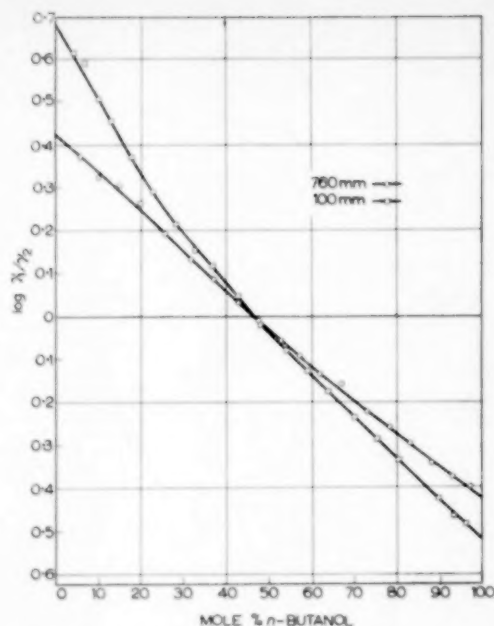
FIG. 7. REDLICH and KISTER plots for n-butanol–ethyl-benzene.

Ethylbenzene–n-butanol

Fig. 4 shows plots of log activity coefficient against concentration for different pressures. It can be seen that for a given concentration, the log of the activity coefficient is increased as the pressure is reduced. Figs. 5 and 6 show a comparison between experimental and van Laar plots for 760 and 100 mm pressure.

On Fig. 7 of the log of the ratio of the activity coefficients is plotted against composition for 760 mm and 100 mm pressure. Similar plots were made for other pressures. In Table 7 a comparison is made of the areas above and below the zero line.

Table 7.

Pressures	Area above the zero line	Area below the zero line	% Error
760	10·05	12·32	18·4
500	11·35	12·5	9·2
300	12·85	13·1	4·0
100	14·55	14·14	−3·0
50	15·40	14·4	−6·9

The percentage error in Table 7 is expressed as the decrease or increase in area below the zero line compared with that above the zero line.

p-*cymene–analine*

Log activity coefficient plots are shown on Fig. 8, and again it can be seen that the log of the activity coefficient increases as the pressure is reduced for a given composition. When a comparison is made between experimental and Van Laar plots the agreement is good.

Table 8.

Pressure (mm Hg.)	Area above the zero line	Area below the zero line	% error
760	9·48	9·52	0·4
500	10·16	10·09	0·69
300	11·22	11·08	0·79
100	13·11	13·00	0·85
50	11·5	11·30	1·75

Table 8 summarizes the area measurements above and below the zero line when for varying pressure the log ratio of the activity coefficients is plotted against composition. The deviations from

$$\int_{0}^{1\cdot0} \log \frac{\gamma_1}{\gamma_2}\, dx_1 = 0$$

are much less for *p*-cymene–aniline than for *n*-butanol–ethylbenzene.

DISCUSSION OF RESULTS

Comparing Tables 7 and 8 it can be seen that there is a greater deviation between the experimental and correlated REDLICH and KISTER [8] results for ethylbenzene–*n*-butanol than for aniline–*p*-cymene. This is mainly due to a significant difference in the boiling ranges of the two systems, although at 760 mm Hg they have the same order of non-ideality. At this pressure, the boiling-point difference for ethylbenzene–*n*-butanol is 15·65°C compared with 7·8°C for aniline–*p*-cymene.

It would therefore appear that as the derivation of the Redlich and Kister correlation is based on the isothermal-isobaric Gibbs–Duhem equation, the application of the Redlich and Kister method to isobaric systems is limited to low boiling ranges.

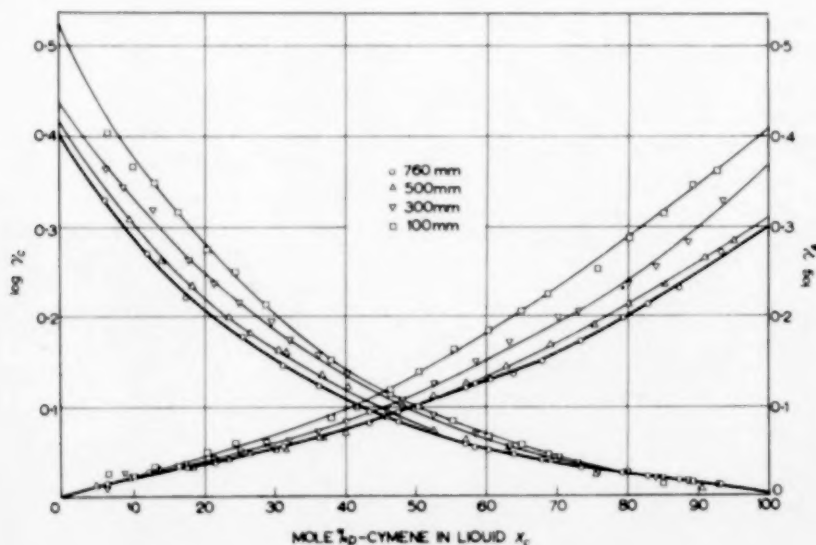HERINGTON [11] and THIJSSEN [12] have related

FIG. 8. Activity coefficient curves for aniline–*p*-cymene.

the variation of activity coefficient with temperature (at constant composition and pressure) to the heat of mixing, and introduced a correction factor into the Redlich and Kister equation for isobaric conditions.

$$\int_{x=0}^{x=1} \left[\ln \frac{\gamma_1}{\gamma_2} - \frac{H_E}{RT^2} \cdot \frac{dT}{dx_1} \right] dx_1 = 0 \qquad (1)$$

where,

H_E = integral heat of mixing for a mole of the mixture

$\dfrac{dT}{dx_1}$ = slope of the boiling-point curve

T = boiling-point of the mixture in °K.

The term $\left[\dfrac{H_E}{RT^2} \cdot \dfrac{dT}{dx} \right]$ is referred to by IBL and DODGE [9] as $\bar{B}$, "the temperature correction factor for isobaric experimental data."

In order to determine $\bar{B}$ values, heats of mixing were calculated by the method of OTHMER [10], $\left[\log \dfrac{\gamma_b}{\gamma_e} - B \right]$ vs. x_b was then plotted for the ethylbenzene–n-butanol system and it was found that at 760 mm Hg the percentage error was reduced from 18·4 per cent to − 6·4 per cent, while at 100 mm Hg it was slightly increased from − 3·0 per cent to − 4·1 per cent.

Since the calculated heats of mixing are not very accurate, as no information was available for the variation of the latent heat of vaporization with temperature, an attempt was made to use calorimetrically determined heats of mixing by BROWN and FOCK [13] for the system benzene-n-butanol at 45·00°C. The assumption was made that the heats of mixing for ethyl benzene-n-butanol are the same as the experimental values for benzene – n – butanol. Fig. 9 gives a plot of $\left[\log \dfrac{\gamma_b}{\gamma_e} - \bar{B} \right]$ vs. x_b for ethylbenzene–n-butanol with a percentage error of only − 0·9 per cent at 760 mm Hg. and − 5·0 per cent at 100 mm Hg. As the boiling range is only 6·3°C at 100 mm Hg the uncorrected Redlich and Kister equation should be applicable.
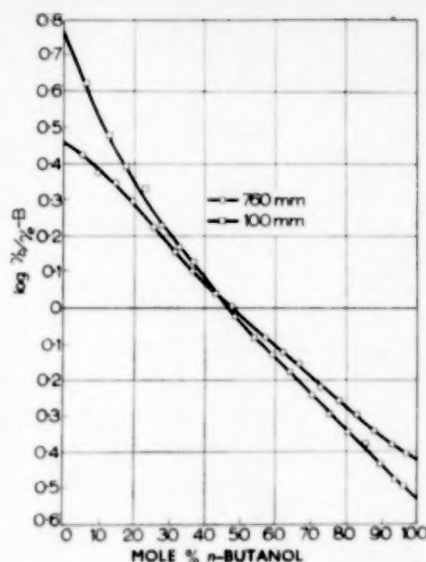

FIG. 9. Plot of equation (1) using experimental heats of mixing.

It would therefore appear that the limitation of low boiling ranges imposed when applying the Redlich and Kister equation to isobaric data, may be overcome to a large extent by the use of equation (1), provided that accurate heat of mixing data are available.

NOTATION

x = composition of the lighter component in liquid

y = composition of the lighter component in vapour

T = boiling point on °K.

Po_1 Po_2 = vapour pressure of pure components

H_E = integral heat of mixing (cal/mole)

R = gas constant

γ = activity coefficient

π = total pressure

Subscripts

1 = lighter component

2 = heavy component

a = aniline

c = p-cymene

b = n-butanol

e = ethyl benzene

REFERENCES

[1] ELLIS S. R. M. and FROOME D. A. *Chem. & Ind.* 1954 237.

[2] FREDERICK M. L. *Industr. Engng. Chem. (Anal.)* 1941 **13** 418.

[3] TIMMERMANS J. *Physical Chemical Consultants of Pure Organic Compounds.* Elsevier, New York 1950.

[4] *International Critical Tables.* Vol. 3 p. 221. McGraw Hill, New York 1927.

[5] *Faraday's Encyclopaedia of Hydrocarbon Compounds* Vol. 5. Chemindex, Manchester England, 1947 – 1954.

[6] *Selected Values of the Properties of Hydrocarbons.* Table No. 14 (a). National Bureau of Standards, American Petroleum Institute Research Project 44, The Carnegie Institute of Technology, April 1952.

[7] STULL D. R. *Industr. Engng. Chem.* 1947 **39** 517.

[8] REDLICH D. and KISTER A. T. *Industr. Engng. Chem.* 1948 **40** 345.

[9] IBL N. V. and DODGE B. F. *Chem. Engng. Sci.* 1953 **2**, 120.

[10] OTHMER D. F. and GILMONT R. *Industr. Engng. Chem.* 1944 **36** 858.

[11] HERINGTON E. F. G. *J. Inst. Petrol.* 1951 **37** 457.

[12] THIJSSEN M. A. *Chem. Engng. Sci.* 1955 **4**, 75.

[13] BROWN I. and FOCK W. *Aust. J. Chem.* 1957 **10** 419.

Tangential Newtonian flow in annuli—I

Unsteady state velocity profiles

R. B. BIRD

Department of Chemical Engineering, University of Wisconsin, Madison, Wisconsin

and

C. F. CURTISS

Department of Chemistry, University of Wisconsin, Madison, Wisconsin

Abstract—An exact solution of the equations of change is given for the unsteady state, laminar, tangential flow of an isothermal, incompressible viscous fluid in the annular space between two cylinders one or both of which may be rotating. The transient behaviour of the velocity profiles is set forth graphically. An approximate solution for short times is also given. These results may be of interest in connexion with problems in lubrication and viscometry.

Résumé—Les auteurs donnent une solution exacte des equations d'échange pour un écoulement tangentiel, laminaire non stationnaire et isotherme d'un fluide incompressible et visqueux dans l'espace annulaire compris entre deux cylindres dont un seul ou deux cylindres peuvent être rotatifs. Le comportement transitoire des profils de vitesse est présenté graphiquement. Une solution approximative est donnée pour des temps courts. Ces résultats peuvent être intéressants par leur rapport avec les problèmes de lubrification et de viscosimétrie.

Zusammenfassung—Für die Änderungsgleichung der nichtstationären laminaren Tangentialströmung einer isothermen inkompressiblen zähen Flüssigkeit in einem Ringspalt zwischen zwei Zylindern wird eine exakte Lösung angegeben und zwar unter der Annahme, dass der eine oder beide Zylinder rotieren. Das nichtstationäre Verhalten der Geschwindigkeitsprofile wird graphisch fortgesetzt. Eine Näherungzlösung für kurze Zeiten wird ebenfalls mitgeteilt. Die Ergebnisse sind für Probleme der Schmierung und Zähigkeitsmessung von Interesse.

1. THE FLOW EQUATIONS

THE equations of continuity and motion for the flow of a compressible, isothermal fluid are [1, 3]:

$$\partial \rho / \partial t + (\nabla \cdot \rho \mathbf{v}) = 0 \qquad (1)$$

$$\rho \left[\partial \mathbf{v} / \partial t + (\mathbf{v} \cdot \nabla) \mathbf{v} \right] = -\nabla p - (\nabla \cdot \boldsymbol{\tau}) + \rho \mathbf{g} \qquad (2)$$

in which ρ is the fluid density, $\mathbf{v}$ is the local velocity, p is the static pressure, $\mathbf{g}$ is the external body force per unit mass and t is the time. The stress tensor $\boldsymbol{\tau}$ is related to the velocity gradients for Newtonian flow thus [1, 3]:

$$\boldsymbol{\tau} = -\mu \left[\nabla \mathbf{v} + (\nabla \mathbf{v})\dagger \right] + \tfrac{2}{3} \mu (\nabla \cdot \mathbf{v}) \boldsymbol{\delta} \qquad (3)$$

in which μ is the coefficient of shear viscosity, $\boldsymbol{\delta}$ is the unit tensor, and $(\nabla \mathbf{v})\dagger$ is the transpose of $(\nabla \mathbf{v})$. Special cases of the above equations in cylindrical co-ordinates are used as the starting point in the following developments.

The assumption above of isothermal flow implies not only that there is no impressed temperature field, but that in addition the viscous dissipation term $(\boldsymbol{\tau} : \nabla \mathbf{v})$ in the energy balance equation is negligible.

2. EXACT EXPRESSION FOR THE VELOCITY DISTRIBUTION

A fluid is contained in the annular region between a pair of infinitely long co-axial cylinders with radii κR and R (see Fig. 1). At time $t < 0$ the fluid within the annulus is at rest. At $t > 0$ the inner and outer cylinders are rotated with constant angular velocities Ω_i and Ω_o respectively.

108

For an incompressible fluid in this situation $v_r = v_z = 0$ and v_θ is a function of r alone so that equations (2) and (3) become [1]:

$$\rho \frac{\partial v_\theta}{\partial t} = \mu \frac{\partial}{\partial r} \left[\frac{1}{r} \frac{\partial}{\partial r} (r v_\theta) \right] \qquad (4)$$

This is to be solved with the boundary and initial conditions: at $r = \kappa R$, $v_\theta = \kappa R \Omega_i$; at $r = R, v_\theta = R \Omega_0$; at $t < 0, v_\theta = 0$. This problem is discussed by KOZENY [5] but his solution is incorrect in that it does not satisfy the initial and boundary conditions. The analogous problem for axial flow in an annulus has been solved by MÜLLER [6].

It is convenient to introduce the dimensionless quantities:

$$\xi = r/R \qquad = \text{radial co-ordinate} \qquad (5)$$

$$\tau = \mu t/\rho R^2 \qquad = \text{time} \qquad (6)$$

$$\phi = v_\theta/R \Delta \Omega = \text{tangential velocity} \qquad (7)$$

$$-\alpha = \Omega_i/\Delta \Omega = \text{angular velocity} \qquad (8)$$

where $\Delta \Omega = \Omega_0 - \Omega_i$. The problem may then be restated as:

$$\frac{\partial \phi}{\partial \tau} = \frac{\partial}{\partial \xi} \left(\frac{1}{\xi} \frac{\partial}{\partial \xi} (\xi \phi) \right) \qquad (9)$$

with boundary and initial conditions: at $\xi = \kappa$, $\phi = -\kappa\alpha$; at $\xi = 1$, $\phi = 1 - \alpha$; and at $\tau = 0$, $\phi = 0$.
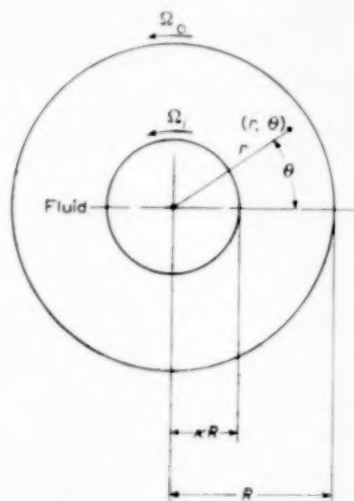

Fig. 1. Annular region in which tangential laminar flow is occurring.

Table 1. The quantities $(1 - \kappa) b_n/n$

n \ κ	0·1	0·2	0·3	0·4	0·5	0·6	0·7	0·8	0·9
1	1·1290	1·0786	1·0485	1·0297	1·0175	1·0097	1·00478	1·00188	1·00042
2	1·0500	1·0256	1·0143	1·00820	1·00464	1·00250	1·00122	1·00047	1·00011
3	1·02640	1·01236	1·00663	1·00373	1·00209	1·00112	1·00054	1·00021	1·00005
4	1·01618	1·00720	1·00379	1·00211	1·00118	1·00063	1·00031	1·00012	1·000026
5	1·01089	1·00469	1·00244	1·00136	1·00076	1·00040	1·00020	1·00008	1·000017
6	1·00780	1·00329	1·00171	1·00094	1·00053	1·00028	1·00014	1·00005	1·000012
7	1·00585	1·00243	1·00126	1·00070	1·00039	1·00021	1·00010	1·000039	1·000009
8	1·00455	1·00187	1·00096	1·00053	1·00030	1·00016	1·00008	1·000029	1·000007
9	1·00363	1·00148	1·00076	1·00042	1·00023	1·00013	1·00006	1·000024	1·000005
10	1·00296	1·00120	1·00062	1·00034	1·00019	1·00010	1·000049	1·000019	1·000004

The steady state solution at $\tau = \infty$ is well-known:

$$\phi_\infty(\xi) = \left[\frac{1 - \alpha(1 - \kappa^2)}{1 - \kappa^2}\right] \xi -$$
$$- \left[\frac{\kappa^2}{1 - \kappa^2}\right] \xi^{-1} \equiv A\xi - B\xi^{-1} \quad (10)$$

Hence the unsteady state solution has the form:

$$\phi(\xi, \tau) = \phi_\infty(\xi) - \phi_t(\xi, \tau) \quad (11)$$

the function $\phi_t(\xi, \tau)$ being the transient contribution, which must satisfy equation (9) but with the boundary and initial conditions: at $\xi = \kappa$, 1, $\phi_t = 0$; at $\tau = 0$, $\phi_t = \phi_\infty(\xi)$.

A transient function of the form $\phi_t(\xi, \tau) = f(\xi) g(\tau)$ is assumed. Application of the method of separation of variables gives:

$$\frac{1}{g}\frac{dg}{d\tau} = -b^2 = \frac{1}{f}\frac{d}{d\xi}\left[\frac{1}{\xi}\frac{d}{d\xi}(\xi f)\right] \quad (12)$$

$$C_n = \frac{\int_\kappa^1 (A\xi - B\xi^{-1}) Z_1(b_n\xi) \, \xi \, d\xi}{\int_\kappa^1 [Z_1(b_n\xi)]^2 \, \xi \, d\xi}$$

$$= \frac{-Ab_n^{-1}\left[Z_0(b_n) - \kappa^2 Z_0(b_n\kappa)\right] + Bb_n^{-1}\left[Z_0(b_n) - Z_0(b_n\kappa)\right]}{\frac{1}{2}\left[Z_0^2(b_n) - \kappa^2 Z_0^2(b_n\kappa)\right]} \quad (16)$$

where $-b^2$ is the separation constant. The solution of the two ordinary differential equations thus generated is straightforward, and one obtains:

$$\phi_t(\xi, \tau) = \sum_{n=1}^\infty C_n (\exp - b_n^2 \tau) Z_1(b_n\xi) \quad (13)$$

wherein

$$Z_1(b_n\xi) = J_1(b_n\xi) Y_1(b_n\kappa) - J_1(b_n\kappa) Y_1(b_n\xi) \quad (14)$$

The functions $Z_1(b_n\xi)$ automatically satisfy the boundary conditions that $Z_1(b_n\xi) = 0$ at $\xi = \kappa$; the requirement that $Z_1(b_n\xi) = 0$ at $\xi = 1$ determines the eigenvalues b_n (some values of b_n are given in Table 1). The C_n are found from the initial condition:

$$\phi_\infty(\xi) = \sum_{n=1}^\infty C_n Z_1(b_n\xi) \quad (15)$$

Multiplication of equation (15) by $Z_1(b_m\xi)\,\xi\,d\xi$ and integration from κ to 1 gives for C_n:

The integrals in equation (16) are evaluated by use of the formulae in JAHNKE and EMDE [4]. The second expression may be simplified by (i) inserting the expressions for A and B from equation (10), (ii) using the relation

$$J_0(x) Y_1(x) - J_1(x) Y_0(x) = -2/\pi x,$$

and (iii) using the defining equation for the b_n. Thereby it may be shown that

$$Z_0(b_n) = -(2/\pi b_n)\left[J_1(b_n\kappa)/J_1(b_n)\right] \quad (17)$$

$$Z_0(b_n\kappa) = -(2/\pi b_n)(1/\kappa) \quad (18)$$

and

$$C_n(\kappa, \alpha) = \frac{\pi J_1(b_n)\left[(1-\alpha)J_1(b_n\kappa) + \alpha\kappa J_1(b_n)\right]}{\left[J_1^2(b_n\kappa) - J_1^2(b_n)\right]} \quad (19)$$

Because of the linear dependence of C_n on α, we may write:

$$C_n(\kappa, \alpha) = (1 - \alpha) C_n(\kappa, 0) + \alpha C_n(\kappa, 1) \quad (20)$$

Hence the values of C_n for any α may be obtained from the tables for $\alpha = 0$ (inner cylinder stationary) and $\alpha = 1$ (outer cylinder stationary) given in Table 2.

The complete expression for the unsteady-state velocity profiles is then:

$$\phi(\xi, \tau) = \left[\frac{1 - \alpha(1 - \kappa^2)}{1 - \kappa^2}\right] \xi - \left[\frac{\kappa^2}{1 - \kappa^2}\right] \xi^{-1} -$$
$$- \pi \sum_{n=1}^\infty \frac{J_1(b_n)\left[(1 - \alpha) J_1(b_n\kappa) + \alpha\kappa J_1(b_n)\right]\left[J_1(b_n\xi) Y_1(b_n\kappa) - J_1(b_n\kappa) Y_1(b_n\xi)\right]}{\left[J_1^2(b_n\kappa) - J_1^2(b_n)\right]} \exp - b_n^2 \tau \quad (21)$$

Table 2. The expansion coefficients C_n

$\alpha = 0$

n \ κ	0·1	0·2	0·3	0·4	0·5	0·6	0·7	0·8	0·9
1	—0·740819	1·44487	—2·26356	—3·10786	—4·28375	—5·06560	8·67573	13·9977	—29·7974
2	0·808087	1·62441	2·36908	3·24969	4·39861	6·05206	8·73960	14·03222	29·7671
3	—0·975122	—1·68653	—2·41438	—3·28186	—4·42176	—6·06855	—8·75081	—14·03880	—29·8134
4	1·01709	1·71367	2·43276	3·29462	4·43109	6·07587	8·75330	14·0410	29·8174
5	—1·04209	—1·72933	—2·44105	—3·30075	—4·43474	—6·07779	—8·75782	—14·0422	—29·7869
6	1·05789	1·73614	2·44646	3·30354	4·43731	6·08131	8·75983	14·0407	29·7553
7	—1·06848	—1·74122	—2·44940	—3·30580	—4·43844	—6·08124	—8·75163	—14·0564	—29·854
8	1·07580	1·74453	2·45115	3·30646	4·43970	6·08231	8·76065	14·040	29·832
9	—1·08125	—1·74897	—2·45288	—3·30759	—4·44150	—6·08266	—8·7572	14·055	—29·785
10	1·08518	1·74876	2·45238	3·30857	4·44083	6·0825	8·7599	14·046	29·759

$\alpha = 1$

| n \ κ	0·1	0·2	0·3	0·4	0·5	0·6	0·7	0·8	0·9
1	0·0165929	0·112692	0·340596	0·764587	1·49593	2·75888	5·07219	10·0119	25·4412
2	0·02388589	0·137775	0·281519	0·815453	1·54993	2·80907	5·11617	10·0392	25·4139
3	0·02780059	0·146787	0·302878	0·827046	1·56085	2·81865	5·12356	10·0439	25·4356
4	0·03003532	0·150773	0·307504	0·831650	1·56525	2·82263	5·12699	10·0463	25·4592
5	0·03143235	0·153088	0·309595	0·833862	1·56696	2·82400	5·12873	10·0472	25·4317
6	0·03238019	0·154096	0·409960	0·834869	1·56817	2·82606	5·13012	10·0460	25·4034
7	0·03288956	0·154851	0·401701	0·835693	1·56870	2·82602	5·12449	10·0585	25·492
8	0·03333078	0·155342	0·402145	0·835930	1·56930	2·82664	5·13069	10·045	25·473
9	0·03361163	0·155258	0·402581	0·836341	1·57005	2·826083	5·1283	10·058	25·430
10	0·03338304	0·155971	0·402455	0·836692	1·56983	2·8267	5·1302	10·050	25·406

111
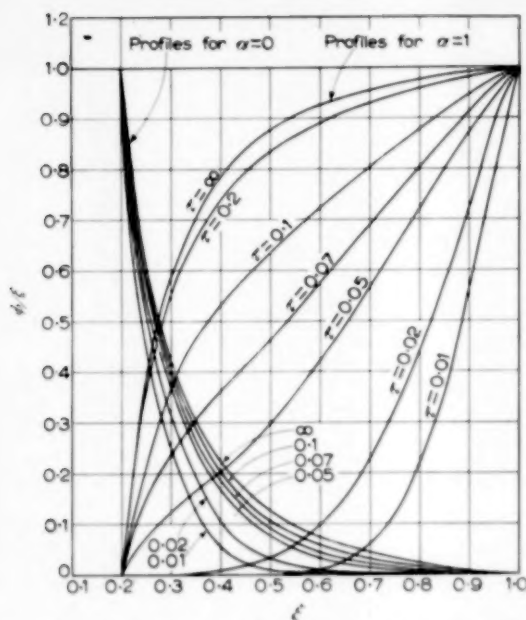
FIG. 2. An illustration of the behaviour of the unsteady-state velocity profiles for $\kappa = 0.2$.

These dimensionless velocity profiles are plotted in Fig. 2 for $\alpha = 0$ and $\alpha = 1$. Velocity profiles for other values of α may be obtained by adding together the velocity profiles for $\alpha = 0, 1$ according to the same rule obeyed by the C_n in equation (20).

The order of magnitude of the times required to establish the steady-state distribution may be illustrated by considering four typical examples with $R = 10$ cm :

(i) for water ($\mu/\rho = 10^{-6}$ m²sec⁻¹), $t = 10^4 \tau$ (sec) ;

(ii) for air ($\mu/\rho = 1.3 \times 10^{-5}$ m²sec⁻¹), $t = 700\tau$ (sec) ;

(iii) for a typical lubricating oil ($\mu/\rho = 10^{-4}$ m²sec⁻¹), $t = 100\tau$ (sec) ;

(iv) for a concentrated aqueous solution of glycerine ($\mu/\rho = 5 \times 10^{-4}$ m²sec⁻¹), $t = 20\tau$.

When $\tau \doteq 1$ steady-state has virtually been established.

3. APPROXIMATE EXPRESSION FOR VELOCITY DISTRIBUTION FOR SHORT TIMES

Equation (21) for the unsteady-state velocity profiles is particularly appropriate for large values of τ. For short times an alternate solution can be derived.

The p-multiplied Laplace transform of equation (9) is :

$$p\bar{\phi} = \frac{d}{d\xi}\left[\frac{1}{\xi}\frac{d}{d\xi}(\xi\bar{\phi})\right] \quad (22)$$

which is to be solved for the boundary conditions : at $\xi = \kappa, \bar{\phi} = -\alpha\kappa/p$; at $\xi = 1, \bar{\phi} = (1-\alpha)/p$. The solution is :

$$\bar{\phi} = \frac{-\{(\kappa\alpha/p)K_1(p^{1/2}) + [(1-\alpha)/p]K_1(p^{1/2}\kappa)\}I_1(p^{1/2}\xi) + \{[(1-\alpha)/p]I_1(\sqrt{p}\kappa) + (\kappa\alpha/p)I_1(p^{1/2})\}K_1(p^{1/2}\xi)}{I_1(p^{1/2}\kappa)K_1(p^{1/2}) - I_1(p^{1/2})K_1(p^{1/2}\kappa)} \quad (23)$$

For large p the hyperbolic Bessel functions may be replaced by the asymptotic expressions $I_1(r) = (1/2\pi r)^{1/2}\exp r$ and $K_1(r) = (\pi/2r)^{1/2}\exp - r$. The resulting expression can then be expanded in a manner analogous to that described by CARSLAW and JAEGER [2]. An inverse Laplace transformation then leads to :

$$(\xi)^{1/2}\phi(\xi, \tau) = -\kappa^{3/2}\alpha\sum_{n=0}^{\infty}\left[\text{erfc}\frac{2n(1-\kappa)+(\xi-\kappa)}{2\sqrt{\tau}} - \text{erfc}\frac{2n(1-\kappa)+(2-\xi-\kappa)}{2\sqrt{\tau}}\right] +$$

$$+ (1-\alpha)\sum_{n=0}^{\infty}\left[\text{erfc}\frac{2n(1-\kappa)+(1-\xi)}{2\sqrt{\tau}} - \text{erfc}\frac{2n(1-\kappa)+(1+\xi-2\kappa)}{2\sqrt{\tau}}\right] \quad (24)$$

which is valid in the limit as τ goes to zero. Equation (24) may be further simplified by replacing erfc x by $\pi^{-1/2}x^{-1}\exp - x^2$ (valid for large x) and using only the first term in the summations.

NOTATION

Scalars — italic
Vectors — bold-face roman
Tensors — bold-face Greek

A, B = functions defined in equation (10)
b = separation constant
C_n = expansion coefficients
$\mathbf{g}$ = gravitational acceleration
J_m = Bessel function of the first kind (m^{th} order)
p = static pressure in Section 1 ; variable introduced in Laplace transform in Section 3.
r = radial co-ordinate

R = radius of outer cylinder
t = time
$\mathbf{v}$ = local velocity vector
v_θ = tangential velocity
Y_m = Bessel function of the second kind (m^{th} order)
$Z_m(b_n\xi) = J_m(b_n\xi)\,Y_1(b_n\kappa) - J_1(b_n\kappa)\,Y_m(b_n\xi)$
α = dimensionless angular velocity (equation 8)
δ = unit tensor
κ = ratio of radius of inner cylinder to that of outer cylinder
μ = coefficient of shear viscosity
ξ = dimensionless radial co-ordinate (equation 5)
ρ = fluid density
τ = dimensionless time (equation 6)
$\boldsymbol{\tau}$ = shear stress tensor
ϕ = dimensionless tangential velocity (equation 7)

REFERENCES

[1] BIRD R. B., STEWART W. E. and LIGHTFOOT E. N. *Notes on Transport Phenomena,* Chapters 3 and 10. John Wiley, New York 1958.

[2] CARSLAW H. S. and JAEGER J. C. *Heat Conduction in Solids,* p. 251. Oxford University Press 1947.

[3] HIRSCHFELDER J. O., CURTISS C. F. and BIRD R. B. *Molecular Theory of Gases and Liquids,* Section 11.1. John Wiley, New York 1954.

[4] JAHNKE E. and EMDE F. *Funktionentafeln.* Dover, New York.

[5] KOZENY J. *Hydraulik — ihre Grundlagen und praktische Anwendung,* p. 456. Springer Verlag, Wien 1953.

[6] MÜLLER W. Z. *Angew. Math. Phys.* 1936 **16** 227.

Tangential Newtonian flow in annuli—II

Steady state pressure profiles

R. B. Bird

Department of Chemical Engineering, University of Wisconsin, Madison, Wisconsin

C. F. Curtiss

Department of Chemistry, University of Wisconsin, Madison, Wisconsin

and

W. E. Stewart

Department of Chemical Engineering, University of Wisconsin, Madison, Wisconsin

Abstract—It is shown how the pressure distribution for isothermal, tangential flow of an *incompressible* fluid in an annulus may be calculated by first solving the problem for a compressible fluid and then taking the limit as the deviation from incompressibility vanishes. An analytical expression for pressure vs. the radial co-ordinate is obtained for either or both of the cylinders in motion.

Résumé—Les auteurs montrent comment calculer la distribution de pression pour l'écoulement isotherme tangentiel d'un fluide incompressible dans une partie annulaire, en résolvant d'abord le problème pour un fluide compressible et en prenant ensuite la limite quand la déviation due à l'incompressibilité disparaît. Une expression analytique de la pression par rapport à la coordonnée radiale est obtenue pour l'un ou pour les deux cylindres en mouvement.

Zusammenfassung—Es wird gezeigt, wie die Druckverteilung für eine isotherme Tangential-strömung einer inkompressiblen Flüssigkeit in einem Ringspalt berechnet werden kann, indem man zunächst das Problem für eine kompressible Flüssigkeit gelöst hat und dann als Grenzüber-gang die Abweichungen von der Inkompressibilität zum Verschwinden bringt. Ein analytischer Ausdruck für den Druck als Funktion der radialen Koordinate wird sowohl für den Fall, dass der eine oder dass beide Zylinder in Bewegung sind, erhalten.

It is desired to compute the pressure distribution which prevails in the system studied in Part I when the velocity distribution is given by $\phi_\infty(\xi)$ in equation (10) for an incompressible fluid. The latter was obtained from the θ-component of the equation of motion. The pressure distribution is obtained from the corresponding r-component of the equation of motion :

$$- \rho (v_\theta{}^2/r) = - dp/dr \qquad (25)$$

This equation could be integrated directly to obtain the radial pressure distribution at a given elevation if the pressure were given at some value of the radial co-ordinate r. In viscometry, however, situations may arise in which one knows only the pressure p_0 of the fluid at rest at the given elevation, and that the volume and fluid content of the annulus are unaffected by rotation. The latter problem is the one considered here.

The problem may be solved by temporarily relaxing the assumption of incompressibility. It can be shown from equation (2) and (3) in component form that equation (4) with the left-hand side equal to zero, and equation (25), are still valid for the isothermal steady flow of a compressible fluid provided that one assumes that μ does not depend upon the pressure. These equations then have to be solved along with the equation of state which is here taken to be the first two
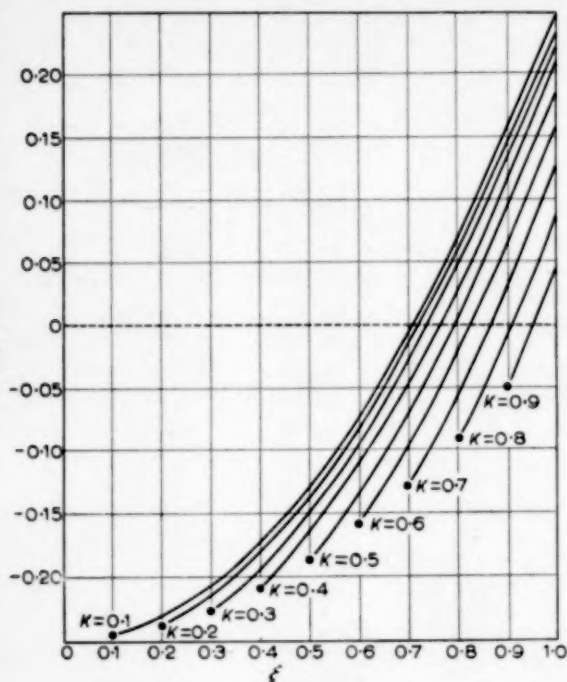
FIG. 1 (a). Steady-state pressure profiles when both cylinders are moving with the same angular velocity.
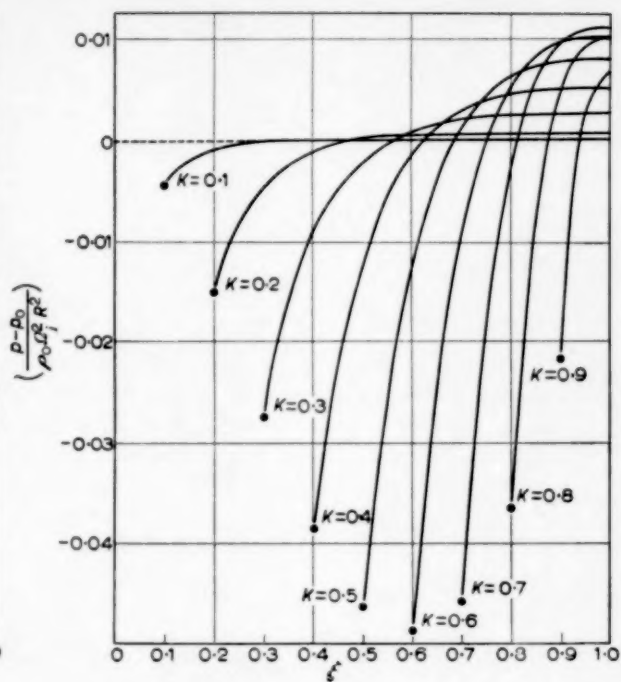
FIG. 1 (b). Steady-state pressure profiles when the inner cylinder is stationary.
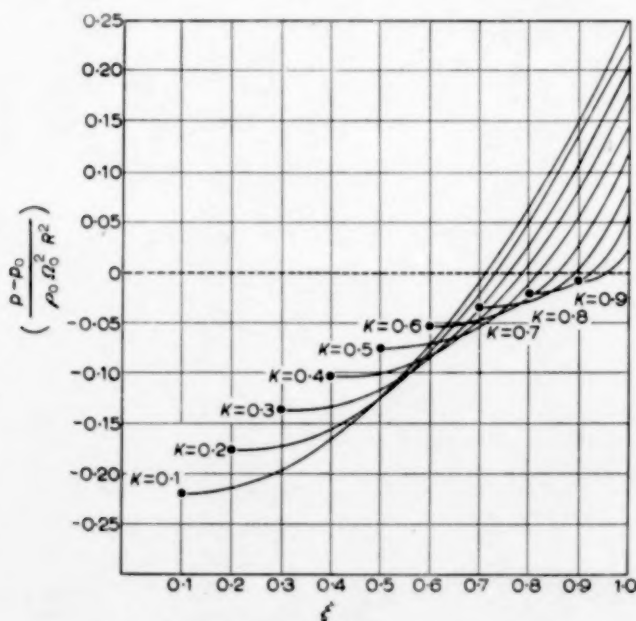
FIG. 1 (c). Steady-state pressure profiles when the outer cylinder is stationary.

115

terms of a Taylor series for ρ as a function of the Gibbs free energy $G = H - TS$:

$$\rho = \rho_0 + \left(\frac{\partial \rho}{\partial G}\right)_0 (G - G_0) + \ldots$$

$$\doteq \rho_0 \left[1 + b_0 (G - G_0)\right]$$

$$= \rho_0 \left[1 + b_0 \int_{p_0}^{p} \rho^{-1} dp\right] \qquad (26)$$

in which p_0 and ρ_0 are the uniform pressure and density of the fluid when the system is at rest, and b_0 is the value of $b = (1/\rho)(\partial \rho/\partial G)_T = (\partial \rho/\partial p)_T$ at $\rho = \rho_0$.

The integration of equation (25) may be performed by inserting the velocity distribution of equation (10) and assuming that ρ is known as a function of p:

$$\int_{p_0}^{p} \rho^{-1} dp = N\left[\frac{1}{2}\left(\frac{\xi^2}{Q^2} - \frac{Q^2}{\xi^2}\right) - 2\ln \xi + C\right] \quad (27)$$

in which N and Q are dimensionless quantities:

$$N = \left(\frac{R\,\Delta\Omega\,(1 - \alpha)\,Q}{1 - Q^2}\right)^2 = (R\,\Delta\Omega)^2\,AB \quad (28)$$

$$Q^2 = \left(\frac{\kappa^2}{1 - \alpha(1 - \kappa^2)}\right) = \frac{B}{A} \qquad (29)$$

The constant of integration C is determined by the normalizing condition that

$$\int_{\kappa}^{1} \rho_0\,\xi\,d\xi = \int_{\kappa}^{1} \rho\xi\,d\xi \qquad (30)$$

which is just a statement of conservation of mass. For the equation of state in equation (26) this reduces to:

$$\int_{\kappa}^{1} \int_{p_0}^{p} \rho^{-1}\,dp\,\xi\,d\xi = 0 \qquad (31)$$

Substitution of equation (27) into equation (31)

yields the integration constant C and hence the final expression for the pressure distribution:

$$\int_{p_0}^{p} \rho^{-1} dp = N\left[\frac{1}{2}\left(\frac{\xi^2}{Q^2} - \frac{Q^2}{\xi^2}\right) - 2\ln \xi - 1 - \frac{1 + \kappa^2}{4Q^2} - \frac{Q^2 + 2\kappa^2}{1 - \kappa^2}\ln \kappa\right] \quad (32)$$

For incompressible fluids the left side of equation (32) just becomes $(p - p_0)/\rho_0$. The same result has been obtained by expressing the equation of state as a Taylor expansion of ρ in powers of $(p - p_0)$, but the development is not as simple as that given above. Three important limiting cases for the pressure distribution are:

(i) $\Omega_i = \Omega_0 = \Omega$:

$$\left(\frac{p - p_0}{\rho_0 \Omega^2\,R^2}\right) = \frac{1}{2}\xi^2 - \frac{1}{4}(1 + \kappa^2) \qquad (33)$$

(ii) $\Omega_i = 0$, $\Omega_0 \neq 0$ (or $\alpha = 0$ and $Q = \kappa$):

$$\left(\frac{p - p_0}{\rho_0 \Omega_0^2\,R^2}\right)\left(\frac{1 - \kappa^2}{\kappa}\right)^2$$

$$= \frac{1}{2}\left(\frac{\xi^2}{\kappa^2} - \frac{\kappa^2}{\xi^2}\right) - 2\ln \xi - 1 -$$

$$- \frac{1 + \kappa^2}{4\kappa^2} - \frac{3\kappa^2}{1 - \kappa^2}\ln \kappa \qquad (34)$$

(iii) $\Omega_i \neq 0$, $\Omega_0 = 0$ (or $\alpha = 1$ and $Q = 1$):

$$\left(\frac{p - p_0}{\rho_0 \kappa^2 \Omega_i^2\,R^2}\right)\left(\frac{1 - \kappa^2}{\kappa}\right)^2$$

$$= \frac{1}{2}\left(\xi^2 - \frac{1}{\xi^2}\right) - 2\ln \xi - 1 -$$

$$- \frac{1 + \kappa^2}{4} - \frac{1 + 2\kappa^2}{1 - \kappa^2}\ln \kappa \qquad (35)$$

These functions are shown graphically in Fig. 1; clearly the largest pressure gradients correspond to equation (33). These results may be used to determine whether or not pressure effects are a disturbing factor in any given concentric cylinder viscometric measurements. They may also be of use in calculating radial pressure distributions in lubrication systems.

NOTATION

A, B = functions defined in equation (10)

b_0 = quantity deferred in equation (26)

p = static pressure

r = radial co-ordinate

R = radius of outer cylinder

v_θ = tangential velocity

α = dimensionless angular velocity (equation 8)

κ = ratio of radius of inner cylinder to that of outer cylinder

μ = coefficient of shear viscosity

ξ = dimensionless radial co-ordinate (equation 5)

ρ = fluid density

ϕ = dimensionless tangential velocity (equation 7)

Precise testing of binary vapour–liquid equilibrium data by the Gibbs–Duhem equation

H. C. VAN NESS*

Department of Chemical Engineering, Rensselaer Polytechnic Institute, Troy, New York

Abstract—The general methods of testing thermodynamic data for binary solutions by the Gibbs–Duhem equation are briefly reviewed, and a new "composition–resolution" test is proposed. Thermodynamically exact methods of testing binary vapour–liquid equilibrium data, both for constant pressure and for constant temperature, are then developed. Application of the "composition–resolution" test is fully discussed, and its advantages are demonstrated.

Résumé—Les méthodes générales de vérification des données thermodynamiques pour des solutions binaires par l'équation de Gibbs–Duhem ont été résumées et une vérification nouvelle "composition–résolution" a été proposée. Les auteurs ont développé des méthodes thermody-namiquement exactes du contrôle des données d'équilibre d'un binaire vapeur liquide à pression constante et aussi à température constante. L'application de la vérification composition–résolution est complètement discutée et ses avantages sont démontrés.

Zusammenfassung—Die allgemeinen Methoden zur Prüfung thermodynamischer Daten für binäre Lösungen durch die Gibbs–Duhem Gleichung werden kurz mitgeteilt und eine neue Zerlegungsmethode vorgeschlagen. Ferner werden thermodynamisch exakte Methoden zur Prüfung der binären Gleichgewichtsdaten dampfförmigflüssig, und zwar sowohl für konstanten Druck wie für konstante Temperatur entwickelt. Die Anwendung der Zerlegungsmethode wird ausführlich mitgeteilt und ihre Vorteile aufgezeigt.

DATA for solutions are most conveniently dealt with by putting them in the form of excess property changes of mixing. If G is taken to represent a property in general, the excess properties of mixing are given by:

$$\Delta G^E = \Delta G - \Delta G^{\text{ideal}} \tag{1}$$

$$\overline{\Delta G_i^E} = \overline{\Delta G_i} - \overline{\Delta G_i^{\text{ideal}}} \tag{2}$$

where ΔG^{ideal} represents the property change which would result if an ideal solution were formed, and the bar indicates a partial molal property change of mixing, i.e. $\overline{\Delta G_i} = \overline{G_i} - G_i$.

There are three general methods for testing the thermodynamic consistency of experimentally determined partial molal excess properties of binary systems. The first is known as the "slope test," and has been recognized for many years. For data at constant temperature and pressure, it requires that:

$$x_A \left(\frac{d\,\overline{\Delta G_A^E}}{dx_A} \right) = - x_B \left(\frac{d\,\overline{\Delta G_B^E}}{dx_A} \right) \tag{3}$$

In other words, for thermodynamically consistent data a definite relationship must exist between the slopes of the curves of $\overline{\Delta G_A^E}$ and $\overline{\Delta G_B^E}$ vs. x_A. The disadvantage of this test is that slopes are very difficult to determine accurately, and the uncertainty of the method is usually at least as great as the uncertainty of the data.

The second method is known as the "area test." A simple and general derivation is given by VAN NESS and MRAZEK [1]. For data at constant temperature and pressure it requires that:

$$\int_0^1 \overline{\Delta G_A^E}\, dx_A = \int_0^1 \overline{\Delta G_B^E}\, dx_A \tag{4}$$

That is, the areas under the curves of ΔG_A^E and

---

* During 1958-59, Visiting Fulbright Lecturer in Chemical Engineering at King's College, University of Durham, Newcastle upon Tyne.

$\overline{\Delta G^E_B}$ vs. x_A should be equal. This is an integral test, and suffers from the disadvantage that it does not represent a point-by-point test of the data. It is entirely possible for this integral or " area " test to be satisfied when the " slope test " at various concentrations is not.

The third method might be called the " composition-resolution " test. It has apparently not been discussed before, and represents a new general method for the testing of data by the Gibbs–Duhem equation which is straightforward and accurate. Furthermore, it allows a point-by-point evaluation of the data. It is based on the observation that a given curve for the excess property change of mixing vs. composition (x_A or x_B) can result from an infinite number of sets of experimentally determined values of $\overline{\Delta G^E_A}$ and $\overline{\Delta G^E_B}$, but only one set of values of $\overline{\Delta G^E_A}$ and $\overline{\Delta G^E_B}$ can result from a given curve for the excess property change of mixing. In other words, if the experimental values of $\overline{\Delta G^E_A}$ and $\overline{\Delta G^E_B}$ are combined according to the equation:

$$\Delta G^E = x_A \overline{\Delta G^E_A} + x_B \overline{\Delta G^E_B} \qquad (5)$$

and the resulting curve of ΔG^E vs. x_A is then used (for example, by the method of tangent intercepts) to calculate values of $\overline{\Delta G^E_A}$ and $\overline{\Delta G^E_B}$, the derived set of values should agree with the experimentally measured set. If they do, the data are consistent. If the data are of poor quality, this method can do no more than reject them. But if they are reasonably accurate, the result of this process of testing will be a set of data smoothed in such a way as to be completely consistent.

The " composition " step of this process as represented by equation (5) presents no difficulty. But the " resolution " step carried out by the classical method of tangent intercepts is usually not sufficiently precise for effective application of the method. VAN NESS and MRAZEK [1] have developed a new method of tangent intercepts which results in the accurate determination of partial molal excess properties. It is based on a plot of $\Delta G^E/x_A x_B$ vs. x_A, or alternatively on a reciprocal plot of $x_A x_B/\Delta G^E$ vs. x_A. Many of the excess property changes of mixing which ΔG^E may represent are set forth in the paper cited [1]. Of these, the one most conveniently

calculated from vapour–liquid equilibrum data is $\Delta F^E/RT$, where ΔF^E is the excess Gibbs free energy of mixing of the liquid phase. Its relation to the activity coefficients of the liquid phase is given by:

$$\Delta F^E/RT = x_A \ln \gamma_A + x_B \ln \gamma_B \qquad (6)$$

Phase equilibrium data for binary systems cannot be taken with both temperature and pressure held constant, as has been assumed in the foregoing discussion, and the method of testing is not quite so direct. Consideration has to be given to two cases: constant-temperature data and constant-pressure data. In either case the general relationship given by equation (6) is valid. The other exact equation which relates the activity coefficients and $\Delta F^E/RT$ for any phase has been derived by the author [2]:

$$d\left(\frac{\Delta F^E}{RT}\right) = \frac{\Delta v}{RT}\,dp - \frac{\Delta H}{RT^2}\,dT + \Sigma(\ln \gamma_i\,dx_i) \qquad (7)$$

where ΔF^E, Δv, ΔH, and the γ_i's are all taken with respect to the pure components at the same temperature and pressure and in the same physical state as the phase considered. We will apply this equation to a binary liquid phase in equilibrium with its vapour, first, at constant temperature, and second, at constant pressure.

For a binary liquid at constant temperature, equation (7) reduces to:

$$\frac{d(\Delta F^E/RT)}{dx_A} = \ln \gamma_A - \ln \gamma_B + \left(\frac{\Delta v}{RT}\right)\left(\frac{dp}{dx_A}\right) \qquad (8)$$

Total derivatives may be used for the case considered because there is but one independent variable, here taken as x_A. Fig. 1 shows a typical plot of $\Delta F^E/RT$ vs. x_A for constant pressure. The slope of a tangent drawn to the curve is, of course, $d(\Delta F^E/RT)/dx_A$, and the tangent is shown intersecting the ordinates at $x_A = 1$ and $x_A = 0$ at points labelled α and β respectively. If the data for $\Delta F^E/RT$ were for constant temperature *and* pressure, then α and β would be partial molal properties and indeed would be identical with $\ln \gamma_A$ and $\ln \gamma_B$. But in the case considered where the pressure varies, α and β differ from $\ln \gamma_A$ and $\ln \gamma_B$ by amounts which are determined as follows: α and β are related to

Constant T or constant p
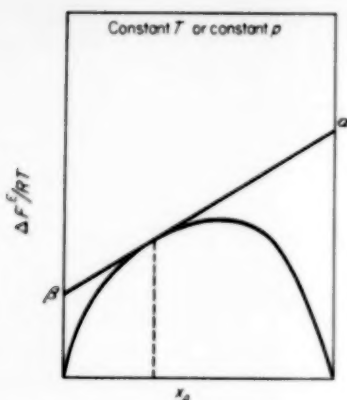
$\Delta F^E/RT$

x_A

FIG. 1. Classical method of tangent intercepts applied to constant-temperature or constant-pressure data.

$\Delta F^E/RT$ by equations which are obvious from inspection of Fig. 1 :

$$\alpha = \frac{\Delta F^E}{RT} + x_B \frac{d\,(\Delta F^E/RT)}{dx_A} \qquad (9a)$$

$$\beta = \frac{\Delta F^E}{RT} - x_A \frac{d\,(\Delta F^E/RT)}{dx_A} \qquad (9b)$$

If equations (9a) and (9b) are each combined with equations (6) and (8), the resulting expressions for α and β are :

$$\alpha = \ln \gamma_A + x_B \left(\frac{\Delta v}{RT}\right)\left(\frac{dp}{dx_A}\right) \qquad (10a)$$

$$\beta = \ln \gamma_B - x_A \left(\frac{\Delta v}{RT}\right)\left(\frac{dp}{dx_A}\right) \qquad (10b)$$

These equations are exact, and show the difference between the tangent intercepts α and β and $\ln \gamma_A$ and $\ln \gamma_B$ for a plot of $\Delta F^E/RT$ vs. x_A at constant temperature. In practice, this difference is usually negligible, because Δv is almost always very small. Hence it is usually entirely satisfactory to treat the tangent intercepts as being identical to the $\ln \gamma_i$'s.

For the case of constant-pressure data, equation (7) becomes :

$$\frac{d(\Delta F^E/RT)}{dx_A} = \ln \gamma_A - \ln \gamma_B - \left(\frac{\Delta H}{RT^2}\right)\left(\frac{dT}{dx_A}\right) \quad (11)$$

A plot of $\Delta F^E/RT$ vs. x_A for data at constant

pressure is identical in form to the plot of constant-temperature data, and is also represented by Fig. 1. Indeed, equations (6) and (9) are equally valid for this case, and equations analogous to equations (10a) and (10b) are readily derived by combining equations (9a) and (9b) with equations (6) and (11) :

$$\alpha = \ln \gamma_A - x_B \left(\frac{\Delta H}{RT^2}\right)\left(\frac{dT}{dx_A}\right) \qquad (12a)$$

$$\beta = \ln \gamma_B + x_A \left(\frac{\Delta H}{RT^2}\right)\left(\frac{dT}{dx_A}\right) \qquad (12b)$$

Again we note the distinction between the intercepts, α and β, and $\ln \gamma_A$ and $\ln \gamma_B$. Here this difference cannot usually be neglected, and it is not in general satisfactory to regard the intercepts as representing values of $\ln \gamma_A$ and $\ln \gamma_B$.

In either case, constant temperature or constant pressure, the treatment of data is in principle the same. Equations (10) and (12) can both be written :

$$\alpha = \ln \gamma_A + x_B \delta \qquad (13a)$$

$$\beta = \ln \gamma_B - x_A \delta \qquad (13b)$$

where

$$\delta = \left(\frac{\Delta v}{RT}\right)\left(\frac{dp}{dx_A}\right) \text{ for constant-temperature data,}$$

and $$\delta = -\left(\frac{\Delta H}{RT^2}\right)\left(\frac{dT}{dx_A}\right) \text{ for constant-pressure data.}$$

It should be noted that :

$$x_A \alpha + x_B \beta = x_A \ln \gamma_A + x_B \ln \gamma_B = \frac{\Delta F^E}{RT} \quad (14)$$

(However, $\alpha \neq \ln \gamma_A$ and $\beta \neq \ln \gamma_B$).

The intercepts, α and β, are related by the equation :

$$x_A \left(\frac{d\alpha}{dx_A}\right) = -x_B \left(\frac{d\beta}{dx_A}\right) \qquad (15)$$

which follows from equations (9a) and (9b) after differentiation of α with respect to x_A and of β with respect to x_B. Equation (15) indicates the appropriate " slope test " of phase-equilibrium data calculated from experimental measurements by equations (13a) and (13b). These same data

may be subjected to an " area test " according to the equation :

$$\int_0^1 \alpha \, dx_A = \int_0^1 \beta \, dx_A \qquad (16a)$$

or

$$\int_0^1 (\alpha - \beta) \, dx_A = 0 \qquad (16b)$$

But $\alpha - \beta = \ln \gamma_A - \ln \gamma_B + \delta$

Therefore :

$$\int_0^1 \ln \frac{\gamma_A}{\gamma_B} \, dx_A = - \int_0^1 \delta \, dx_A \qquad (17)$$

This particular test was discussed by THIJSSEN [3]. Both the " slope test " and the " area test " suffer from disadvantages already discussed. The " composition–resolution " test proposed here is also applicable, and represents a much more satisfactory procedure.

Values of $\Delta F^E / RT$ are calculated from the experimental data, and are plotted vs. x_A. Values of α and β can then be determined by the usual method of tangent intercepts, and the results are used to calculate values of $\ln \gamma_A$ and $\ln \gamma_B$ by equations (13a) and (13b). If the derived values of $\ln \gamma_A$ and $\ln \gamma_B$ correlate with the values calculated directly from the data, then the data are consistent.

As previously explained, there is considerable inherent uncertainty in drawing tangents to the curves of $\Delta F^E / RT$ vs. x_A and in extrapolating to get values of α and β. The procedure for overcoming this problem has been described by VAN NESS and MRAZEK [1]. Rather than plotting $\Delta F^E / RT$ vs. x_A one plots $\Delta F^E / x_A x_B RT$ vs. x_A as shown in Fig. 2. The tangent intercepts on this plot, I_0 and I_1, are related to α and β by the equations :

$$\alpha = x_B^2 \left[2 \frac{\Delta F^E}{x_A x_B RT} - I_0 \right] \qquad (18a)$$

$$\beta = x_A^2 \left[2 \frac{\Delta F^E}{x_A x_B RT} - I_1 \right] \qquad (18b)$$

and $\ln \gamma_A$ and $\ln \gamma_B$ are given by :

$$\frac{\ln \gamma_A}{x_B} = x_B \left[2 \frac{\Delta F^E}{x_A x_B RT} - I_0 \right] - \delta \qquad (19a)$$

$$\frac{\ln \gamma_B}{x_A} = x_A \left[2 \frac{\Delta F^E}{x_A x_B RT} - I_1 \right] + \delta \qquad (19b)$$
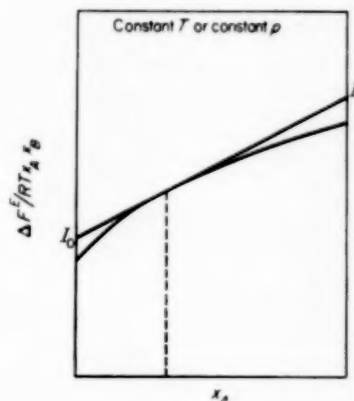

FIG. 2. Method of VAN NESS and MRAZEK applied to constant-temperature or constant-pressure data.

It should be noted that :

$$\frac{\Delta F^E}{x_A x_B RT} = \frac{\ln \gamma_A}{x_B} + \frac{\ln \gamma_B}{x_A} \qquad (20)$$

Thus the comparison here is most conveniently made between experimental and derived values of $(\ln \gamma_A)/x_B$ and $(\ln \gamma_B)/x_A$. The reasons for the superiority of this procedure are given in the paper cited [1]. It is also explained that in some cases the reciprocal plot of $x_A x_B RT / \Delta F^E$ vs. x_A can be used to greater advantage.

For constant-pressure data the rigorous testing procedure requires a knowledge of the heat of mixing as a function of composition and temperature. In practice this means the determination of the heat of mixing as a function of composition at two temperatures. Since the heat of mixing at a given composition is almost always essentially linear with temperature, interpolation for the effect of temperature is very easy. Unfortunately, at present the necessary heat-of-mixing data are usually lacking.

For constant-temperature data it is usually satisfactory to take δ as zero. Hence the recommended testing procedure requires no additional

data beyond phase-equilibrium measurements. In Fig. 3 data of Röck and Schröder [4] for the acetone–chloroform system at the constant temperature of 30°C are subjected to the " composition–resolution " test. The data have been corrected for the non-ideality of the vapour phase. This appears to be essential even for sub-atmospheric pressures, because the method
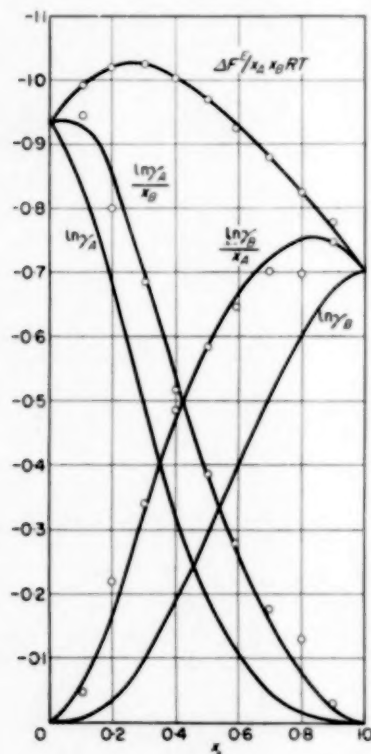

FIG. 3. Acetone – chloroform system at 30°C [4].

is very sensitive to deviations of any kind. The points shown on Fig. 3 represent values calculated from the experimental data. The curve of $\Delta F^E/x_A x_B RT$ vs. x_A has been drawn through the data points so as to give a smooth relation. The curves of $(\ln \gamma_A)/x_B$ and $(\ln \gamma_A)/x_A$ vs. x_A have been derived from the $\Delta F^E/x_A x_B RT$ curve by equations (19a) and (19b), with δ taken as being negligible. These curves are seen to correlate the experimental points reasonably well, and it is concluded that the data are essentially consistent.

Moreover, the derived curves represent the data smoothed in such a way as to be completely consistent. Curves of the smoothed values of $\ln \gamma_A$ and $\ln \gamma_B$ are also shown on Fig. 3. It should be noted that if the curve of $\Delta F^E/x_A x_B RT$ is expressed in equation form, analytical expressions for $\ln \gamma_A$ and $\ln \gamma_B$ can be readily derived from it. If this curve is a straight line, then the 2-constant Margules equations result. If the reciprocal plot, $x_A x_B RT/\Delta F^E$ vs. x_A, is a straight line, then the Van Laar equations are obtained.

For constant-pressure data, where δ cannot usually be neglected, the quantities derived from the $\Delta F^E/x_A x_B RT$ vs. x_A curve are α and β (see equations 18a and 18b] and not $\ln \gamma_A$ and $\ln \gamma_B$. Hence derived analytical expressions are for α and β, and again Margules and van Laar equations arise (for α and β) if the appropriate curves are straight lines. Correct equations for $\ln \gamma_A$ and $\ln \gamma_B$ can be obtained only by expressing δ as well in analytical form. In general, the nature of δ is such that this is most difficult, and it is probably best treated graphically.

An alternative procedure for the case of constant-pressure data is to make use of ΔF^E itself rather than $\Delta F^E/RT$. A plot of ΔF^E vs. x_A at constant pressure would be similar to Fig. 1. In this case we will designate the tangent intercepts by α' and β'. The required equations are :

$$\alpha' = \Delta F^E + x_B \left(\frac{d \Delta F^E}{dx_A}\right) \qquad (21a)$$

$$\beta' = \Delta F^E - x_A \left(\frac{d \Delta F^E}{dx_A}\right) \qquad (21b)$$

$$\Delta F^E = x_A RT \ln \gamma_A + x_B RT \ln \gamma_B \qquad (22)$$

By differentiation :

$$\frac{d (\Delta F^E/RT)}{dx_A} = - \frac{\Delta F^E}{RT^2} \left(\frac{dT}{dx_A}\right) + \frac{1}{RT} \left(\frac{d \Delta F^E}{dx_A}\right)$$

If this is combined with equation (11), the result is :

$$\frac{d \Delta F^E}{dx_A} = \left(\frac{\Delta F^E - \Delta H}{T}\right) \left(\frac{dT}{dx_A}\right) + {} + RT \ln \gamma_A - RT \ln \gamma_B$$

or

$$\frac{d \, \Delta F^E}{dx_A} = RT \ln \gamma_A - RT \ln \gamma_B - \Delta S^E \left(\frac{dT}{dx_A} \right) \quad (23)$$

Combination of equations (21), (22), and (23) gives:

$$\alpha' = RT \ln \gamma_A - x_B \, \Delta S^E \left(\frac{dT}{dx_A} \right) \quad (24a)$$

$$\beta' = RT \ln \gamma_B + x_A \, \Delta S^E \left(\frac{dT}{dx_A} \right) \quad (24b)$$

In practice, of course, one should plot $\Delta F^E / x_A x_B$ vs. x_A and use the method of VAN NESS and MRAZEK for determining values of α' and β'.

A possible advantage of equations (24) over equations (12) is that ΔS^E may be small even though ΔH is not. This is the basis for the many suggestions in the literature that it is preferable to deal with $T \ln \gamma_i$ rather than with $\ln \gamma_i$ itself for constant-pressure data. Although this is not necessarily true, it is sometimes the case. It is doubtful, however, that the ΔS^E term of equation (24) is very often negligible.

Another possible advantage to the use of ΔS^E rather than ΔH is that ΔS^E may not vary nearly so rapidly with temperature. In this case values of ΔS^E need be determined at just one temperature, whereas ΔH must be known as a function of temperature.

The area test in terms of these variables is readily deduced from either equation (23) or (24), and requires:

$$\int_0^1 RT \ln \frac{\gamma_A}{\gamma_B} \, dx_A = \int_0^1 \Delta S^E \left(\frac{dT}{dx_A} \right) dx_A \quad (25)$$

Thus it is seen that the suggestion of BROUGHTON and BREARLEY [5] that the left-hand integral in equation (25) is zero is not in general correct.

One other question often arises in connexion with constant-pressure data: Do the curves of $\ln \gamma_A$ and $\ln \gamma_B$ vs. x_A have to be tangent to the horizontal at their respective origins? The answer is an unequivocal *yes*. This may be seen by differentiation of equation (13a), which gives:

$$\frac{d \ln \gamma_A}{dx_A} = \frac{d \alpha}{dx_A} - x_B \left(\frac{d \delta}{dx_A} \right) + \delta$$

As x_A approaches unity, x_B, δ, and $d \alpha / dx_A$ all approach zero, and all terms on the right-hand side of this equation vanish. That $d \alpha / dx_A$ approaches zero can be seen from equation (15). This conclusion is based on the premise that none of the derivatives, $d \alpha / dx_A$, $d \beta / dx_A$, or dT / dx_A, becomes infinite as x_A approaches zero or unity.

At an azeotropic point δ becomes zero for both constant-pressure and constant-temperature data. Moreover, the curves of $\Delta F^E / RT$ vs. x_A for constant pressure and for constant temperature which pass through a given azeotropic point are tangent at this point.

It has been the object of this paper to develop thermodynamically exact equations for the treatment of vapour-liquid equilibrium data at both constant pressure and constant temperature. In addition, precise methods for the testing and smoothing of such data have been presented.

NOTATION

ΔF^E = excess Gibbs free energy change of mixing

G = a thermodynamic property in general

G_i = a molal property of pure i at the T and p of the solution

$\bar{G}_i$ = a partial molal property

ΔG = a property change of mixing per mole of mixture

$\overline{\Delta G_i}$ = a partial molal property change of mixing

ΔG^E = an excess property change of mixing

$\overline{\Delta G_i}^E$ = an excess partial molal property change fo mixing

ΔG^{ideal} = a property change of mixing for an ideal solution

$\overline{\Delta G_i}^{\text{ideal}}$ = a partial molal property change of mixing for an ideal solution

ΔH = heat of mixing per mole of mixture = ΔH^E

I_0, I_1 = tangent intercepts as shown in Fig. 2

p = pressure

R = universal gas constant

ΔS^E = excess entropy change of mixing per mole of mixture

T = absolute temperature

Δv = volume change of mixing per mole of mixture

x_i = mole fraction of component i in solution

α, α' = tangent intercepts at $x_A = 1$ as shown in Fig. 1

β, β' = tangent intercepts at $x_A = 0$ as shown in Fig. 1

δ = deviation term defined following equation (13)

γ_i = activity coefficient of component i in solution

References

[1]   Van Ness H. C. and Mrazek R. V. *A.I.Ch.E. Journal.* 1959 **5** No. 2.

[2]   Van Ness H. C. *Chem. Engng. Sci.* 1959 **10** 225.

[3]   Thijssen H. A. C. *Chem. Engng. Sci.* 1955 **4** 75.

[4]   Röck H. and Schröder W. Z. *Phys. Chem.* 1957 **11** 41.

[5]   Broughton D. B. and Brearley C. S. *Industr. Engng. Chem.* 1955 **47** 838.

Dispersion in flow through a network of capillaries

P. G. Saffman

Cavendish Laboratory, Cambridge

Abstract—This paper presents the results of an analysis of dispersion in a porous medium, for the case when Dorcy's law is valid and the Péclet number is large. It is shown that, after a sufficiently long time, the effective longitudinal diffusivity is a logarithmic function of the Péclet number.

Résume—Analyse de la dispersion d'un écoulement dans un milieu poreux, lorsque la loi de Dorcy s'applique et pour des nombres de Péclet considérables. On montre qu'apres un temps suffisant, la diffusivité longitudinale est une fonction logarithmique du nombre de Péclet.

Zusammenfassung—Untersuchungsergebnisse über die Durchmischung in einem porösen Medium werden mitgeteilt im Bereich des Dorcyschen Gesetzes und bei grosser Pécletzahl. Nach genügend langer Zeit ist die effektive Längsdurchmischung eine logarithmische Funktion der Pécletzahl.

1. Description of the Model

One of the difficulties in calculating the properties of flow through porous media is that the detailed geometry of the medium is not usually known and the flow field cannot be computed in detail. Theoretical work is at present confined to the investigation of models which can be handled mathematically. This note summarizes an investigation (Saffman [2]) of the dispersion of a dynamically neutral material quantity in flow through a particular model, first considered by Josselin de Jong [1], and suggested independently by Sir Geoffrey Taylor.

The model consists of a random, statistically isotropic, network of straight circular capillaries of length l and radius a, several capillaries starting and finishing at each junction. The case is considered in which the Reynolds number of the flow through the capillaries is small so that Poiseuille flow exists in each capillary or pore. To a good approximation, the pressure gradient along a pore making an angle θ with the direction of the mean flow can be taken as $\cos \theta \, \partial P/\partial x$, where $\partial P/\partial x$ is the mean pressure gradient and the mean flow is supposed uniform and in the x-direction. The velocity profile in this capillary is

$$q = \frac{1}{4\mu} \cos \theta \, \frac{\partial P}{\partial x} (a^2 - r^2) \qquad (1)$$

where r is the distance from the axis of the pore and μ is the viscosity of the fluid. The proportion of pores with θ lying between θ and $\theta + d\theta$ is $\sin \theta \, d\theta$, and the mean interstitial velocity (in the x-direction) is therefore

$$\int_0^{\frac{1}{2}\pi} \int_0^a q \cos \theta \, \frac{2r}{a^2} \, dr \sin \theta \, d\theta = \frac{a^2}{24\mu} \frac{\partial P}{\partial x} = U, \text{ say} \quad (2)$$

The filter velocity is σU, where σ is the porosity, and therefore the permeability of the model is

$$k = \frac{1}{24} \sigma a^2 \qquad (3)$$

In terms of U, (1) may be written

$$q = 6 U \cos \theta (1 - r^2/a^2) \qquad (4)$$

2. The Longitudinal Dispersion of a Fluid Particle

Consider the motion of a fluid particle. After passage through one capillary it has gone a distance $l \cos \theta$ in the x-direction in a time $t = l/q$. Since the network is random, it may be assumed that the values of θ and r for successive

pores traversed by the particle are random variables and statistically independent. The probability distribution of the displacement and time after a fluid particle has passed through n pores can then be calculated, using well known methods of statistics. It is then possible to obtain the probability distribution (p.d.) of the longitudinal displacement, x, of the particle after a given time T.

It is found that the mean displacement is given by

$$\bar{x} = U\,T \qquad (5)$$

so that the centre of a cloud of marked fluid particles moves with the interstitial velocity U.

For the dispersion about the mean, it is found that $(x - \bar{x})/\bar{x}^{\frac{1}{2}}$ is asymptotically normal as $\bar{x} \to \infty$, and that

$$\frac{\overline{(x - \bar{x})^2}}{\bar{x}} \sim \frac{l}{48}\left(\log\frac{54\bar{x}}{l}\right)^2 \qquad (6)$$

where the bar denotes a mean, and it is necessary that $\log(\bar{x}/l) \gg 1$ before equation (6) applies.

It is to be noted that the p.d. of $x - \bar{x}$ is *not* asymptotically normal; it has a tail for negative values of $x - \bar{x}$, whose effect on the cumulants of the probability distribution is negligible when weighted with $\bar{x}^{-1/2}$, but not otherwise.

If an effective diffusivity, k_l, for the longitudinal dispersion is defined by the formula $\overline{(x - \bar{x})^2} = 2k_l\,T$, then k_l/Ul is not constant but is an increasing function of $\bar{x}/l$. This result is not in accordance with diffusion processes in general, and arises here because the time of passage of a fluid particle through a pore, t, becomes infinite as $r \to a$ or $\theta \to (1/2)\pi$. If the quantity being dispersed is subject to molecular diffusion with a diffusivity D, it is clearly not physically sensible to suppose that elements of the material quantity may spend an infinite time in a pore, however small D may be. It is therefore necessary to investigate the effects of molecular diffusion, even though $D \ll k_l$.

3. EFFECTS OF MOLECULAR DIFFUSION

Molecular diffusion acts in two ways: (i) it transports material across a capillary, the time scale for this process being $a^2/8D = t_a$, say (cf.

TAYLOR [3]) ; and (ii) it transports material along a capillary with a time scale $l^2/2D = t_l$, say. These processes are negligible if t_a and t_l are very much greater than l/q, where q is to be interpreted as the velocity of the fluid particle at the point where a material element enters a capillary. But however small D, provided it is not identically zero, there are values of r and θ for which these conditions are not satisfied.

An exact calculation of the effects of molecular diffusion presents great difficulties. However, if

$$t_l > t_a > l/U \qquad (7)$$

molecular diffusion can be taken into account in an approximate manner by assuming that its effect is to impose " cut-offs " on the possible values of t. Two " cut-offs " are required : firstly to express the idea that material near the capillary walls will diffuse away from the walls in a time of order t_a to where it will be convected with a velocity of order $3U\cos\theta$, and secondly that material diffuses along a pore in a time of order t_l. These may be expressed formally by saying that the time spent by a material element in a capillary is the least of l/q, $t_a + l/3U\cos\theta$, and t_l. One reason for believing that this rough approximation is not too unreasonable lies in the fact that the results depend logarithmically upon D and are not sensitive to variations of t_a and t_l.

The p.d. of the displacement of material elements after a given time can then be calculated and it is found that the mean displacement still moves with the velocity U, i.e. equation (5) is satisfied. The dispersion about the mean now depends, however, on the relative values of the dimensionless quantities $\bar{x}/l$, Ut_a/l and Ut_l/l. The following results are obtained, where the square of the dispersion is denoted by $s^2 = \overline{(x - \bar{x})^2}$, which are valid when (7) is satisfied.

(a) If, roughly, $(\bar{x}/l)^{1/2} > Ut_l/l > Ut_a/l > 1$, then

$$\frac{s^2}{\bar{x}l} \doteq \frac{1}{3}\log\frac{3Ut_l}{l} + \frac{1}{12}\left(\log\frac{6Ut_a}{l}\right)^2 -$$
$$- \frac{1}{4}\log\frac{6Ut_a}{l} + \frac{19}{24}, \quad (8a)$$

a more precise condition for the validity of (8a) being

$$\frac{Ut_l/l}{(\bar{x}/l)^{1/2}(\log 3Ut_l/l)^{1/2}} < 1 \qquad (8b)$$

$\bar{x}/l = N$, say, is proportional to the average number of pores which a fluid particle goes through in the time T. $l/t_l = 2D/l = v_l$, say, can be called the "velocity of diffusion along a pore," and $l/t_a = 8Dl/a^2 = v_a$, say, the "velocity of diffusion across the pore." Then $Ut_l/l = Ul/2D = U/vl$ and $Ut_a/l = Ua^2/8Dl = U/v_a$. The condition (7) can be expressed as $U > v_a > v_l$, and the rough condition for case (a) as $N^{1/2} > U/v_l > U/v_a$. This can be satisfied by taking N sufficiently large, however small D may be.

Expressions for other relative values of the parameters are:

(b) If, roughly, $Ut_l/l > (\bar{x}/l)^{1/2} > Ut_a/l > 1$, then

$$\frac{s^2}{\bar{x}l} \doteq \frac{1}{6}\log\frac{27\bar{x}}{2l} + \frac{1}{12}\left(\log\frac{6Ut_a}{l}\right)^2 -$$
$$- \frac{1}{4}\log\frac{6Ut_a}{l} + \frac{19}{24} \qquad (9a)$$

more precise conditions being

$$\log\left(\frac{\bar{x}}{l}\right)^{1/2} > 1, \frac{3Ut_a/l}{(\bar{x}/l)^{1/2}\{\log(\bar{x}/l)^{1/2}\}^{1/2}} < 1,$$
$$\frac{3Ut_l/l}{(\bar{x}/l)^{1/2}\{\log(\bar{x}/l)^{1/2}\}^{1/2}} > 1 \qquad (9b)$$

(c) If, roughly, $Ut_l/l > Ut_a/l > (\bar{x}/l)^{1/2} > 1$, then

$$\frac{s^2}{\bar{x}l} \doteq \frac{1}{48}\left(\log\frac{54\bar{x}}{l}\right)^2, \qquad (10a)$$

more precise conditions being

$$\log\left(\frac{\bar{x}}{l}\right)^{1/2} > 1, \frac{4Ut_a/l}{(\bar{x}/l)^{1/2}\log(\bar{x}/l)^{1/2}} > 1,$$
$$\frac{4Ut_l/l}{(\bar{x}/l)^{1/2}\log(\bar{x}/l)^{1/2}} > 1. \qquad (10b)$$

It may be that t_a and t_l differ by a factor of 100 or more, in which case the condition

$$t_l > l/U > t_a \qquad (11)$$

may possibly be satisfied, i.e. the time scale for diffusion of material across the capillary is small compared with the time spent in the pore. In this case, the material will be uniformly concentrated across a cross-section and the material is effectively convected along the pore with the average velocity $3U\cos\theta$ (see TAYLOR [3]). The analysis leading to the above results can then be repeated taking the time spent by a material element in a capillary as $l/(3U\cos\theta)$, and assuming that the effect of molecular diffusion is to "cut-off" the possible values of the time by an upper bound t_l. The results valid when (11) is satisfied are that $\bar{x} = UT$ and as follows:

(d) If, roughly, $(\bar{x}/l)^{1/2} > \dfrac{Ut_l}{l} > 1$, then

$$\frac{s^2}{\bar{x}l} \doteq \frac{1}{3}\log\frac{3Ut_l}{l} - \frac{1}{12}, \qquad (12)$$

more precise conditions being

$$\frac{Ut_l/l}{(\bar{x}/l)^{1/2}(\log 3Ut_l/l)^{1/2}} < 1 \qquad (12b)$$

(e) If, roughly, $Ut_l/l > (\bar{x}/l)^{1/2} > 1$, then

$$\frac{s^2}{\bar{x}l} \doteq \frac{1}{6}\log\frac{27\bar{x}}{2l}, \qquad (13a)*$$

more precise conditions being

$$\log\left(\frac{\bar{x}}{l}\right)^{1/2} > 1, \frac{3Ut_l/l}{(\bar{x}/l)^{1/2}\{\log(\bar{x}/l)^{1/2}\}^{1/2}} > 1. \quad (13b)$$

The precise magnitude of "$>$" in these formulae is not certain, but interpreting it as "greater than by a factor of five" should not lead to serious error.

The p.d. of $(x - \bar{x})/\bar{x}^{1/2}$ is in each case approximately normal, but that of $x - \bar{x}$ is not, having a long tail for negative values of $x - \bar{x}$. The third moment has been calculated for cases (a) and (d), and it is found that

$$\overline{(x - \bar{x})^3} \sim -\frac{3}{4}\bar{x}\,U l\,t_l \to \quad \infty \text{ as } \bar{x} \to \infty. \quad (14)$$

(The third moment of $(x - \bar{x})/\bar{x}^{1/2}$ is $O(\bar{x}^{-1/2})$ which $\to 0$ as $\bar{x} \to \infty$).

---

* This is effectively the result given by JOSSELIN DE JONG [1].

4. DISCUSSION

Although the theory applies strictly only to a network of capillaries, it is expected that it will have some relevance, qualitatively at least, to dispersion in flow through an actual porous medium, with the length of the capillaries, l, identified with the grain size of the medium, and the radius a estimated from the permeability and porosity by means of equation (3). It is to be noticed, anyway, that the results are not quantitatively accurate because they depend upon the precise form of the cut-off conditions, although not to any great extent.

For given values of U and D, and $\bar{x}$ varying, the dispersion must eventually be given by cases (a) or (d) since the conditions for one of these cases can always be satisfied by taking $\bar{x}$ sufficiently large; however, the larger Ul/D, the larger must be $\bar{x}$. The dispersion is then proportional to $\bar{x}^{1/2}$, in accordance with the usual behaviour of diffusion processes, and is also a logarithmic function of Ul/D. (Compare TAYLOR [3] where dispersion in a straight capillary is found to be inversely proportional to D).

If $D \to 0$ (i.e. t_a and $t_l \to \infty$), with $\bar{x}$ and U kept fixed, case (c) eventually obtains, which is of course identical with (6) which was derived on the assumption that $D = 0$. (10b) therefore gives the condition that molecular diffusion should be negligible. Notice that $\log (\bar{x}/l)^{1/2}$ must be large compared with unity for the distribution to be gaussian, which implies values of $\bar{x}/l$ of at least 2×10^4. In this case the dispersion is proportional to $\bar{x}^{1/2} \log \bar{x}$, although in practice the logarithmic dependence would be difficult to observe.

Equivalently, suppose that $\bar{x}$ and D are fixed and U varies. For the small (but not too small) values of U, cases (a) or (d) will obtain. As U increases, the dispersion increases, because, in effect, molecular diffusion has less time to decrease concentration gradients, and (c) eventually obtains.

These comments are illustrated in the figure, where $s^2/\bar{x}l$ is plotted against Ul/D on a logarithmic scale, with, for the sake of example, $\bar{x}/l = 10^6$ and $a/l = 1/5$. The full curves are the values given by the various results in the region of their
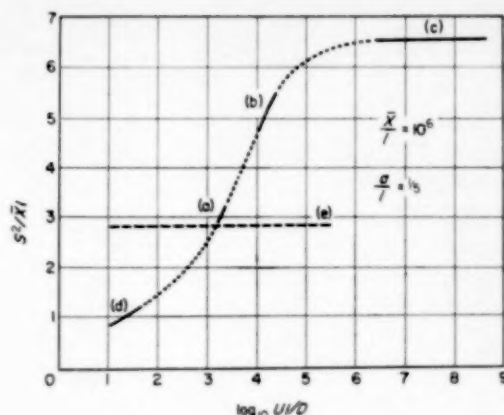

FIG. 1.

$s^2/\bar{x}l$ as a function of Ul/D, for $\bar{x}/l = 10^6$ and $a/l = 1/5$. The full lines give the results for the case of the accompanying letter, and the dotted lines are obtained by interpolation. The horizontal dotted line is the value given by case (e).

validity and the letter denotes the corresponding case. It will be noticed that much of the range is not covered by the cases, but the value of $s^2/\bar{x}l$ can then be obtained by interpolation, shown by the dotted lines on the figure. The values shown for very large values of Ul/D may be academic, since the value of U cannot be too large else Poiseuille flow will not exist in the capillaries. Roughly speaking, this requires $Ua/v < 1$, where v is the kinematic viscosity of the fluid. The horizontal dotted line is the value given by (13a), i.e. the dispersion according to (e) if the conditions for that case were satisfied.

One point seems worth emphasizing, and that is that the results of laboratory experiments with relatively small values of $\bar{x}/l$ must apparently be applied with care to situations occurring in practice where the value of $\bar{x}/l$ may be very different, especially if Ul/D is extremely large.

5. THE LATERAL DISPERSION

It is found that the lateral or transverse displacement in a direction perpendicular to the mean motion has a p.d. which is normally distributed with zero mean and variance.

$$\bar{y^2} = 3/8 \; Ul \; T = 3/8 \; l\bar{x}, \tag{15}$$

provided $(\bar{x}/l)^{1/2} \gg 1$. This expression is equiva-

lent to an effective lateral diffusivity $k_l = (3/16)\, l\, \bar{x}$. This result is independent of molecular diffusion, provided of course $D \ll Ul$. However, its derivation assumes that the direction of successive pores through which a marked fluid particle moves are statistically independent, and there are reasons based on continuity arguments for believing that this assumption is not valid for the lateral dispersion, although reasonable for the longitudinal dispersion. The lateral dispersion may therefore be an order of magnitude less than that given by (15).

A full discussion of the assumptions and a description of the analysis are given in [2]. Also, the theory is there compared with some experimental data, and the agreement is found to be not unreasonable.

NOTATION

a = radius of capillary

D = molecular diffusivity

k_l = effective longitudinal diffusivity

k_t = effective lateral diffusivity

k = permeability

l = length of capillary

P = mean pressure

q = velocity in a capillary

r = distance from axis of a capillary

$s = \sqrt{(x - \bar{x})^2}$ = longitudinal dispersion

$t_a = a^2/8D$ = cut-off time for diffusion across a capillary

$t_l = l^2/2D$ = cut-off time for diffusion along a capillary

U = axial component of the interstitial velocity

$\bar{x}_l = UT$ = mean longitudinal displacement in time T.

μ = viscosity of fluid

ν = kinematic-viscosity

σ = porosity

θ = angle between directions of capillary and the mean flow.

REFERENCES

[1] JOSSELIN DE JONG G. *Trans. Amer. Geophys. Union* 1958 **39** 67.

[2] SAFFMAN P. G. *J. Fluid Mech.* **6** 321.

[3] TAYLOR SIR GEOFFREY *Proc. Roy. Soc.* 1953 **A.219** 186.

Gas-phase mass-transfer in a disk-column

N. A. WARNER

School of Metallurgy, University of New South Wales, P. O. Box 1, Kensington, New South Wales, Australia

Abstract—Mass-transfer rates in a disk-column were studied by vaporizing liquids in a range of counter-current flowing gases. The results of these studies are well correlated by a " relative j_D factor," which takes into account the relative velocity of the gas and liquid streams.

The importance of the gas-liquid relative velocity in the analysis of packed-column absorption studies is illustrated by showing how the true effect of diffusivity can be masked.

For a disk-column, a simple correlation is established between the gas-film mass-transfer coefficient, the diffusion coefficient and the gas-phase pressure drop. The relationship provides excellent support for the 2/3 exponent on the diffusivity.

Résumé—L'auteur étudie les vitesses d'échange massique dans une colonne à disque avec des liquides se vaporisant dans un gaz circulant à contre-courant. La résultats de ces études sont reliés convenablement par un " facteur relatif j_D" qui tient compte de la vitesse relative des courants de gaz et de liquide.

L'importance de la vitesse relative gaz liquide, de l'absorption dans les colonnes de garnissage est mise en évidence en montrant combien l'effet exact de la diffusion peut être masqué.

L'auteur établit pour une colonne à disque une relation simple entre le coefficient de transfert de masse gaz-film, le coefficient de diffusion et la perte de charge dans la phase gazeuse. La relation montre la valeur de l'exposant 2/3 du coefficient de diffusion.

Zusammenfassung—In einer Scheibenkolonne wurden Stoffübergangswerte durch Verdampfung von Flüssigkeiten in entgegenströmende Gase untersucht. Die Ergebnisse lassen sich gut durch einen " relativen j_D-Faktor " wiedergeben, der die relative Geschwindigkeit zwischen Gas und Flüssigkeit berücksichtigt.

Die Bedeutung dieser relativen Geschwindigkeit bei der Untersuchung von Füllkörper-Absorptionskolonnen wird dadurch bewiesen, das gezeigt wird, wie die wahre Wirkung der Diffusion überdeckt werden kann.

Für eine Scheibenkolonne wird eine einfache Beziehung zwischen dem Stoffübergangskoeffizient auf der Gasseite, dem Diffusionskoeffizient und dem gasseitigen Druckabfall angegeben. Der Exponent 2/3 für den Diffusionsterm wird gut bestätigt.

INTRODUCTION

THE disk-column, as introduced by STEPHENS and MORRIS [1], has been used primarily for the investigation of gas absorption systems in which the liquid-film is the major diffusional resistance. All previous measurements of gas-film controlled mass-transfer rates in a standard disk-column [1], [2] and [3] have been made with air as the principal gas phase. Further investigation was considered desirable to establish the effects of the properties of other gases on the gas-phase mass-transfer process. It seemed reasonable to expect that such a study might also elucidate some of the factors generally influencing mass transfer: e.g.

the relative velocity of the fluid streams; the true effects of diffusivity and the relation between the pressure drop and the mass-transfer coefficient. It is possible to investigate these variables in a disk-column, because of the known gas-liquid interfacial area.

In this investigation, the gas-phase mass-transfer process was studied by measuring the rates of vaporization of liquids in different gases for a wide range of counter-current gas and liquid flow rates. Using this technique, complications arising from diffusional resistance in the liquid phase were absent and the gas-film mass-transfer coefficients could be measured directly.

EXPERIMENTAL

During a preliminary investigation, the liquid velocity on the disks was determined by hold-up measurements on an eighty disk assembly. For water, at liquid flow rates less than 240 lb/hr ft these velocities compared favourably with those calculated according to the method of COOPER, *et al.* [4]. At greater liquid flow rates, a departure from the theoretical equation was evident. The observed velocities were less than those obtained by calculation. This is presumably due to the formation of ripples on the rims of the disks at high liquid rates. Ripple formation was reported by TAYLOR and ROBERTS [3].

In the experiments, the gas-phase mass-transfer process was studied by measuring the rates of vaporization of water into counter-current streams of hydrogen, air, carbon dioxide, dichlorodifluoromethane and the vaporization of *n*-heptane by air in a standard disk-column. The column and the auxilliary equipment used has been described previously by the author [5]. The principal dimensions of the column are given in Table 1. The column was operated under conditions such that no spray or splashing of the liquid was observable. To achieve these conditions in the *n*-heptane experiments, extremely small liquid rates were required.

Table 1. Disk-column, principal dimensions

Number of disks	27
Dry surface area of disks*	0·161 ft^2
Average disk diameter	0·0484 ft
Average disk thickness	0·0148 ft
Tube internal diameter	0·082 ft
Free space (dry)	89%
Mean perimeter for liquid flow	0·122ft
Equivalent diameter for gas flow	0·052 ft

*Uncorrected for liquid film thickness or loss of area at points of contact, but used throughout as an approximation of the true liquid surface area.

The partial pressure of the diffusing component in the outlet gas stream was measured continuously with a calibrated gas analysis cell of the thermal conductivity type. The inlet gas to the column was analysed at the beginning and end of each series of run. The change was too small to warrant continuous analysis. The equilibrium vapour pressures were interpolated from the extensive tables compiled by STULL [6].

The diffusion coefficients for the water vapour systems were taken from the table of selected experimental data given by WILKE and LEE [7] and the diffusion coefficient for the air–*n*-heptane system was obtained from the measurements of SCHLINGER *et al.* [8]. The relevant diffusion data are given in Table 2.

The rates of vaporization were calculated from the steady-state partial pressure of vapour in the exit gas stream, the inlet partial pressure and the gas flow rate. For the *n*-heptane experiments, the calculated true mean driving force was used to evaluate the mass-transfer coefficient. However, in the water vaporizations, because of the very much higher liquid rates, negligible error was introduced by using the log mean of the terminal driving forces, based on bulk liquid temperatures. The calculated gas-film mass-transfer coefficients and other relevant results for the systems studied are given in Table 3.

Table 2. Published diffusion data

System	Temp. (°C)	Diffusion coefficient (cm^2/sec)	Schmidt number
H_2–H_2O	20	0·850	1·25
Air–H_2O	25	0·260	0·60
CO_2–H_2O	25	0·164	0·48
CCl_2F_2–H_2O	25	0·105	0·25
Air–*n* C_7H_{16}	21	0·073	2·05

CORRELATION AND DISCUSSION OF RESULTS

For a disk-column, STEPHENS and MORRIS [1] and TAYLOR and ROBERTS [3] have shown that the relative velocity of the gas and liquid streams can be used to correlate results of countercurrent and co-current absorptions of ammonia in water from a dilute ammonia–air mixture. The basis for using the relative velocity of the gas and liquid streams for a particular type of absorption, i.e. either countercurrent or co-current has not been investigated before.

131

Table 3. Experimental and calculated results

Liquid rate (lb/hr ft)	Gas velocity (ft/sec)	Liquid velocity (ft/sec)	Relative velocity (ft/sec)	Partial pressure of diffusing component (mm Hg)		Temperature (°C)				Gas film mass transfer coefficient lb mole / (hr ft² atm)
				Inlet	Outlet	Liquid inlet	Liquid outlet	Gas inlet	Gas outlet	
				Vaporization of water with hydrogen						
325	5·15	1·08	6·23	0·4	13·8	25.4	24.4	26.3	25.9	1.23
325	9·44	1·08	10·52	0·5	11·4	25·4	23·8	26·2	25·6	1·70
325	12·19	1·08	13·27	0·5	10·7	24·4	23·5	26·2	25·5	2·03
325	14·59	1·08	15·67	0·6	10·1	25·4	23·1	25·9	25·3	2·26
325	16·99	1·08	18·07	0·7	9·5	25·4	22·8	25·4	25·2	2·42
325	8·24	1·08	9·32	0·4	11·5	25·1	23·6	25·9	25·2	1·55
325	12·87	1·08	13·95	0·4	10·1	25·1	23·0	26·0	25·0	2·05
325	14·76	1·08	15·84	0·5	9·8	25·1	22·8	26·2	25·0	2·26
325	21·63	1·08	22·71	0·5	9·0	25·1	22·0	26·0	24·7	3·02
325	26·78	1·08	27·86	0·6	8·5	25·1	21·5	25·0	24·2	3·50
325	19·40	1·08	20·48	0·6	9·2	25·1	22·0	23·8	24·0	2·76
325	15·62	1·08	16·70	0·7	9·8	25·0	22·5	23·6	24·2	2·39
325	10·13	1·08	11·21	0·7	11·3	25·0	23·1	24·0	24·6	1·86
325	5·56	1·08	6·64	0·7	13·4	25·0	23·8	24·8	25·1	1·29
				Vaporization of water with air						
325	8·24	1·08	9·32	2·6	11·8	24·0	22·6	23·5	23·6	1·52
325	7·21	1·08	8·29	2·6	12·3	24·0	22·8	23·5	23·7	1·42
325	6·18	1·08	7·26	2·6	12·5	24·0	22·9	23·6	23·7	1·25
325	4·98	1·08	6·06	2·6	13·4	24·0	23·0	23·6	23·8	1·14
325	3·84	1·08	4·92	2·6	14·3	24·0	23·1	23·6	23·8	1·00
325	2·68	1·08	3·76	2·6	14·8	23·9	23·2	23·5	23·7	0·75
325	1·92	1·08	3·00	2·6	16·4	23·9	23·3	23·4	23·7	0·67
325	1·22	1·08	2·30	2·6	18·6	23·8	23·4	23·1	23·5	0·60
298	1·70	1·04	2·74	2·8	18·9	26·2	25·6	24·9	25·2	0·60
240	1·70	1·00	2·70	2·8	18·6	26·1	25·4	24·6	24·9	0·59
149	1·70	0·74	2·44	2·8	18·1	25·8	24·8	24·0	24·3	0·58
64	1·70	0·43	2·13	2·8	16·5	25·3	23·6	23·9	24·0	0·52
298	2·40	1·04	3·44	2·8	15·2	23·5	22·8	21·6	22·2	0·74
240	2·40	1·00	3·40	2·8	15·0	23·5	22·6	21·9	22·3	0·73
149	2·40	0·74	3·14	2·8	14·2	23·2	22·1	21·9	22·2	0·68
64	2·40	0·43	2·83	2·8	13·2	22·8	21·0	21·6	21·8	0·62
298	3·78	1·04	4·82	2·6	12·9	22·7	21·8	21·1	21·5	0·97
240	3·78	1·00	4·78	2·6	12·7	22·9	21·9	21·1	21·6	0·89
149	3·78	0·74	4·52	2·6	12·1	22·7	21·3	21·1	21·4	0·84
64	3·78	0·43	4·21	2·6	11·3	22·2	19·8	20·7	20·7	0·80
298	4·81	1·04	5·85	2·8	12·1	22·8	21·8	21·0	21·8	1·02
240	4·81	1·00	5·81	2·8	11·8	22·8	21·6	21·3	22·1	0·98
149	4·81	0·74	5·55	2·8	11·5	22·9	21·4	21·5	22·2	0·93
64	4·81	0·43	5·24	2·8	10·7	22·7	20·1	21·8	22·0	0·87
298	5·94	1·04	6·98	2·8	11·7	23·0	22·0	22·2	22·6	1·16
240	5·94	1·00	6·94	2·8	11·1	23·0	21·8	22·3	22·6	1·05
149	5·94	0·74	6·68	2·8	10·6	23·0	21·3	22·4	22·5	1·01
64	5·94	0·43	6·37	2·8	10·2	23·0	20·0	22·4	22·3	0·97

Table 3—contd. *Experimental and calculated results.*

Liquid rate (lb/hr ft)	Gas velocity (ft/sec)	Liquid velocity (ft/sec)	Relative velocity (ft/sec)	Partial pressure of diffusing component (mm Hg)		Temperature (°C)				Gas film mass transfer coefficient lb mole (hr ft² atm)
				Inlet	Outlet	Liquid inlet	Liquid outlet	Gas inlet	Gas outlet	
				Vaporization of water with carbon dioxide						
325	1·51	1·08	2·59	1·6	18·8	26·7	26·2	29·4	29·4	0·52
325	1·82	1·08	2·90	1·7	18·4	26·9	26·3	29·1	29·2	0·58
325	2·06	1·08	3·14	1·9	16·7	26·9	26·3	29·0	29·3	0·54
325	3·67	1·08	4·75	2·3	14·2	26·9	26·0	26·7	28·6	0·72
325	2·82	1·08	3·90	2·5	16·4	27·0	26·2	27·5	29·2	0·69
325	2·47	1·08	3·55	2·7	17·1	27·0	26·4	28·3	29·7	0·65
325	2·09	1·08	3·17	2·8	17·5	27·0	26·5	29·0	30·0	0·57
325	1·65	1·08	2·73	2·9	18·4	27·0	26·6	29·9	30·5	0·50
325	1·08	1·08	2·16	3·1	19·8	27·1	26·8	31·0	31·0	0·37
325	0·88	1·88	1·96	3·2	21·5	27·1	26·9	31·0	31·2	0·37
				Vaporization of water with dichlorodifluoromethane						
325	0·61	1·08	1·69	0	15·8	23·1	22·8	20·8	21·2	0·24
325	0·93	1·08	2·01	0	13·7	23·1	22·8	20·5	21·3	0·28
325	1·14	1·08	2·22	0	13·4	23·1	22·7	20·3	21·4	0·33
325	1·11	1·08	2·19	0	13·6	23·1	22·6	20·5	21·3	0·33
325	1·56	1·08	2·64	0	12·5	23·1	22·5	20·2	21·3	0·43
325	0·84	1·08	1·92	0	15·1	23·1	22·7	20·2	21·3	0·32
325	0·79	1·08	1·87	0	14·4	23·1	22·7	20·2	21·3	0·26
				Vaporization of n-heptane with air						
15	1·58	0·25	1·83	0	8·0	13·7	7·5*	12·8	12·3	0·21†
15	2·40	0·25	2·65	0	6·1	13·1	5·5*	12·5	11·0	0·25†
15	3·60	0·25	2·85	0	4·8	12·7	4·0*	12·2	10·0	0·30†
15	5·15	0·25	5·40	0	4·2	12·3	3·0*	11·3	9·2	0·39†
15	6·65	0·25	6·90	0	3·8	12·2	3·2*	11·7	9·3	0·45†
15	8·58	0·25	8·83	0	3·2	12·4	3·2*	11·7	9·0	0·48†

*These temperatures measured close to the last disk by copper–constantan thermocouple with cold junction at 0°C.
†Corrected for true mean driving force.

In an earlier publication [5] the author has shown that a conventional Reynolds number vs. friction factor type of graph is not satisfactory for correlating the gas-phase pressure drops across a disk-column, when the disks are irrigated with water. A further analysis of these results has since been made [9], in which the significant velocity term was taken as the relative velocity of the gas an liquid streams. Pressure drops across the dry column and those when irrigated with water at rates less than that required for ripple formation can all be correlated by a single line on a " relative friction factor " vs. " relative Reynolds number " graph. These findings were considered to support the contention that the relative velocity of the gas and liquid streams is also the significant velocity term in the mass-transfer process.

If the gas–liquid relative velocity were significant in the original dimensional analysis of the mass-transfer process, then a modified approach could be derived.

i.e.
$$\frac{k_c L}{D} = \psi\left[\left(\frac{Lv_R \rho}{\mu}\right), \quad \left(\frac{\mu}{\rho D}\right), \quad \left(\frac{p_{BM}}{P}\right)\right] \quad (1)$$

A " relative j_D " factor can then be defined:

Relative $j_D = (j_D)_R = \dfrac{k_c}{v_R} \dfrac{p_{BM}}{P} \left(\dfrac{\mu}{\rho D}\right)^{23}$ (2)

$\qquad = \dfrac{k_g}{v_R} \dfrac{p_{BM}}{\rho_m} \left(\dfrac{\mu}{\rho D}\right)^{23}.$ (3)

It is proposed that the " relative j_D factor " should be a function of the " relative Reynolds number "

$$(R_e)_R = \left(\dfrac{L v_R \rho}{\mu}\right).$$ (4)

The newly defined " relative j_D factor " and the conventional j_D correlation were applied to the experimental results. Fig. 1 is a comparison of the two methods of correlation. " The relative

FIG. 1. Comparison of the j_D and $(j_D)_R$ correlations.
(a) Constant liquid rate $\Gamma = 325$ lb/hr ft
    Water vaporization
       △ hydrogen
       ● air
       ◑ carbon dioxide
       + dichlorodifluoromethane
       ○ air $\Gamma = 298$ lb/hr ft
(b) All liquid rates.
    Water vaporization
       △ hydrogen
       ● air
       ◑ carbon dioxide
       + dichlorodifluoromethane
    n-Heptane vaporization
       ⊕ air

j_D " correlation includes all liquid rates. The j_D correlation is only for the constant liquid rate of 325 lb/hr ft.

The conventional j_D type of correlation shows the hydrogen results as being displaced below the air points, particularly at low Reynolds numbers, where the effects of relative velocity are greatest. The difference between the air and hydrogen points decreases with increased Re. This is to be expected, if the relative velocity is significant, as at higher values of Re, the liquid velocity has a much smaller effect, because of the higher gas velocities. The dichlorodifluoromethane points, however, do not exhibit the same trend. To be consistent, these results should be displaced above the air whereas they are also displaced below.

Irrespective of liquid flow rate, the newly proposed " relative j_D " vs. " relative Re " plot correlates all the results except the dichlorodifluoromethane points, which are displaced well below the line of best fit through the other points. A similar discrepancy is observed for the two low velocity carbon-dioxide points. These two carbon-dioxide points and the bulk of the dichlorodifluoromethane points represent cases in which the liquid velocity on the disks is greater than the upward gas velocity.

At low gas velocities, the gas is carried downward by the liquid and the resulting reverse flow mixes the gas vertically in the column so that the mean driving force is less than for true countercurrent contact. Under these conditions, mass-transfer coefficients, evaluated by assuming no longitudinal mixing, are considerably smaller than the true coefficients. COOPER et al. [10] reported similar anomalies in a packed tower when the downward liquid velocity exceeded the upward gas velocity.

GAS/LIQUID RELATIVE VELOCITY EFFECTS IN PACKED-COLUMNS

The effect of diffusivity on the rate of gas-phase mass-transfer in packed-columns has been the subject of conflicting reports and apparent anomalies for many years. In general, it would appear the experimental results for systems in which there is no liquid flow (e.g. pre-wetted
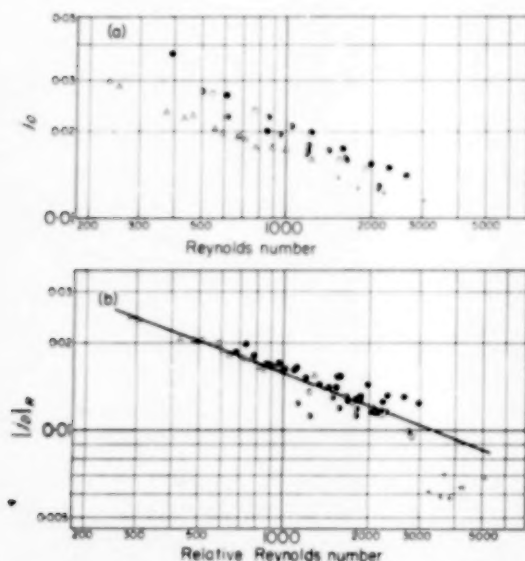
raschig rings, naphthalene berl saddles, etc.) can be well correlated using the j_D factor with the 2/3 exponent on the Schmidt number, whereas for irrigated systems a range of exponents from 0·15 to 0·90 has been required to correlate the results. SHULMAN *et al.* (11) has shown that differences in effective interfacial areas can explain the low exponent of 0·15 obtained by SUROSKY and DODGE [12]. The exponents on the SCHMIDT number of 0·90 and 0·77 obtained by LYNCH and WILKE [13] and YOSHIDA [14], respectively, cannot be explained by differences in interfacial areas, because only one liquid phase was used. It is proposed that the true effect of diffusivity in these studies is masked by the relative velocity of the gas and liquid streams.

Although a formal analysis of relative velocity effects in a packed-column requires knowledge of the flow paths of both the gas and liquid, the effect of the gas/liquid relative velocity on the exponent of the Schmidt number can be demonstrated by evaluating the relative velocities in terms of an unknown tortuosity (β) of the gas flow path and an assumed true mean liquid velocity (v_L). The true mean gas velocity can be calculated in terms of β by equation (5).

$$v_g = \beta \left(\frac{G}{\rho \epsilon} \right). \quad (5)$$

Now since $v_R = v_g + v_L$

$$v_R = \beta \left(\frac{G}{\rho \epsilon} + \frac{v_L}{\beta} \right). \quad (6)$$

For example, the results of LYNCH and WILKE [13] can be correlated by the " relative j_D factor" with the 2/3 exponent on the Schmidt number, if the magnitude of v_L/β in equation (6) is assumed to be 0·1 ft/sec. This assumption corresponds with a liquid velocity of 0·067 ft/sec when the value of β is 1·5. Both of these figures are of an order which would be expected in a packed-column. The selected recalculated results are plotted as the product $\beta \left[a \left(j_D \right)_R \right]$ vs. $1/\beta \left(v_R \rho / \mu \right)$ on a log–log scale in Fig. 2. The points plotted cover the range of LYNCH and WILKE's experiments up to the observed loading points.

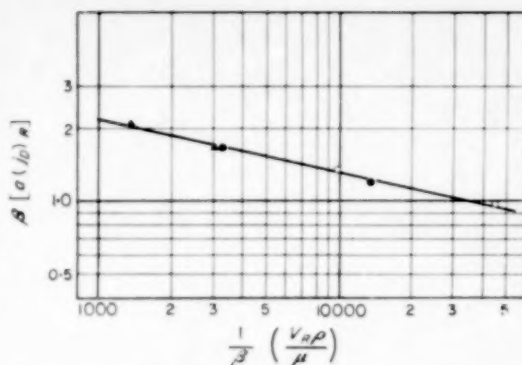The good correlation of the points in Fig. 2

FIG. 2. Correlation of LYNCH and WILKE [13] data using " relative j_D factor " and " relative Reynolds number." Data of LYNCH and WILKE – liquid rate = 1575 lb/hr ft² recalculated assuming $\frac{v_L}{\beta} = 0·1$ ft/sec. water vaporization

▲ helium
● air
○ dichlorodifluoromethane

shows very clearly the marked effect of the small liquid velocity correction. In the main, this is due to the very low apparent dichlorodifluoromethane gas velocities of 0·25 to 1·4 ft/sec. The exponent of the Schmidt number in this correlation is 2/3 as compared with the exponent of 0·9 obtained by LYNCH and WILKE [13] when using the conventional correlation.

CORRELATION OF THE MASS-TRANSFER COEFFICIENTS IN TERMS OF THE PRESSURE DROP

The gas-phase pressure drop across the disk-column was measured with a micromanometer for each of the mass transfer runs. These readings were converted to the pressure drop across one disk by correcting for the pressure drop due to the column shell and by dividing by the number of disks in the assembly. A formal theoretical analogy between the pressure drops and the mass-transfer coefficients was not possible because of the unknown contribution of form drag to the measured total pressure drop. An entirely empirical approach was used to determine if any consistent relationship existed.

For a given system, it seemed reasonable to expect the pressure drop and the mass transfer

135

coefficient to be affected similarly by changes in gas velocity and liquid rate. A plot of k_g versus ΔP_d for the air–water system showed that these quantities could be correlated by a straight line on a log–log graph as shown in Fig. 3. This method of correlation is very attractive, particularly as the uncertain effects of liquid flowing over the disks are eliminated, because the mass-transfer coefficient and the pressure drop are affected equally by these uncertainties.
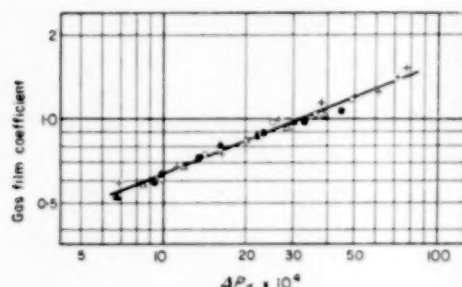

FIG. 3. The relation between pressure drop and the mass-transfer coefficient. Air – water system.

Water vaporization with air

$+$ $\Gamma = 325$ lb/hr ft
$\bigcirc$ $\Gamma = 298$ lb/hr ft
$\bullet$ $\Gamma = 240$ lb/hr ft
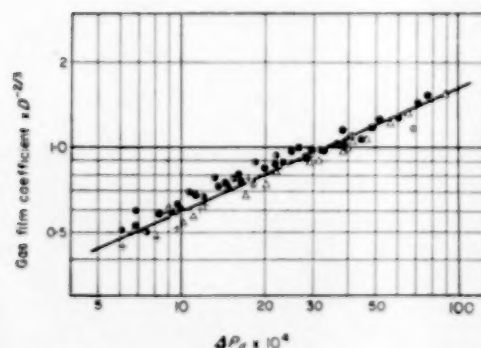$\triangle$ $\Gamma = 149$ lb/hr ft
$\blacktriangle$ $\Gamma = 64$ lb/hr ft

FIG. 4. Generalized correlation of gas-film mass-transfer coefficients in terms of the diffusivity and the pressure drop.

Water vaporization

$\triangle$ hydrogen
$\bullet$ air
$\mathbb{O}$ carbon dioxide
$+$ dichlorodifluoromethane

n-Heptane vaporization

$\odot$ air

All the mass transfer results of this investigation can be well correlated by a log–log plot of $k_g D^{-2/3}$ vs. ΔP_d as shown in Fig. 4. This type of correlation has not been reported previously. The 2/3 exponent on the diffusivity is considered to lend excellent support for the use of this exponent in correlating gas-phase mass-transfer results, because the uncertain effects of liquid velocity, associated with other published investigations, are eliminated in this approach.

NOTATION

a = area of interphase contact in a packed column ft^2/ft^3

D = molecular diffusivity ft^2/hr

G = gas superficial mass velocity $lb/hr\,ft^2$

$j_D = \dfrac{k_g\,p_{BM}}{v_g\,\rho_m}\left(\dfrac{\mu}{\rho D}\right)^{2/3}$ dimensionless

$(j_D)_R = \dfrac{k_g\,p_{BM}}{v_R\,\rho_m}\left(\dfrac{\mu}{\rho D}\right)^{2/3}$ dimensionless

k_c = mass-transfer coefficient   lb mole/hr ft^2 lb mole/ft^3

k_g = mass-transfer coefficient   lb mole/hr ft^2 atm

L = characteristic dimension   ft

P = total pressure   atm

ΔP_d = pressure drop across a disk lb/ft^2

p_{BM} = logarithmic mean of the partial pressure of the non-diffusing component at the phase boundary and the bulk of the fluid   atm

Re = Reynolds number $= \dfrac{Lv\,\rho}{\mu}$ dimensionless

$(\text{Re})_R$ = " relative Reynolds number " $= \dfrac{Lv_R\,\rho}{\mu}$ dimensionless

v = fluid velocity   ft/hr

v_g = average gas velocity   ft/hr

v_L = average liquid velocity   ft/hr

v_R = relative velocity of the gas and liquid streams   ft/hr

β = tortuosity of the gas fluid path in a packed column   dimensionless

ϵ = packed bed porosity   dimensionless

Γ = liquid rate per wetted perimeter   lb/hr ft

ρ = gas density lb/ft^3

ρ_m = molar gas density   lb moles/ft^3

μ = gas viscosity   lb/ft hr

References

[1] STEPHENS E. J. and MORRIS G. A. *Chem. Engng. Progr.* 1951 **47** 232.

[2] ROPER G. H. *Chem. Engng. Sci.* 1953 **2** 18.

[3] TAYLOR R. F. and ROBERTS F. *Chem. Engng. Sci.* 1956 **5** 168.

[4] COOPER C. M., DREW T. B. and MCADAMS W. H. *Trans. Amer. Inst. Chem. Engrs.* 1933–4 **30** 158.

[5] WARNER N. A. *Chem. Engng. Sci.* 1954 **3** 77.

[6] STULL D. R. *Industr. Engng. Chem.* 1947 **39** 517.

[7] WILKE C. R. and LEE C. Y. *Industr. Engng. Chem.* 1955 **47** 1253.

[8] SCHLINGER W. G., REAMER H. H., SAGE B. H. and LACEY W. N. *Fundamental Research on Occurrence and Recovery of Petroleum.* Report of Progress. American Petroleum Institute 1952–1953. p. 70.

[9] WARNER N. A., Ph.D. Thesis in Chemical Engineering. New South Wales University of Technology 1958.

[10] COOPER C. M., CHRISTL R. and PEFRY L. C. *Trans. Amer. Inst. Chem. Engrs.* 1941 **37** 979.

[11] SHULMAN H. L., ULLRICH D. F. and WELLS N. *A.I.Ch.E. Journal* **1** 247 1955.

[12] SUROSKY A. E. and DODGE B. F. *Industr. Engng. Chem.* 1950 **42** 1112.

[13] LYNCH E. J. and WILKE C. R. *A.I.Ch.E. Journal* 1955 **1** 9.

[14] YOSHIDA F. *Chem. Engng. Progr.* Symposium Series No. 16 1955 **51** 59.

Book Reviews

Chemical Engineering Practice. Edited by H. W. CREMER and T. DAVIES. Vol. V. Fluid Systems I. Butterworths Scientific Publications, London and Academic Press, New York, 1958. vi + 695 + xxiv pp. London 95s. $13.30

Chemical Engineering Practice. Edited by H. W. CREMER and T. DAVIES. Vol. VI. Fluid Systems II. Butterworths Scientific Publications, London and Academic Press, New York, 1958. 600 pp. 95s. $13.30.

IT is fashionable at the present time to regard the " unit operations " concept in chemical engineering as obsolescent, and this idea is certainly being fostered in the chemical engineering schools. Nevertheless, there are no chemical engineers who do not know what is meant by unit operations, and it is with certain of these transfer processes, to use the current description, that most of Volumes 5 and 6 of Chemical Engineering Practice are concerned, although the books carry the titles Fluid Systems I and II respectively.

The first half of Volume 5 follows logically from Volume 4, which contained a large section on the academic ideas of fluid mechanics. In Volume 5, these ideas are supplemented by a useful practical discussion of the selection and performance of pumps, fans, blowers and compressors, and descriptions of pipe systems for liquid and gases. Worked examples of design calculations are included for those who regard this series as handbooks of procedures. Next in the book is an authoritative chapter on the design of high pressure vessels, in which the academic origin is very obvious, but which does contain a lot of useful practical information. The next chapter on the production of vacuum combines a good description of the various kinds of equipment with a valuable section containing worked examples on flow rates and pumping rates for the molecular flow regions, pump-down times and so on.

The rest of Volume 5 consists of a 327 page contribution on solvent extraction and distillation processes. All the usual text-book material is included in a commendably brief form, supplemented by critical comments on the latest work and by comprehensive references. The chapters in this section have the headings, " Liquid–liquid equilibrium ; liquid-liquid stagewise contact ; extraction equipment ; vapour–liquid equilibria ; rectification of binary mixtures ; multi-component distillation, and distillation equipment." The authors are all associated with the Department of Chemical Engineering at Birmingham and are known for their original contributions to the subject. The practical equipment side is adequately covered in the space available. Taking the section as a whole, it appears that this will be the starting point of a literature survey for many future research students. Volume 6 continues the discussion of gas–liquid systems by chapters on gas absorption and on the operating characteristics of packed absorption columns. Once again, there is the apparently inevitable mixture of text-book and a good deal of practical information and design data obtained from actual operating plant, although much of the latter has been previously published. The final chapter dealing with gas–liquid systems is a very good one on evaporation practice, with the emphasis really on the practice. The combination of text and illustrations is very informative indeed.

Gas–solid systems are considered next. There are chapters on fluidization and fluidized beds, and on the general applications of fluidization with special reference to the carrying out of chemical reactions. These sections contain an orthodox discussion of fluidizing velocity, pressure drop, mass and heat transfer and a description of some of the processes for which fluidized beds are used, together with some good practical points. Anyone expecting up-to-the-minute information will be disappointed at the omission of such topics as the effect of bubble formation which has recently attracted a good deal of attention. The other topic which can be considered under the heading of gas–solid systems is Adsorption and the chapter on this topic is a general description of the elementary principles, together with useful illustrations of how the process is used in industry.

Chapters on the liquefaction and fractionation of gases and on refrigeration practice can best be described as a useful introduction to these subjects, and are accompanied by exhaustive references. The next main heading, " Liquid–liquid Systems " is mainly concerned with the separation processes of leaching, crystallization, filtration and centrifuging. The authors of these chapters have contrived to blend an adequate amount of the simple theory with a good deal of useful practical information, particularly in the selection and operation of filters. There is a chapter on colloids, which comprises nearly all a student needs to know in a degree course, and the Volume is completed with a chapter on sublimation and vacuum freeze drying.

If an attempt is to be made to assess the value of the work as a whole, reference must be made to what H. W. CREMER, the General Editor, wrote in the preface to Volume I of the series, " The chemical engineer is increasingly at a loss to find ready-made answers to his problems. There still remains a great gulf fixed between theory and practice, a space which, of necessity, he must on occasion himself endeavour to fill." Do these volumes help him ? The blend of practical information with the academic approach which is characteristic in all the contents certainly deserves to be successful. And perhaps Mr. CREMER would now agree that since he wrote his preface the gulf between theory and practice is narrowing perceptibly.

E. S. SELLERS

Low Temperature Physics and Chemistry. Edited by J. R. DILLINGER. University of Wisconsin Press, 1958. 676 pp. $6.00.

THIS book contains summaries of the 225 papers presented at the Fifth International Conference on Low Temperature held at the University of Wisconsin in August, 1957. It is obviously impossible to review such a book but it may be useful to the reader to list the main headings under which the papers were grouped. These follow:

I. Viscosity and flow properties of liquid He^4.

II. Heat flow in, and specific heat of, liquid He^4.

III. Dielectric constant. Refractive index, film thickness and rotation of liquid He^4.

IV. Heat diffraction, sound transmission and structure of He^4.

V. Liquid He^3 and He^4.

VI. Theory of liquid He^4 and liquid He^3.

VII. Solutions of He^3 in He^4.

VIII. The temperature scale and temperature measurement.

IX. Instrumentation: He^3 Dewar systems, heat switches, a liquefier, computer elements; techniques.

X. Theories of superconductivity.

XI. Properties of some superconductors.

XII. Intermediate state of superconductors.

XIII. Superconductivity of thin films, contact resistance, pressure effects and volume changes in superconductivity.

XIV. Millimeter wave absorption and the paramagnetic effect in superconductors.

XV. Thermal and electrical conductivity of elements and compounds.

XVI. Thermal and electrical conductivity of alloys.

XVII. Measurements of specific heats of solids.

XVIII. Analyses of specific heat data.

XIX. De Haas–Van Alphen and other oscillatory effects.

XX. Magnetoresistance, thermoelectricity, resistivity and hall effect.

XXI. Mechanical properties of solids including solidified gases

XXII. Paramagnetism and resonances.

XXIII. Magnetic susceptibilities.

XXIV. Ferromagnetism and general magnetic properties.

XXV. Thermal expansion, absorption spectra, dielectric properties, rotational transitions, polymers and nuclear magnetic resonance.

XXVI. Nuclear orientation experiments.

It can be seen from this list that the papers deal almost entirely with phenomena at the temperature of liquid helium and below. There is practically nothing which is of direct interest to the chemical engineer.

B. F. DODGE

O. KUBASCHEWSKI and E. Ll. EVANS: **Metallurgical Thermochemistry.** (Third Edition – revised). Pergamon Press, London, 1958, xiv + 426 pp. 63s.

READERS of the earlier editions, and in the field of physical chemistry there must be many indeed, will recall that the book was divided into five sections, namely: The Theoretical Basis; Experimental Methods; The Estimation of Thermochemical Data; Thermochemical Data; Examples of Thermochemical Treatment of Metallurgical Problems. These divisions are retained in the third edition. The first and third sections remain materially the same in this later edition, whilst in the second section there have been a few changes illustrating new apparatus and techniques, particularly in the part dealing with calorimetry. Two additional examples in the fifth section are to be welcomed, and the tables of thermochemical data in the fourth section have been revised and extended. It is disappointing, however, in this very useful fourth section, to find that the data on dilute solutions, which included information on the solubilities of gases in metals, have been omitted from this edition.

One cannot help feeling that anyone already possessing a copy of the second edition would have perhaps preferred a supplementary volume containing only the revised and extended tables of thermochemical data, particularly as the third edition of the book has increased in price by eight shillings.

However, for those interested in modern thermochemistry, this book remains one of the outstanding works in its field. One can argue the theoretical section would have to be supplemented by additional reading, and that the experimental section is uneven in that the review of calorimetric methods is more complete than, for example, the parts dealing with cells and gas-condensed phase equilibria measurements; it is certain, though, that the last three sections would immeasurably benefit anyone who has to handle thermochemical data.

The book obviously has a metallurgical bias but the writer believes that this in no way detracts from its general appeal. It is the emphasis on the critical assessment of thermochemical data and the correct manipulation of such data, together with the reference tables, which make the book so valuable to anyone who is interested in the practical application of chemical thermodynamics.

B. C. H. STEELE

A. REGNER: **Electrochemical Processes in Chemical Industries.** Constable. 1957. 464 pp. 30s.

ON ACCOUNT of the title one would suppose that all electrochemical processes finding application in industry are covered. This however is not the case: the book describes only processes in aqueous solutions and so the electrolysis of molten salts (manufacture of aluminium, sodium, etc.) and the electrochemistry of gases (e.g. the

manufacture of ozone) are not dealt with. On the other hand some processes, such as the manufacture of hydrochloric acid from salt and sulphuric acid, which have no relation at all to electrochemistry, are included.

The first 170 pages contain a survey of theoretical electrochemistry. The objection could be made that this part is rather superfluous as, in the first place, there are already many books covering this subject and, secondly, because many of the theoretical explanations are not referred to when dealing with the applications. So, for instance, the theory of the conductance of strong electrolytes, that of galvanic cells and that of the cathodic precipitation of metals which have no follow-up in the second part.

The description of many processes is more elaborate than may be found in other books covering the same field (BILLITER, MANTELL) which naturally is an advantage. On the other hand however obsolete processes are treated, e.g. the old processes for the manufacture of bleaching powder, the electrolytical manufacture of hypochlorite and the Griesheim-Elektron cell which are of no more than historical interest.

The bibliography is not at all adequate. All that is given is a list of about thirty books, only twelve of them being less than twenty years old, and half of these are in Russian. One of the consequences is that one always doubts whether the given process data originate from own experience or are taken from literature. The same applies for some explanations of reaction mechanisms which are sometimes not very likely. For instance, is it not true that the anodic evolution of chlorine from a chloride solution is due to overvoltage of oxygen, neither is the reasoning why ammonium sulphate gives a higher output of persulphate than sulphuric acid as an electrolyte very convincing.

In conclusion it must be said that this book has hardly any advantage above the existing textbooks and owing to its lack of literature references, it is useless as a reference book.

J. G. HOOGLAND

W. MIALKI : **Kernverfahrenstechnik. Eine Einführung für Ingenieure.** Springer-Verlag, Berlin/Göttingen/ Heidelberg 1958. 483 S. 78,60 DM.

Es gibt in der Bundesrepublik noch nicht viele gute Einführungen in die Reaktortechnik. So hat der Verfasser eine echte Lücke ausgefüllt, indem er in Anlehnung an die vorzüglichen amerikanischen Einführungen VON GLASSTONE, STEPHENSON und MURRAY ein deutsches Lehrbuch verfasste. Aus der speziellen Fachrichtung des Verfassers ist es wohl zu erklären, dass er sein Buch " Kern-Verfahrenstechnik " genannt hat, obwohl es sich mehr um " Reaktortechnik " handelt. Beim Bemühen, die Verfahrenstechnik dennoch nicht zu kurz kommen zu lassen, mussten im Stoff Kompromisse geschlossen werden, die der Einheitlichkeit und Ausgewogenheit des Buches abträglich sind.

Dass der Verdampfungsvorgang bewusst nicht berücksichtigt wurde, ist angesichts der Wichtigkeit der Siedewasserreaktoren allzu einseitig ; demgegenüber wurde der Wärmeübergang bei flüssigen Metallen eher zu ausführlich behandelt. Die Moderatoren sollten wegen ihrer Wichtigkeit eingehender besprochen, die Kühlmittel nicht in der Gliederung als Werkstoffe bezeichnet werden.

In einer Neuauflage sollte eine Reihe von Fehlern (z.B. Coulomb'sches Gesetz, S. 83–87) oder Ungenauigkeiten (z.B. Diffusionslänge L und Fermialter τ sind als wirkliche mittlere Entfernungen angegeben) vermieden werden. Auch sollten möglichst für die Wirkungsquerschnitte die allgemein üblichen Bezeichnungen gewählt werden, also

$$\sigma_{total} = \sigma_{Absorption} + \sigma_{Streuung} ;$$
$$\sigma_{Absorption} = \sigma_{Spaltung} + \sigma_{Strahlungseinfang} .$$

Zu den unbestreitbaren Vorzügen des Buches gehört das wohlgeglückte Bemühen des Verfassers, die physikalischen Vorgänge anschaulich zu behandeln, wodurch es sich für Studierende empfiehlt.

K. JAROSCHEK

BOOKS RECEIVED

H. JEBSEN-MARWEDEL (editor): Glastechnische Fabrikationsfehler. Springer–Verlag 1959.

SELECTION OF CURRENT PAPERS OF INTEREST TO CHEMICAL ENGINEERS

P. DEBYE and R. L. CLELAND : Flow of liquid hydrocarbons in porous Vycor (glass). (Flow through this porous medium deviates from Poiseuille's law). *J. Appl. Phys.* 1959 **30** 843–849.

U. P. OPPENHEIM : Experimental verification of theoretical relations between total gas absorptivities and total gas emmisivities for CO. *J. Appl. Phys.* 1959 **30** 803–807.

S. A. ZWICK : Behaviour of small permanent gas bubbles in a liquid. Part I. Isolated bubbles. *J. Math. Phys.* 1958 **37** 246–286. Part II. Bubble clouds. *Ibid.* 1959 **37** 339–353. Part III. A forced vibration problem. *Ibid.* 1959 **37** 354–370.

J. N. FRANKLIN : Numerical stability in digital and analog computation for diffusion problems. *J. Math. Phys.* 1959 **37** 305–315.

L. N. HOWARD : Hydrodynamic stability of a jet (two-dimensional viscous incompressible fluid). *J. Math. Phys.* 1959 **37** 283–298.

Y. CHIA-SHUN : Thermal instability of viscous fluids. *Quart. Appl. Math.* 1959 **17** 25–42.

W. NACHBAR, F. WILLIAMS and S. S. PENNER : The conservation equations for independent coexistent continua and for multicomponent reacting gas mixtures. *Quart. Appl. Math.* 1959 **17** 43–54.

D. A. SENIOR : A theoretical treatment of combustion in a spherical underwater gas bubble. *Proc. Roy. Soc.* 1959 A **251** 493–503.

D. G. CHRISTOPHERSON and D. DOWSON : An example of minimum energy dissipation in viscous flow (a sphere falling in a tube of slightly greater diameter). *Proc. Roy. Soc.* 1959 A **251** 550–564.

D. H. BOWEN : Hydrogen liquefaction. *Nature Lond.*, 1959 **183** 1504–1506.

W. EGUCHI and S. NAGATA : Concentration gradient in a continuous countercurrent extraction column with longitudinal back mixing. *Mem. Fac. Engng. Kyoto Univ.* 1959 **21** (Part 1) 70–83.

T. KATSUHARA : Pressure drop due to friction for upward flow of mixtures of vapour and water in a perpendicular pipe (1st report). (In Japanese). *Bull. Kyushu Inst. Tech.* 1958 No. 8 7–11.

T. OTAKE and E. KUNUGITA : Performance of irrigated packed towers—residence time of liquid. *Tech. Rep. Osaka Univ.* 1958 **8** 417–426.

T. SHIROTSUKA and N. HONDA : Fluidized bed reactor for the production of maleic anhydride from benzene. (In Japanese). *Bull. Sci. Engng. Res. Lab., Waseda Univ.* 1958 No. 10 33–38.

T. SHIROTSUKA and N. HONDA : The effect of pulsation to the absorption in columns (*sic*). (In Japanese). *Bull. Sci. Engng. Res. Waseda Univ.* 1958 No. 8 58–62.

M. TSUYAMA and M. TAGA : On the flow of the air–water mixture in the branch pipe. I. Experiment on the horizontal branch pipe which is equal to the main one in diameter (*sic*). *Bull. Jap. Soc. Mech. Engrs.* 1959 **2** 151–156.

H. ITŌ . Friction factors for turbulent flow in curved pipes. *J. Basic Engng.* (*Trans. Amer. Soc. Mech. Engrs.* Series D.) 1959 123–134.

R. B. JACOBS, K. B. MARTIN and R. J. HARDY : Direct measurement of net positive suction head. *J. Basic Engng.* (*Trans. Amer. Soc. Mech. Engrs.* Series D) 1959 pp. 147–152.

A. H. BOERDIJK : Contribution to the general theory of thermocouples. *J. Appl. Phys.* 1959 **30** 1080–1083.

F. BUECHE : Non-Newtonian viscosity of synthetic rubber and its solutions. *J. Appl. Phys.* 1959 **30** 1114.

F. S. HAM : Shape-preserving solutions of the time-dependent diffusion equation. (The rate of growth of a particle by material diffusing from a solution). *Quart. Appl. Math.* 1959 **17** 137–145.

141

YAN PO CHANG : Wave theory of heat transfer in film boiling. *J. Heat Transfer (Trans. Amer. Soc. Mech. Engrs. Series C)* 1959 **81** 7–12.

E. M. SPARROW and J. L. GREGG : A boundary layer treatment of laminar film condensation. *J. Heat Transfer (Trans. Amer. Soc. Mech. Engrs. Series C)* 1959 **81** 13–18.

W. A. WOLFE : Transient response of heated air in an enclosure with heat losses. *J. Heat Transfer (Trans. Amer. Soc. Mech. Engrs. Series C)* 1959 **81** 19–23.

R. SIEGEL and E. M. SPARROW : Transient heat transfer for laminar forced convection in the thermal entrance region of flat ducts. *J. Heat Transfer (Trans. Amer. Soc. Mech. Engrs. Series C)* 1959 **81** 29–36.

S. LEVY : Generalized correlation of boiling heat transfer. *J. Heat Transfer (Trans. Amer. Soc. Mech. Engrs. Series C)* 1959 **81** 37–42.

K. ENGELBERG-FORSTER and R. GREIF : Heat transfer to a boiling liquid—mechanism and correlations. *J. Heat Transfer (Trans. Amer. Soc. Mech. Engrs. Series C)* 1959 **81** 43–53.

G. M. DUSINBERRE : Calculation of transients in a cross-flow heat exchanger. *J. Heat Transfer (Trans. Amer. Soc. Mech. Engrs. Series C)* 1959 **81** 61–67.

R. G. DEISSLER and A. L. LOEFFLER : Heat transfer and friction for fluids flowing over surfaces at high temperatures and high velocities. *J. Heat Transfer (Trans. Amer. Soc. Mech. Engrs. Series C)* 1959 **81** 89–91.

F. KREITH, J. H. TAYLOR and J. P. CHANG : Heat and mass transfer from a rotating disk. *J. Heat Transfer (Trans. Amer. Soc. Mech. Engrs. Series C)* 1959 **81** 95–105.

L. S. HAN : Laminar heat transfer in rectangular channels. *J. Heat Transfer (Trans. Amer. Soc. Mech. Engrs. Series C)* 1959 **81** 121–128.

S. LEVY, R. A. FULLER and R. O. NIEMI : Heat transfer to water in thin rectangular channels. *J. Heat Transfer (Trans. Amer. Soc. Mech. Engrs. Series C)* 1959 **81** 129–143.

R. T. LANCET : The effect of surface roughness on the convection heat transfer coefficient for fully developed turbulent flow in ducts with uniform heat flux. *J. Heat Transfer (Trans. Amer. Soc. Mech. Engrs. Series C)* 1959 **81** 168–174.

R. D. CESS and E. C. SHAFFER : Heat transfer to laminar flow between parallel plates with a prescribed wall heat flux. *Appl. Sci. Res. Hague* 1959 A **8** 329–344.

C. L. TIEN : On the eddy diffusivities for momentum and heat. *Appl. Sci. Res. Hague* 1959 A **8** 345–348.

A. McD. MERCER : The growth of the thermal boundary layer in laminar flow between parallel plates. *Appl. Sci. Res. Hague* 1959 A **8** 357–365.

H. A. LAUWERIER : A diffusion problem with chemical reaction (Cylindrical Poiseuille flow, diffusion and chemical reaction). *Appl. Sci. Res. Hague* 1959 A **8** 366–376.

J. HIGGINS : Method for measuring the moisture content of air. *J. Sci. Instrum.* 1959 **36** 300–302.

H. GOLDENBURG : Transient temperature rise due to a line source in a semi-infinite medium, with a radiation boundary condition at the interface. *Brit. J. Appl. Phys.* 1959 **10** 314–317.

D. R. OLIVER and S. G. WARD : Studies of the viscosity and sedimentation of suspensions. 5. The viscosity of settling suspensions of fine particles. *Brit. J. Appl. Phys.* 1959 **10** 317–321.

H. E. ROSE and R. M. E. SULLIVAN : Rapid estimation of the specific surface of a powder. *Nature Lond.*, 1959 137–138.

D. S. HOFFMAN and J. H. WEBER : K's for aromatics (Vaporization equilibrium constants). *Petrol. Refin.* 1959 **38** 137–138.

D. W. MOORE : The rise of a gas bubble in a viscous liquid. *J. Fluid Mech.* 1959 **6** 113–130.

SELECTION OF CURRENT SOVIET PAPERS OF INTEREST
TO CHEMICAL ENGINEERS*

A. B. Davankov and V. M. Laufer : On the problem of elution of noble metals from anionites after adsorption. *Zh. prikl. Khim.* 1959 **32** 727–734.

G. N. Gasyuk, A. G. Bolshakov, A. V. Kortnev and P. Ya. Krainy : Effect of hydrodynamic factors on the process of carbonization of ammonia liquor in an apparatus of the air-lift type. *Zh. prikl. Khim.* 1959 **32** 770–777.

V. G. Gleim and I. K. Shelomov : On the physical chemistry of foams. *Zh. prikl. Khim.* 1959 **32** 778–785.

P. A. Mochalova and M. Kh. Kishinevski : On calculation of height of apparatus for chemical interaction of gases and liquids. *Zh. prikl. Khim.* 1959 **32** 785–789. Absorption accompanied by chemical reaction.

V. V. Kafarov and B. M. Babanov : Interfacial area of immiscible liquids in mixing by mechanical stirrers. *Zh. prikl. Khim.* 1959 **32** 789–796.

V. M. Govorkov and Ya. D. Averbukh : On methods of calculating mass transfer in equipment with continuous value of driving force and in equipment of stagewise type. *Zh. prikl. Khim.* 1959 **32** 800–867. Calculation of height of a packed column and of number of plates in a plate column.

L. D. Berman : General view of basic equations for mass transfer in equipment with fixed contact area between phases. *Zh. prikl. Khim.* 1959 **32** 807–812. Dimensional analysis.

I. N. Bushmakin : Apparatus for determination of vapour–liquid equilibria. *Zh. prikl. Khim.* 1959 **32** 812–817.

V. B. Kogan, V. M. Fridman and T. G. Romanova : Separation of mixtures of alcohols and hydrocarbons by extraction. *Zh. prikl. Khim.* 1959 **32** 847–852.

M. A. Proskurnin : Prospects of carrying out radiochemical processes in the chemical industry. *Khim. Prom.* 1959 (2) 99–106.

N. M. Zhavoronkov and Yu. M. Martinov : Investigation of kinetics of absorption of nitrogen oxides in water and in aqueous solutions of nitric acid. *Khim. Prom.* 1959 (2) 150–155.

Yu. N. Brodski : Drying of sulphur anhydride by solid sorbents. *Khim. Prom.* 1959 (2) 155–163.

D. K. Kollerov : Hydrodynamics of porous media. *Khim. Prom.* 1959 (2) 163–169.

V. G. Fastovski, Yu. V. Petrovski and R. A. Akchurin : Investigation of resistance and effectiveness of operation of a contact plate utilizing kinetic energy of the lighter phase. *Khim. Prom.* 1959 (2) 169–174. Performance and pressure drop of Kittel plates.

V. I. Smirnova and B. F. Ormont : Determination of surface tension of substances at high temperatures by the pendant and creeping drop methods. *Zh. fiz. Khim.* 1959 **33** 771–779.

G. M. Martinyuk and A. I. Shlygin : On the mechanism of hydrogenation of nitrobenzene in the presence of a liquid phase. *Zh. fiz. Khim.* 1959 **33** 852–857.

A. T. Davidov and Ya. A. Tolmacheva : Study of the dynamics of ion exchange on sulphocarbon. *Zh. fiz. Khim.* 1959 **33** 858–862.

I. P. Budarov : Equation for the rate of vaporization of liquids under conditions of forced convection. *Zh. fiz. Khim.* 1959 **33** 920–921.

O. P. Fedoseeva, E. P. Cherneva and N. N. Tunitski : Studies of the kinetics of ion-exchange sorption. II. Kinetics of exchange with the participation of hydrogen ions. *Zh. fiz. Khim.* 1959 **33** 936–942.

---

*To assist readers, translations of any article appearing in the above list can be obtained at a reasonable charge. All orders should be addressed to the Administrative Secretary of the Pergamon Institute at either Headington Hill Hall, Oxford or 1404 New York Avenue N.W., Washington 5, D.C. whichever is more convenient.

A. S. Nevski : About the influence of contamination of screen surfaces on the effectiveness of screening. *Teploenergetika* 1959 **6** (4) 56–61.

V. A. Kirilin and S. A. Oulibin : Experimental determination of specific volumes of heavy water. *Teploenergetika* 1959 **6** (4) 67–72.

D. I. Orochko, V. A. Basov and T. Kh. Melik–Akhnazarov : On the method of hydrodynamic calculation of stagewise contact equipment. *Khim. Tekhnol. Topl. Masel.* 1959 **4** (4) 54–59. Stagewise gas–solid contact in fluidized beds.

L. M. Zysina–Molozhen : Approximate method of calculation of a non–isothermal boundary layer. *Zh. tekh. Fiz.* 1959 **29** 632–639.

V. N. Tsvetkov and S. I. Klenin : Concentration dependance of the diffusion coefficient of a polymer in solution. *Zh. tekh. Fiz.* 1959 **29** 640–646.

S. S. Litvinkov : A boundary value problem for linearized equations of viscous flow dynamics. *Dokl. Akad. Nauk SSSR* 1959 **125** 998–1001.

V. P. Pavilov and G. V. Vinogradov : Heat effects involved in the motion and stopping of flow of anomalously viscous bodies. *Dokl. Akad. Nauk SSSR* 1959 **125** 1061–1064.

L. S. Palatnik and Yu. F. Komnik : Condensation kinetics of metals *in vacuo*. *Dokl. Akad. Nauk SSSR* 1959 **126** 74–77.

S. N. Ganz, G. I. Vilesov, S. I. Gorbman and S. B. Leibovich : Combination of the process of purification of hydrogen–nitrogen mixtures from CO_2 with manufacture of ammonium carbonate salts. *Zh. prikl. Khim.* 1959 **32** 969–975.

S. N. Ganz, S. B. Leibovich and S. I. Gorbman : Investigation of the rate of conversion of $CaSO_4$ into $(NH_4)_2 SO_4$ during combination of this process with the absorption of NH_3 and CO_2 under highly turbulent conditions. *Zh. prikl. Khim.* 1959 **32** 975–978.

V. I. Atroschenko and B. Bibr : Investigation of the conversion of carbon monoxide by water vapour at elevated pressures. *Zh. prikl. Khim.* 1959 **32** 997–1004.

M. E. Pozin, B. A. Kopylev and E. Ya. Tarat : Effect of foam height on a sieve plate on absorption of carbon dioxide by solutions of caustic soda. *Zh. prikl. Khim.* 1959 **32** 1004–1010.

M. E. Pozin, B. A. Kopylev and E. Ya. Tarat : Absorption of carbon dioxide by solutions of caustic soda in the foam regime. *Zh. prikl. Khim.* 1959 **32** 1011–1016.

M. Kh. Kishinevski and L. A. Mochalova : On interfacial resistance in absorption processes. *Zh. prikl. Khim.* 1959 **32** 1016–1021. Low values of mass transfer coefficients in absorption of CO_2 by 1N NaOH are explained by interfacial resistance.

A. A. Medvedev and P. G. Romankov : Some problems in the analogy of diffusional and thermal processes. *Zh. prikl. Khim.* 1959 **32** 1021–1029.

I. P. Levsh and O. B. Balandina : Bubbling of air through viscous liquids. *Zh. prikl. Khim.* 1959 **32** 1029–1039.

V. G. Gleim, I. K. Shelomov and B. R. Shidlovski : Stability of electrolytic foams. *Zh. prikl. Khim.* 1959 **32** 1046–1050.

I. M. Alekseev : Dispersion of pigments in highly viscous media. *Khim. Nauka i Prom.* 1959 **4** 365–371.

M. D. Kuznetsov and V. M. Leonenko : Heat transfer in transitional regime. *Khim. Nauka i Prom.* 1959 **4** 406–407. Variation in the value of the heat transfer coefficient in the range of Re between 1000 and 10000.

E. L. Zorina and V. K. Semenchenko : Effect of sodium sulphate on critical phenomena in the system triethylamine–water. *Zh. fiz. Khim.* 1959 **33** 961–969.

Ya. Z. Kazavchinski and G. I. Tosoyman : Equation of state for Freon 41 (methylfluoride). *Zh. fiz. Khim.* 1959 **33** 992–996.

K. A. Golbert and A. V. Alekseeva : Kinetics of physical adsorption of gases and their mixtures. I. Differential method of measuring the kinetics of physical adsorption. *Zh. fiz. Khim.* 1959 **33** 1035–1041.

144

V. Ya. Basevich : Investigation of the rate of burning of atomized fuel in turbulent flow. *Zh. fiz. Khim.* 1959 **33** 1080–1086.

L. S. Aleksandrova, S. Yu. Elovich and K. V. Chmutov : Dynamic ionic sorption on various types of cation exchangers. II. Diffusion kinetics of dynamic sorption. *Zh. fiz. Khim.* 1959 **33** 1119–1125.

O. P. Fedoseeva and N. N. Tunitski : Studies of kinetics of ion exchange sorption. III. Complete exchange between univalent and divalent ions in resins. *Zh. fiz. Khim.* 1959 **33** 1140–1146.

K. A. Alekseeva, V. S. Dragunskaya, D. M. Rudkovski and A. G. Trifel : Solubility of synthesis gas in some hydro-carbons and oxygen-containing products in the reaction of oxysynthesis. *Khim. Tekhnol. Topl. Masel* 1959 **4** (5) 24–28.

V. G. Pavlov and A. A. Chechulin : Hydraulic resistance of a bed of granular material. *Khim. Tekhnol. Topl. Masel* 1959 **4** (5) 60–65.

V. A. Ragozin and N. F. Ronzhina : Formation of static electricity in reactive fuels. *Khim. Tekhnol. Topl. Masel* 1959 **4** (6) 55–60.

Z. I. Geller : On the problem of choice of a type of preheater for high-viscosity fuels. *Teploenergetika* 1959 **6** (5) 38–45

G. B. Froyshteter : On the problem of determining the resistance of a burning bed of coal. *Teploenergetika* 1959 **6** (5) 50–55.

A. V. Arseev : Heat transfer and hydraulic resistance of pipes in high temperature air heating. *Teploenergetika* 1959 **6** (6) 67–72.

S. R. Sergyenko, L. N. Kvitkovski and A. A. Petrov : Viscosity–temperature properties of high-molecular hydro-carbons of mixed structure. *Dokl. Akad. Nauk SSSR* 1959 **126** 798–801.

Ya. P. Berkman and S. V. Kushnir : Production of carbon disulphide by " non-equilibrium " recovery of sulphurous gas by methane. *Zh. prikl. Khim.* 1959 **32** 1211–1218.

N. G. Chekh : Radiometric investigation of adsorption of some ions in connexion with corrosion of metals in salt solutions. *Zh. prikl. Khim.* 1959 **32** 1255–1259.

A. B. Zdanovski and N. A. Karazhanov : Determination of rate-of-dissolution coefficients of crushed crystals. *Zh. prikl. Khim.* 1959 **32** 1259–1267.

I. N. Bushmakin, S. P. Versen and N. P. Kuznetsova : Vapour–liquid equilibrium in the system methylcyclohexane – 2, 2, 4-trimethylpentane. *Zh. prikl. Khim.* 1959 **32** 1274–1279.

I. N. Kuzminikh and A. I. Rodionov : Mass transfer on sieve plates as a function of weir height. *Zh. prikl. Khim.* 1959 **32** 1279–1285.

I. S. Pavlushenko : New method of calculation of heat transfer equipment. *Zh. prikl. Khim.* 1959 **32** 1286–1290.

I. P. Mukhlenov, D. G. Traber, V. G. Sarkits and T. P. Bondarchuk : Heat removal from a fluidized catalyst bed to a heat transfer surface. *Zh. prikl. Khim.* 1959 **32** 1291–1296.

Yu. A. Gorin : Vapour-phase hydration of acetylene into acetaldehyde on non-mercury catalysts. *Khim. Prom.* 1959 (3) 194–200.

I. Ya. Tyupyaev, T. N. Mukhina, A. N. Bushin and P. S. Gurina : Catalytic dehydrogenation of propane under semi-industrial conditions. *Khim. Prom.* 1959 (3) 201–202.

N. M. Zhavoronkov and K. I. Sakodynski : Industrial methods of heavy water production. *Khim. Prom.* 1959 (3) 221–234.

N. P. Dolinin : Concentration of sulphuric acid by superheated steam. *Khim. Prom.* 1959 (3) 238–241.

M. N. Shendrik and G. K. Boreskov : Calculation of adiabatic reactor for endothermic processes. *Khim. Prom.* 1959 (3) 241–243.

I. I. Ioffe and A. F. Grigorov : On the theory of rate of reaction in fluidized catalyst beds. *Khim. Prom.* 1959 (3) 243–250.

I. G. Averyanov and L. S. Akselrod : Conditions of uniform operation of bubble-cap plates. *Khim. Prom.* 1959 (3) 250–256.

K. P. Shumski : Investigation of the condensation process in condensers of sublimation plants. *Khim. Prom.* 1959 (3) 256–259.

V. K. Semenchenko and E. L. Zorina : Effect of nonyl alcohol on critical phenomena in the system triethylamine–water. *Zh. fiz. Khim.* 1959 33 1176–1183.

A. N. Baratov : Effect of initial temperature on the concentration limits of inflammation of combustible gaseous mixtures. *Zh. fiz. Khim.* 1959 33 1184–1188.

G. P. Luchinski : Physico-chemical investigation of the system $H_2O - SO_3$. II. Heats of interaction of the components in the system $H_2O - SO_3$ with the liquid phase of varying composition. *Zh. fiz. Khim.* 1959 33 1275–1279.

A. V. Komandin and V. Ya Rozlovski : Densities and molar volumes of some organic compounds over a wide temperature range. *Zh. fiz. Khim.* 1959 33 1280–1282.

A. V. Komandin and V. Ya. Rozlovski : Dielectric constants of some organic compounds over a wide temperature range. *Zh. fiz. Khim.* 1959 33 1283–1286.

D. A. Vyakhirev and A. I. Bruk : Effect of experimental parameters on chromatographic separation of substances in gaseous and vapour phases. II. Effect of nature of carrier gas on the separation of mixtures of gaseous hydrocarbons. *Zh. fiz. Khim.* 1959 33 1309–1317.

I. R. Krichevski and G. D. Efremova : Phase equilibria in the system melamine–ammonia. *Zh. fiz. Khim.* 1959 33 1328–1335.

V. B. Kogan and V. M. Safronov : Method of calculation of vapour–liquid equilibrium data in ternary systems. II. *Zh. fiz. Khim.* 1959 33 1353–1359.

K. S. Kazanski, S. G. Etelis and N. M. Chirkov : Solubility of gaseous *iso*butylene in water. *Zh. fiz. Khim.* 1959 33 1409–1413.

V. A. Marinin : Temperature dependence of the coefficient of diffusion of some substances in tetrachloroethane. *Zh. fiz. Khim.* 1959 33 1430–1433.

B. P. Bering, M. M. Dubinin and V. V. Serpinski : Calculation of differential heats of vapour adsorption on active charcoal. *Izv. Akad. Nauk SSSR, Otd. khim. Nauk* 1959 (6) 981–988.

A. V. Kiselev and N. V. Kovaleva : Effect of thermal treatment of various carbon blacks on vapour adsorption. *Izv. Akad. Nauk, Otd. Khim. Nauk* 1959 (6) 989–998.

L. N. Galperin, V. M. Maltsev and P. F. Pokhil : Measurement of flame temperature of condensed systems. *Dokl. Akad. Nauk SSSR* 1959 159 131–134.

G. V. Vinogradov, A. A. Mamakov and V. P. Pavlov : Flow of anomalously viscous systems under the action of two pure stresses in mutually perpendicular direction. *Dokl. Akad. Nauk SSSR* 1959 159 362–365.

M. Ya. Gen, M. S. Ziskin and Yu. I. Petrov : Study of dispersion of aluminium aerosols as a function of conditions of their formation. *Dokl. Akad. Nauk SSSR* 1959 159 366–368.

A. K. Vnukov and A. A. Madoyan : Automation of ball mills according to the level of fuel in the drum. *Teploenergetika* 1959 6 (7) 19–22.

L. D. Berman and S. N. Fuks : Design of surface heat exchange equipment for condensation of steam from steam–water mixtures. *Teploenergetika* 1959 6 (7) 74–83.

G. L. Antipenko, E. S. Beletskaya and Z. I. Koroleva : Density of N_2O_4 solutions in strong nitric acid. *Zh. prikl. Khim.* 1959 32 1462–1466.

S. N. Ganz and M. A. Lokshin : Investigation of the rate of absorption in horizontal mechanical absorbers with the aid of the theory of similarity. *Zh. prikl. Khim.* 1959 32 1477–1483.

I. N. Kuzminikh and A. I. Rodionov : Mass transfer on sieve and grid-type plates. *Zh. prikl. Khim.* 1959 32 1489–1495. Effects of gas velocity, free area, liquid rate and foam height on the mass transfer coefficient.

I. S. PAVLUSHENKO and A. V. YANISHEVSKI : On the magnitude of interfacial area in mechanical stirring of mutually-insoluble liquids. *Zh. prikl. Khim.* 1959 **32** 1495–1502.

K. A. ANDRYANOV, S. A. GOLUBTSOV and I. V. TROFIMOVA : Interaction of silicon and hydrogen chloride in a fluidized bed. *Zh. prikl. Khim.* 1959 **32** 1620–1623.

E. R. SHENDEREY, YA. D. ZELVENSKI and F. P. IVANOVSKI : Solubility of carbon dioxide in methanol at low temperatures under pressure. *Khim. Prom.* 1959 (4) 328–331.

A. A. ZHELNIN, N. B. PAVLOV and A. N. NEVEROR : Beneficiation of sylvinite ore by flotation. *Khim. Prom.* 1959 (4) 331–334.

S. M. KRUGLITY : Distribution of evaporated water between effects in multiple effect evaporators. *Khim. Prom.* 1959 (4) 335–338.

F. B. MOIN : Some problems in calculation of equilibrium in rectification of multicomponent mixtures. *Khim. Prom.* 1959 (4) 338–339.

V. V. KAFAROV and V. B. TIKHOMIROV : Ejector column for diffusional processes. *Khim. Prom.* 1959 (4) 340–342

S. F. YAVOROVSKAYA : Rapid method of separation of organic chlorine compounds in air. *Khim. Prom.* 1959 (4) 355–357.

B. P. BERING and V. V. SERPINSKI : Adsorption of gas mixtures. 5. Adsorptive equilibrium in water–ethyl chloride–activated charcoal system. *Izv. Akad. Nauk SSSR, Otd. khim. Nauk* 1959 (7) 1186–1195.

I. R. KRISHEVSKI, N. E. KHAZANOVA, YU. V. TSEKHANSKAYA and L. R. LINSHITS : Critical phenomena in the system hexamethyleneimine–water. I. Solubility curve near the critical solution temperature. *Zh. fiz. Khim.* 1959 **33** 1484–1491.

V. B. KOGAN, V. M. FRIDMAN and T. G. ROMANOVA : Phase equilibria in systems formed by paraffin hydrocarbons and aliphatic alcohols. *Zh. fiz. Khim.* 1959 **33** 1521–1525.

L. D. BELYAKOVA and A. V. KISELEV : Adsorption and chemisorption of methanol by silica gel with different degrees of surface hydration. *Zh. fiz. Khim.* 1959 **33** 1534–1543.

A. B. KONDRATEY and B. K. MARUSHKIN : On calculation of minimum reflux ratio in rectification of complex mixtures. *Khim. Tekhnol. Topl. Masel* 1959 **4** (7) 31–37.

N. F. VOLKOV and Z. I. GELLER : Some peculiarities of heat transfer in pipe heaters and distribution of radiant flux. *Khim. Tekhnol. Topl. Masel* 1959 **4** (7) 38–47.

M. E. AEROV, N. I. NIKITINA, S. S. TRAININA and I. V. GUSEV : Heat and mass transfer in granular beds. IV. Local coefficients of heat and mass transfer in a bed of spheres. *Zh. tekh. Fiz.* 1959 **29** 924–927.

A. V. NIKOLAEV, S. M. SHUBINA and N. M. SINITSYN : Extraction of nitric acid by derivatives of butyphosphinic acids. *Dokl. Akad. Nauk SSSR* 1959 **127** 578–580.

B. I. DAVIDOV : On the statistical dynamics of an incompressible turbulent fluid. *Dokl. Akad. Nauk SSSR* 1959 **127** 768–771.

L. V. CHERKESOV : Development of surface waves caused by periodic translocation of pressure. *Dokl. Akad. Nauk SSSR* 1959 **127** 774–776.

B. I. DAVIDOV : On the statistical theory of turbulence. *Dokl. Akad. Nauk. SSSR* 1959 **127** 980–982.

E. S. RUDAKOV : Interrelation between physico-chemical characteristics of polar liquids. *Dokl. Akad. Nauk SSSR* 1959 **127** 1058–1061.

P. YA. SIVER : Mutual influence of diffusion streams in multicomponent systems. *Dokl. Akad. Nauk SSSR* 1959 **127** 1062–1065.

P. E. SOBOLEVSKI : Non-stationary equations of viscous fluid dynamics. *Dokl. Akad. Nauk SSSR* 1959 **128** 45–48.

B. DOLAPCHEV and B. SENDOV : Symmetrical flow around a cylinder with two vortices behind it. Trajectories of the vortices and resistance of the cylinder. *Dokl. Akad. Nauk SSSR* 1959 **128** 53–56.

R. L. BABKIN and E. M. YAKIMETS : On the methods of determining small quantities of oxygen dissolved in water. *Teploenergetika* 1959 **6** (8) 6–9.

Errata

T. J. GILBERT: Liquid mixing on bubble-cap and sieve plates. *Chem. Engng. Sci.* 1959 **10** 243.

Equation (4) on p. 249 should read as follows:

$$\frac{D}{uh} = 0.45 \left(\frac{h_f}{h}\right)^{2.4} \cdot \left(\frac{1}{u}\right)^{0.4}$$

Selection of Current Soviet Papers of Interest to Chemical Engineers. *Chem. Engng. Sci.* 1959 **11** 73.

The last reference on p. 74 should read as follows.

N. L. KAFENGAUZ and T. D. BOCHAROV: Effect of height of a flat rectangular conduit on heat transfer to water. *Teploenergetika* 1959 **6** (3) 76–78.